CHARACTERIZING A REINFORCED CONCRETE CONNECTION FOR PROGRESSIVE COLLAPSE ASSESSMENT

By

LOO YONG TAN

A THESIS PRESENTED TO THE GRADUATE SCHOOL
OF THE UNIVERSITY OF FLORIDA IN PARTIAL FULFILLMENT
OF THE REQUIREMENTS FOR THE DEGREE OF
MASTER OF SCIENCE

UNIVERSITY OF FLORIDA

2010

To my lovely wife in Singapore

ACKNOWLEDGMENTS

I would like to express my gratitude to my thesis advisor, Professor Theodor Krauthammer for his decisive guidance and advice. I would like to thank Dr Sedar Astarlioglu for his patience with my questions and encouragement. I would like to thank Dr Yim Hyun Chang for his advice on the finite element software. I am grateful for the Defence Science and Technology Agency, Singapore, for the postgraduate scholarship. I thank all my friends at the Center for Infrastructure Protection and Physical Security and my Singaporean friends in Gainesville for their support and making my stay here a wonderful experience.

Lastly, I would like to thank my wife for her sacrifices and support from my family in Singapore throughout my course.

TABLE OF CONTENTS

page

LIST OF TABLES

LIST OF FIGURES

LIST OF ABBREVIATIONS

A_c	Current area
A_s	Area of steel reinforcement
A_0	Initial area
a_v	Shear span
b_b	Transverse width of beam
b_c	Transverse width of column
b_j	Effective connection width
$\{B\}$	Strain displacement matrix
$\{C\}$	Constitutive matrix
$[C]$	Damping matrix
d_b	Diameter of reinforcement
$\{d\}$	Nodal displacements
$\{D\}$	Nodal displacement vector
DL	Dead load
E_c	Elastic modulus of concrete
f_{bs}	Bond stress
$f_c^{'}$	Concrete's cylinder strength
f_{cr}	Split-cylinder strength of concrete
F_c	Force due to the concrete
f_s	Stress applied to reinforcement
F_s	Force due to the reinforcement

f_r	Modulus of rupture of concrete
$f_t^{'}$	Direct tensile strength of concrete
f_y	Yield stress of reinforcement
f_{yi}	Yield stress of radial hoops
$\{f\}$	External nodal load
$\{F\}$	Force matrix
h	Depth of column
K_0, k_i	Initial rotational stiffness
K	Ratio of second stress invariant on the tensile meridian to compressive meridian
$\{K\}$	Element stiffness matrix
$[K]$	Global stiffness matrix
l	Anchorage length
l_{dh}	Minimum development length
l_p	Length of plastic hinge
LL	Live load
M	Moment
$[M]$	Mass matrix
n	shape factor
$\{N\}$	Shape function
$\{u\}$	Displacement matrix
$\{\dot{u}\}$	Velocity matrix

$\left\{\ddot{u}\right\}$	Acceleration matrix
V_u	Design shear force
V_n	Nominal shear strength
w_c	Density of concrete
z	Distance of critical section to the point of contraflexure of a cantilever
ϕ	Diameter of reinforcement
α	Stress multiplier for reinforcement
θ	Rotation of connection
θ_0	Plastic rotation of connection
λ	Load factor
ε_c	Strain of concrete
ε_s	Strain of reinforcement
ε_0	Strain of concrete corresponding to maximum stress
ε_{nom}	Nominal strain
$\varepsilon_{\ln}^{pl}$	Plastic strain
$\{\varepsilon\}$	Strain vector
$\{\sigma\}$	Stress vector
φ	Dilation angle of concrete
ϕ	Friction angle of concrete
$fb0/fc0$	Ratio of unibiaxial compressive strength to intial uniaxial strength of concrete in CDP
ε	Eccentricity of plastic potential surface of concrete in CDP

μ	Viscosity parameter in CDP
σ_{true}	True stress or Cauchy stress
σ_{nom}	Nominal stress

Abstract of Thesis Presented to the Graduate School
of the University of Florida in Partial Fulfillment of the
Requirements for the Degree of Master of Science

CHARACTERIZING A REINFORCED CONCRETE CONNECTION FOR PROGRESSIVE COLLAPSE ASSESSMENT

By

Loo Yong Tan

May 2010

Chair: Theodor Krauthammer
Major: Civil Engineering

Advanced numerical tools, such as finite element codes, are required for accurate assessment of reinforced concrete frames for progressive collapse mitigation. Previous studies of moment resisting steel frames have shown that the accuracy in modeling the connections had a large effect on the accuracy of the entire simulation. This study is focused on a particular type of reinforced concrete (RC) beam-column connection subjected to monotonic loading. The main objective is to use a high fidelity continuum model to derive a simplified mechanical model of the connection under monotonic loadings to be used for progressive collapse assessment. The approach was validated by comparing simulations for RC elements with available test data. The derived resistance functions for the connections will be incorporated in numerical model of a full scale RC frame that is scheduled for progressive collapse tests. The numerical results will eventually be compared with the test data for assessing the effectiveness of the proposed numerical approach.

CHAPTER 1
PROBLEM STATEMENT

Reinforced concrete (RC) structures are very common in many countries due to the easily availability and relatively low cost of the raw materials. The convenience and advantage of in-situ construction in which the “wet” concrete could be made to the contours of different shapes and sizes of the buildings and the boom in population and economic activities further drive up the need for new buildings, especially RC structures.

RC beam-column connections, however, have complex stress distributions due to load and geometric discontinuities and cannot be described by the classical Beam theory (Krauthammer, 2008). The behavior of beam-column connections under abnormal loads is not well understood and only a few models exist in the literature for design of such connections.

When subjected to an abnormal loading, such as blast, the beam-column connection may become the primary plane of weakness. In essence, the failure may be initiated at the connection even though the loads have not reached the design load levels of the primary structural members. This results in catastrophic consequences in which a portion or the entire structure may fail from progressive collapse of the main structural elements, causing injuries or even fatalities and destruction of properties. Watson and Inkester (1982) clearly identified the importance of connections relative to the main structural elements here:

> A joint was studied because it has been seen from bomb damage that joints often sustain more damage than the point of impact.(Watson and Inkester, 1982)

Advanced numerical tools are seldom used for progressive collapse analysis of RC structures because it is computationally too expensive and time consuming to model

an entire RC structure for progressive collapse simulation. Currently, engineers design buildings against progressive collapse by following guidelines by authorities such as Unified Facilities Criteria (UFC) or General Services Administration (GSA).

Objectives and Scope

The main objectives of this study are to develop a better understanding of the behavior of RC beam-column connections under monotonic loads by employing an predominantly continuum typed finite element (FE) model, and extract from it a simplified connector model that can be used along structural type elements for fast progressive collapse analysis.

The scope of this study is limited to the analysis of a particular type of reinforced concrete interior connection of a RC building that is scheduled to be tested for progressive collapse in late 2010. It will ignore the effects on the connections from the transverse RC beams and slabs. It will also not look into other types of reinforced concrete connections.

Research Significance

By using the simplified connector model and structural elements to represent the beams and columns, it is faster and computationally inexpensive to simulate the progressive collapse of a RC structure. This can act as an additional check for buildings designed to current progressive collapse guidelines.

CHAPTER 2
BACKGROUND AND LITERATURE REVIEW

Introduction

The primary structural elements of a reinforced concrete structure can only fully exhibit their design strength and ductility if the connections between these elements are adequately designed to transmit such forces. Due to constraints posed on the dimensions of the connection because of the sizes of the columns and beams framing into it and inadequate detailing of reinforcement, the connections often have reduced ductility compared to the structural members they are adjoining. To ensure properly detailed joint reinforcements, it is critical to understand the complex forces within the connection that result from the forces in the connecting structural elements. This chapter will look into detail the forces within a connection and the design of the connection accordingly to these forces. It will also look at material models, various tests and models, and experiments on beam-column connections being carried out by others.

Beam-Column Connections

> A beam-column joint is defined as that portion of the column within the depth of the deepest beam that frames into the column. (ACI 352R-02, 2002)

Beam-column connections (slabs not shown) can be classified into many types shown in Figure 2-1. Nilson, Darwin and Dolan (2004) gave a good representation of internal and exterior joints as shown in Figure 2-2. A typical internal joint is made up of all four beams coming together into the column. An exterior joint is formed by either beam 1, 2 and 3 or only beam 1 and 3 coming together into the column. A corner joint is formed by beam 1 and 2 coming together into the column. According to ACI 352-R02, type 1 connection is a moment-resisting connection designed on the basis of the

strength in accordance to ACI 318-02 for structural members without significant inelastic deformation. Type 2 connects members that are required to have sustained strength and dissipate energy through reversals of deformation into the inelastic range.

Two-Member Connections / Knee Connections

A two-member connection or knee-connection is most commonly found at the corner of portal frames. The connection may be subjected to either opening or closing load. MacGregor and Wight (2005) portrayed the behavior for a knee-connection under opening loads in Figure 2-3. The strut-and-tie model can be used to describe the behavior of a knee connection.

Nilsson and Losberg (1976) and Balint and Taylor (1972) conducted several tests for a large number of connections with different bar details. The test shown that the efficiency of a joint, the ratio between the theoretical and the measured moment capacities is highest at lower reinforcement ratio.

Nilsson (1973) showed that addition of diagonal bars in the connection increases the efficiency of a joint. The diagonal bar resisted the crack from developing at the inner corner and allows the compressive stress to flow around the corner, thus preventing tensile cracks from occurring. It is shown that the area of reinforcement required for this diagonal bar is half of the area of the main tensile steel. Another effect of the diagonal stirrups is that it helps to increase confinement in the concrete core and thus increase the strength and ductility of the joint.

Krauthammer and Ku (1996) developed a numerical model to determine the influence of diagonal and radial reinforcements (Figure 2-4) on knee-connections. Diagonal bars were determined to increase the strength of the connection by resisting the diagonal tensile forces at the inside corner. Radial bars act against the diagonal

tensile forces across the connection. However, radial bars were found to affect the tensile stress of the diagonal bars.

Three-Member Connections / T-Connections

A three-member connection or T connection is usually found at roof beam-column joints, exterior column-connections or at base of retaining walls (Figure 2-5). Each T connection will be subjected to both an opening and closing load. Tests by (Balint and Taylor, 1972) and (Taylor, 1974) shown that connections are stronger in closing loads than opening loads. Figure 2-6 indicates the strut-and-tie model for the T-connection.

Four Member Connections / Interior Connections

An interior connection or a four-member connection is designed to resist forces due to gravity or lateral loadings as shown in Figure 2-7. The joint must be designed to resist all the forces, including moments, shears and axial loads that the beam and column transfer through the joint.

Connection Behavior

To ensure connections are being adequately designed, it is critical to understand the mechanics and behavior of the connection. Different models of explanation and theories on the behavior of the connection lead to emphasis on different characteristics of the connection and correspondingly different design and detailing requirements.

Strut-And-Tie Model

Nilson, Darwin and Dolan (2004) illustrated the use of a strut-and-tie model to analyze the beam-column connection as shown in Figure 2-8. It shows an interior connection subjected to a lateral load causing clockwise moments from the beams balanced by anti-clockwise moments from the columns. The compressive force from the moments develops compressive struts within the joints, balanced by the tension ties.

There must be adequate development length for the tension bars to achieve its yield strength. In the case of a corner connection, hook anchorages in the form of L-bar or U-bar is used. The maximum force experienced in the connection is not the force determined by structural analysis, but it is the force calculated based on the nominal strengths of the connecting members. In this case, the maximum tensile force in the tensile steel is $A_s f_y$ where A_s is the area of the tensile steel while f_y is the yield stress of the tensile steel.

In a strut-and-tie model, column ties are required by conventional design procedures to prevent buckling of the column ties, provide containment to the concrete within the joint under compression and prevent cracking which might occur due to the tension force perpendicular to the compression strut.

Compressive Strut and Truss Mechanism Model

Park and Paulay (1975) idealized the behavior of a connection into two mechanisms, shear transfer by compression strut and shear transfer through truss mechanism, assuming the two mechanisms are additive. The compressive forces and shear forces combined to form the diagonal strut which is resisted by the compressive strength of the concrete. In the truss mechanism, the bond forces in the steel set up diagonal compressive forces and vertical or horizontal tensile forces within the entire panel zone. The diagonal compressive forces can be resisted by the concrete while vertical and horizontal reinforcement are required to resist the tensile forces.

Equilibrium Criteria

Paulay (1989) and Paulay and Priestly (1992) used the laws of statics or equilibrium criteria to show that connection shear forces due to lateral (seismic) loading

caused extensive diagonal cracks in the concrete core which in turn generated significant orthogonal tensile forces. The diagonal cracks in the concrete core due to the large lateral force causes a shift in the internal tensile forces along the column and lead to the development of significant tensile forces in all vertical column bars. Tensile concrete strength lost due to the cracking of the concrete needs to be replaced by orthogonal tensile reinforcement to continually sustain the shear resistance. As a consequence of these effects, significant orthogonal tensile forces are generated. Paulay suggested that the connection shear reinforcement is required to sustain the diagonal compression field rather than to provide confinement to the compressed concrete.

Connection Design Parameters

For the connection to perform its intended function to connect the different elements of a structure and fully exhibit the intended strength and ductility, it must be designed to meet the following requirements.

Column Longitudinal Reinforcement

Park and Paulay (1975), Paulay (1989) and Paulay and Priestly (1992) determined that the tensile forces developed within the concrete core must be resisted by the longitudinal reinforcement of the column. In normal design, the column longitudinal reinforcement that runs through the connection will be sufficiently strong enough to resist the tensile forces developed in the connection, hence the code requirements is more focused towards a uniform distribution of the longitudinal reinforcements within the joint.

- ACI 352-08 indicates that column longitudinal reinforcements need to satisfy CL 10.9.1 and 10.9.2 of ACI 318-05, which states:

- Area for the longitudinal reinforcement, A_{st} should be larger than greater than $0.01A_g$ (gross sectional area of column) but less than $0.08A_g$.

- The minimum numbers of longitudinal reinforcements are three, four, and six for triangular ties, rectangular ties or circular ties, and bars enclosed by spirals, respectively. ACI 352R-02 also gives guidance on the detailing requirements for both Type 1 and 2 connections for the offsetting of the longitudinal reinforcements within a joint. For Type 2 connections, the distance between longitudinal bars should be less than the larger of 8 inch or 1/3 of the column cross-section dimension (or diameter), and not larger than 12 inch.

Connection Transverse Reinforcement

Park and Paulay (1975) reported that the diagonal compressive stresses within the connection are responsible for the failure of the concrete core due to cyclic loading, especially if the transverse reinforcement is allowed to yield. Effective confinement through transverse reinforcement is critical for improving the connection performance. Nilson, Darwin and Dolan (2004) indicated that confinement strengthened the core concrete, improved its strain capacity, and prevented the vertical column bars from buckling outward. Panatazopoulou and Bonacci (1993) reported that the shear resistance of joints increases with the amount of hoop reinforcements in the joint.

> The primary functions of ties in a tied column are to restrain the outward buckling of the column longitudinal bars, to improve the bond capacity of column bars, and to provide some confinement to the joint core. Confinement of the joint core is intended to maintain the integrity of joint concrete toughness and to reduce the rate of stiffness and strength deterioration. (ACI 352R-02, 2002)

For Type 1 connections, transverse reinforcement is not necessary as adequate confinement is provided as shown in Figure 2-9 (Nilson, Darwin and Dolan, 2004). Confinement in the other direction is not considered in the presence of a third beam framing into the column. Transverse reinforcement is required for the direction which is not adequately confined by the beams.

Vertical joint transverse reinforcement is also required for connections with discontinuous columns. In this case, vertical reinforcement must be provided throughout the depth of the connection and there must be at least 2 layers between the outermost longitudinal column bars.

Type 2 connections have different detailing requirements specified under ACI 352R-02. The main difference is that Type 2 connections have transverse reinforcements that are closed with a seismic hook.

Shear Strength

Joint transverse reinforcement, combined with uniformly distributed longitudinal column reinforcement, has been shown to increase the shear resistance of connections by Hanson and Conner (1967).

Panatazopoulou and Bonacci (1992) have shown that shear strength of a connection depends on the compressive strength of the concrete that can be mobilized. Stirrups not only increase the shear stiffness of the reinforcement, but also the shear stiffness of the concrete core through confinement.

The maximum shear within a connection is limited by amount of shear reinforcement and the magnitude of the diagonal compressive stresses (Paulay and Priestley, 1992). To ensure constructability, the amount of shear reinforcement that can be placed within the connection, considering the amount of beam and column reinforcement passing through the connection, is limited. A large diagonal compressive force may cause extensive diagonal cracking within the connection core. Therefore, it is necessary to limit the horizontal shear force to prevent the connection core from cracking and causing the failure of the connection. The horizontal shear force may be

limited by maintaining the angle of the diagonal compressive forces within acceptable limits.

$$V_u \le 0.25 f_c^{'} \le 1300\, psi \tag{2-1}$$

ACI 352R-02 limits the shear force on a horizontal plane passing through a connection to values established by tests.

$$V_u \le \phi V_n \tag{2-2}$$

where V_u refers to the design shear force and V_n is the nominal shear strength of the connection and ϕ is taken as 0.85.

The nominal shear strength is given by

$$V_n = \gamma \sqrt{f_c'} b_j h \qquad \text{(psi)} \tag{2-3}$$

$$V_n = 0.083 \gamma \sqrt{f_c'} b_j h \quad \text{(MPa)} \tag{2-4}$$

where b_j is the effective connection width, h is the depth of the column in the direction of the load, $f_c^{'}$ is the concrete compressive strength of concrete at 28 days. Strength of the concrete is limited to 6000 psi due to the lack of research on high strength concrete. γ value is a constant that varies according to the confinement of the connection provided by the beam framing into it as shown in Table 2-1.

There are restrictions to be applied when determining γ values. For interior connections, the width of the beams must be at least ¾ the width of the columns and the depth of the shallowest beam must be at least ¾ the depth of the deepest beam. Connections that do not meet these criteria will be considered exterior connection. An exterior connection must have at least 2 beams framing from opposite sides of the connection. The width of the beam of the 2 opposite face should be at least ¾ the width

of the column and the depth of the two beams should not be less than ¾ the total depth of the deepest beam. Connections that do not meet these criteria will be considered corner connection.

ACI 352-R02 states that the effective connection width, b_j depends on both the average width of the beams (b_b) that frame into the column and the width of the column (b_c). . In the case of b_b smaller than b_c, b_j is:

$$b_j = \frac{b_b + b_c}{2} \quad \text{and} \quad b_j \le b_b + h \tag{2-5}$$

If the beam is flushed with one surface of the column, effective connection width b_j is as given:

$$b_j = \frac{b_b + b_c}{2} \quad \text{and} \quad b_j \le b_b + \frac{h}{2} \tag{2-6}$$

And if b_b exceeds b_c, effective connection width b_j is the same as b_c.

Flexure

For Type 2 connections that are a part of the primary resistance to seismic loading, it is important to maintain a weak beam-strong column ratio. This is to ensure that plastic hinges are formed in beams rather than columns. A structure needs to be sufficiently ductile to dissipate the seismic energy through inelastic rotations within the beams (Uma, 2006). Having inelastic rotations within the beams instead of the column ensures that the inelastic rotational demand is not excessively high such that detailing within the connection is not possible.

ACI 352R-02 recommends that the minimum column-flexural strength be at least 1.2 times the beam-flexural strength at the connection. The value of 1.2 is

recommended as a compromise to prevent plastic hinging from occurring at the column and the need to keep column sizes and reinforcement within economic and constructability purposes, although studies have shown that that a higher factor than 1.2 has been required in cases where the structure is extremely flexible and higher modes of failure contributes to the response.

Ehsani and Wight (1984) recommend a value of greater than 1.4 for bare connections and 1.2 for connections where slab and transverse beams are present, for plastic hinges to form in the beams for ductile frames. For a stiff frame, where the value is 1.0, the plastic hinge will form in the column.

Development of Reinforcement

For connections, it is important that the anchorage length of the reinforcement (Figure 2-10) is sufficient to fully develop the tensile and compressive forces caused by the design loads on the structural element (Holmes and Martin, 1983) to prevent premature failure of the bond between concrete and the rebar.

One can determine the length that is necessary to prevent bond failure equating the force in the bar to the bond stress,

$$f_s . \frac{\pi(\phi)^2}{4} = f_{bs} . \pi \phi l \qquad (2\text{-}7)$$

where f_s is the stress applied to the bar, f_{bs} is the bond stress and the anchorage length l

$$l = \frac{f_s \phi}{4 f_{bs}} \qquad (2\text{-}8)$$

While there is sufficient length to provide anchorage for interior connections where the flexural reinforcement of the beam enters a connection and continues straight on to

become the flexural reinforcement of the opposite beam, there is not sufficient length to provide anchorage for the tensile reinforcement in exterior and corner connections. In such cases, 90º hooks extending towards and beyond the connection are used. The bottom reinforcements only require to make a ninety degree hook if it the beam is part of a lateral load resisting system.

Beam Transverse Reinforcement

For Type 2 connections, where the beam is wider than the column with computed beam shear stresses less than $2\sqrt{f_c'}(psi)$ or $0.17\sqrt{f_c'}(MPa)$, the maximum spacing of reinforcement within the beam's plastic hinging zone should be the least of ½ the effective beam's depth, eight times the diameter of the longitudinal bar or 24 times the diameter of the stirrup according to ACI 352-R02. This is to address the lower shear stresses experienced in wide beams compared to current stringent provisions for shear.

However, ACI 352-02 does not provide guidance on the detailing for the wide-beams' longitudinal bars into the beam-column connections. If the outer reinforcement of a wide beam passes outside the width of the column, the diagonal strut will form outside the column width. In such cases, the vertical compressive strut needed to balance the diagonal strut cannot be developed. Nilson et al. (2004) suggested placing all the beam outer bars within the outer bars of the column or if this is not possible, placing vertical stirrups throughout the connection to balance the diagonal strut.

Plastic Hinge

Reinforced concrete beam-column connections are designed with strong column – weak beam philosophy. Type 2 connections (ACI 352R-02) can undergo significant inelastic deformations and the sum of the column flexural strengths will be more than

the sum of the beam flexural strengths. When subjected to large shear forces, the column above and below a joint will remain elastic while plastic hinges will develop in the beams (Paulay, 1989). Plastic hinges are allowed to develop in the beams because it is possible to design for the inelastic deformations through proper detailing (Uma and Prasad, 2006) but is difficult to cater to the inelastic demand through detailing in the columns if plastic hinges are allowed to form in the columns.

With the rotation of the beam due to the formation of the plastic hinges, one can represent the behavior of a reinforced concrete beam-column connection with a moment-rotation curve. The rotation of the plastic hinges can be determined from actual tests or through simulation models while the moment is simply the product of the force/pressure onto the beam and the lever arm.

Several empirical formulas are proposed for the effective plastic hinge length. Paulay and Priestley (1992) gave a good estimate of effective plastic hinge length of a cantilever beam with a tip load as shown below. In the case of typical beam and column sections, $l_p \approx 0.5h$.

$$l_P = 0.08l + 0.022d_b f_y (MPa) \tag{2-9}$$

$$l_P = 0.08l + 0.15d_b f_y (ksi) \tag{2-10}$$

where *l* is the length of the cantilever, h is the section depth, d_b is the diameter of the longitudinal reinforcement and f_y is the strength of the reinforcement.

Corley (1966) proposed that the equivalent plastic hinge length to be:

$$l_p = 0.5d + 0.2\sqrt{d}(\frac{z}{d}) \tag{2-11}$$

where d is the effective depth of the beam in inches and z is the distance from the critical section to the point of contraflexure or tip of a cantilever.

Mattock (1967) suggested that the equivalent plastic hinge length to be:

$$l_p = 0.5d + 0.05z \tag{2-12}$$

Finally, Sawyer (1964) proposed the equivalent plastic hinge length to be:

$$l_p = 0.25d + 0.075z \tag{2-13}$$

ASCE (1999) stated that the plastic hinge size is about equal to the member's depth for plastic hinge to be developed in flexure.

Modeling of Beam-Column Connections

Alath and Kunnath (1995) modeled inelastic shear deformation in reinforced concrete beam-column connections by idealizing the connection region as a panel zone characterized by pure shear deformation. The column moments and rotation are assumed to be different for the beam moments and rotation. M_b, θ_b, M_c and θ_c are the moments and rotations of the joint region and γ_p is the shear deformation of the joint region or the relative difference in the rotations. The prediction by the model was able to correlate well with the test results conducted at Cornell (Beres, El-Borgi, White and Gergely, 1992).

$$\gamma_p = \theta_b - \theta_c \tag{2-14}$$

The relationship between the moments and the rotations is:

$$\begin{Bmatrix} M_c \\ M_b \end{Bmatrix} = V_p G \begin{bmatrix} 1 & -1 \\ -1 & 1 \end{bmatrix} \begin{Bmatrix} \theta_c \\ \theta_b \end{Bmatrix} \tag{2-15}$$

where V_p = volume of the panel and G = shear modulus of the material

El-Metwally and Chen (1988) used thermodynamic field theory to develop the moment-rotation relationships for reinforced concrete beam-column connections idealizing the connections as a rotational spring. The rotational spring is characterized by three parameters: initial rotational stiffness of the connection, ultimate capacity of the connection and internal variable that reflects the energy dissipation of the connection. The model assumes the connection to be properly designed, detailed and has sufficient shear strength. The results generated from the model showed good agreement with the experimental data conducted by Viwathanatepa, Popov and Bertero (1979). The analytical model slightly overestimates experimental data because the model was based on the assumption that the free and dissipated energies of the RC connections are unbounded at failure. In reality, the RC connections have a limited capacity to gain free energy and dissipate energy and thus both the energies are bounded at failure

Panatazopoulou and Bonacci (1992) idealized connections as 2 dimensional (2-D) panels reinforced in both orthogonal directions, and acted upon by in-plane shear and normal stresses. The total shear stiffness K of the panel consists of K_c, shear stiffness for concrete, and K_s, shear stiffness for the reinforcement and both inter-dependent. In tests where the connection transverse reinforcements were replaced by longitudinal beam reinforcements uniformly distributed along the height of the connections, the connections were able to resist the shear demanded to develop beam hinging but a rapid deterioration of joint shear resistance was observed with cyclic loads. The tests showed the stirrups were able to increase the shear resistance of the connections directly by increasing the shear stiffness of the steel and indirectly by confining the concrete core and thus increasing the shear stiffness of the concrete, thereby

increasing the overall shear stiffness. The stress of concrete decreased after yielding of the stirrup and loss of confinement within the concrete. Yielding of the stirrup will be followed by either the yielding of the longitudinal column reinforcement or the crushing of concrete in the direction of the principal compressive stress.

Lowes and Altoontash (2003) developed numerical models to simulate reinforced concrete beam-column connections subjected to cyclic loading. A classical super element, composed of 4 internal nodal translations and thirteen one-dimensional components was used to model the connection element. Behavior of the connection is characterized by a combination of one-dimensional shear panel, bar slip and interface-shear components. Each external node consists of two translations and one rotation and each internal node consists of a translation. The sixteen internal and external nodal displacements are complemented by 16 internal and external nodal resultants and can be represented by the following component deformations, forces and equations.

$$\begin{Bmatrix} \Delta_1 \\ \vdots \\ \vdots \\ \Delta_4 \end{Bmatrix} = A \begin{Bmatrix} u_1 \\ \vdots \\ u_9 \\ v_1 \\ \vdots \\ v_4 \end{Bmatrix} \tag{2-16}$$

$$\begin{Bmatrix} F_1 \\ \vdots \\ F_{12} \\ \Phi_1 \\ \vdots \\ \Phi_4 \end{Bmatrix} = A^T \begin{Bmatrix} f_1 \\ \vdots \\ f_{13} \end{Bmatrix} \tag{2-17}$$

where $\Delta =$ vector of component deformations, $u =$ internal nodal displacements, $v =$ external nodal displacements, $f =$ component forces, $F =$ external nodal resultants, $\Phi =$ internal nodal resultants

Constitutive models are developed for the load deformation response for the shear panel and bar-slip based on material properties, joint geometry and the distribution of the reinforcements' distribution. The model was able to represent well the fundamental characteristics of response for the connections based on the comparison with actual observed test data.

Krauthammer and Ku (1996) used a hybrid finite element (FE) – finite difference (FD) approach to investigate the behavior, response and influence of reinforcements in structural concrete knee-connections (two-member connections) under impulsive opening loads. The connection area was modeled using FD numerical method while the adjoining structural elements were modeled using the FE code DYNA3D.

The FD approach was advantageous for simple geometry but the FE approach has the advantageous when the boundary and loading conditions are complicated. In the FD approach, computing time and memory requirements are reduced since no stiffness and mass matrices need to be calculated. In the case of FE method, much time is required in the constant updating of the matrices is required in the inelastic domain. Non-linear material models are also developed for concrete and reinforcements. For the dynamic response, the FE code DYNA3D was used to calculate the stress and strains, due to impulsive loads, at the nodal points between the connection boundaries and this output is passed to the FD code to determine the displacement fields of the connections. The displacement field is then used to compute

strains and lastly, the material constitutive model is used to compute the stresses. For both time steps, the steel and concrete were checked for possible failures. Figure 2-11 shows the computational flow chart of the FD portion.

Experiments and Tests

Hii (2007) carried out tests on four beam-column sub assemblages to develop a better understanding of beam-column connections subjected to monotonic loads. Three of the specimens have higher column strength than the beam and connection's concrete strength, with two of them carrying different reinforcements within the connection and the last one did not have any additional reinforcements within the connection but had the same column and beam strength. Figure 2-12 shows the experimental setup.

All the specimens failed because of diagonal cracking within the connection. The addition of reinforcement in the joints increase the failure loads and caused the diagonal cracks to be more organized and delayed its formation. The specimen which had a higher concrete strength only had a slight higher failure load which indicates that the strength of the connection does not vary much for small increase in concrete strength. However, small increase in concrete strength may result in significant increase in shear strength.

Nilsson (1973) performed several tests on beam-column connections such as the one shown in Figure 2-13. The connections are laid onto the floor with the "T" lying on the ground on roller bearings to eliminate the effects of self weight in the test. A point load was applied at the tip of the column and the load-deflection history was observed.

Load-deflection curve of Test T16 is shown in Figure 2-14. The ultimate test moment of 2465kgfm is about 94% of that of the design moment of 2630kgfm.

Nilsson also performed tests on corner RC beam-column connections or knee-joints shown in Figure 2-15. The conditions for the tests are similar to those of the T-connections. Load-deflection of Test U25 is shown in Figure 2-16. The ultimate failure load is 3600kgf.

Another series of tests Nilsson did was on interior RC connections subjected to monotonic loads as shown in Figure 2-17. The testing conditions were similar to that of the previous 2 tests and the load-deflection curve of U69 is shown in Figure 2-18.

Moment-Rotation Resistance of Connections

Reinforced beam-column connections are loaded statically or dynamically to determine the moment-rotational resistance function that characterizes the behavior of the connection. FE modeling is one of the methods able to simulate the moment-rotational resistance to represent the behavior of the connection.

Mathematical expressions are also used to quantify the moment-rotational relationship in steel connections. The Power Model or the Richard-Abbot equation (Richard and Abbott, 1975) is commonly used to represent moment-rotational relationships of steel connections. Yim (2007) used the Power Model to describe the resistance function simulated in Abaqus reasonably well.

$$M = \frac{k_i \theta}{\left\{1+\left(\frac{\theta}{\theta_0}\right)^n\right\}^{\frac{1}{n}}} \tag{2-18}$$

where k_i is the initial connection stiffness, θ is the rotation, θ_0 is the plastic rotation, n is the shape factor and M is the moment.

Materials

Concrete Compressive and Tensile Strength

In general, concrete compressive strength is measured in reference to the uniaxial compressive strength obtained by the compression of concrete in a standard test cylinder. Composed of different materials, it is not a homogenous compound and thus has variations in its strength.

The modified Hognestad stress-strain curve (Figure 2-19) is commonly used to represent the stress-strain relationship for concrete with strengths up to 6000 psi. It consists of a quadratic function with a maximum stress of $f_c"$, where $f_c" = 0.9 f_c'$, at a strain of $1.8 f_c" / E_c$ and a straight line with a negative slope terminating at stress of $0.85 f_c"$ and strain of 0.0038. Elastic modulus E_c is given in ACI 318-08 as:

$$E_c = w_c^{1.5} 33 \sqrt{f_c'} \tag{2-19}$$

for concrete with density of $90 lb/ft^3 \le w_c \le 160 lb/ft^3$

$$E_c = 57000 \sqrt{f_c'} \tag{2-20}$$

for normal weighted concrete.

Although weak in tension, tensile stress in concrete is measured in terms of f_r, modulus of rupture through different tests (Table 2-5). ACI recommends that $f_r = 7.5 \sqrt{f_c'}$ normal weight concrete. This value is multiplied by 0.85 for “sand lightweight” concrete and 0.75 for “all lightweight” concrete.

Reinforcement

Concrete is strong in compression but weak in tension. In reinforced concrete structures, reinforcement is added to develop the tensile force within the structure while the compressive forces will be resisted by the concrete.

Hsu (1993) observed that reinforcement behave differently when they are embedded within the concrete. The stress-strain curve of a reinforcement (Figure 2-20) refers to the stress-strain at a particular location while the stress-strain curve for a reinforcement embedded in concrete refers to the average stress-strain value of a large length of bar over many cracks. Hsu proposed the following bi-linear average stress-strain properties for reinforcement embedded within concrete.

$$f_s = E_s.\varepsilon_s \text{ for } f_s \le f_y' \tag{2-21}$$

$$f_s = \left(1 - \frac{2 - \theta_c / 45°}{1000\rho}\right)\left[(0.91 - 2B) f_y + (0.02 + 0.25B) E_s \varepsilon_s\right] \text{ for } f_s \succ f_y' \tag{2-22}$$

$$f_y' = (1 - \frac{2 - \theta_c / 45°}{1000\rho})(0.93 - 2B) f_y \tag{2-23}$$

$$B = \frac{1}{\rho}\left(\frac{f_{cr}}{f_y}\right)^{1.5} \tag{2-24}$$

Finite Element Analysis

Finite element analysis (FEA) is commonly used nowadays to solve engineering analysis problems especially with the advances made in computers. In the field of civil engineering, FEA is commonly used to analyze a structure subjected to certain loadings. Bathe (1996) summarizes the procedure using FEA to solve a physical problem (Figure 2-21).

The initial step is to idealize the physical problem into a mathematical model. The mathematical model will be governed by numerous assumptions and differential equations. It must be noted that the solution obtained by FEA is characterized by the mathematical model defined, governed by the assumptions and differential equations.

> Even very accurate FEA may be at odds with physical reality if the mathematical model is inappropriate or inadequate. (Cooks, Malkus, Plesha and Witt, 2002).

It is almost compulsory to validate FEA by employing it in certain classic problems with known solution in whichever field that the FEA will be employed in. Only then, can the FEA be used with confidence to obtain valid results for the problem to be investigated.

In finite element, we are concerned with the numerical solution of field problems (Cooks et.al, 2002). The spatial displacement of an element within a body is given by:

$$\{u\} = [N]\{d\} \tag{2-25}$$

where $\{u\}$ is the displacement of the element, $[N]$ is the shape function, also known as interpolation function which approximates the displacement of a point based on the nodal displacements, $\{d\}$ is the nodal displacements.

$$\{\varepsilon\} = [B]\{d\} \tag{2-26}$$

where $\{\varepsilon\}$is the strain vector and $[B]$ is the strain displacement matrix.

From Hooke's Law, we can determine the constitutive relationship:

$$\{\sigma\} = [C]\{\varepsilon\} \tag{2-27}$$

where $[C]$ is the constitutive matrix

By applying the virtual work principle:

Internal work done = External work done

$$[k]\{D\} = \{f\} \tag{2-28}$$

where $[k]$ is the element stiffness matrix, $[k] = \int [B]^T [C][B] dv$, v is the volume of the element, $\{f\}$ is the external nodal load and $\{D\}$is the nodal displacement vector.

Verification and Validation

Verification and validation of FE codes is necessary before the FE code is used for analysis and simulation for any topics of interest. This is to impart greater confidence in the FE codes used and the results obtained. It is even more critical to determine the reliability and robustness for complicated or high-consequence systems that could not ever be physically tested (Oberkampf, Trucano and Tirsch, 2002).

The process of verification is (Figure 2-58) necessary to ensure that the accuracy of the solution to computational model with a known solution. It provides evidence that the computational solution corresponds to the conceptional model. It does not, however, attempt to relate the relationship of the conceptional model with the real world.

Validation (Figure 2-59) on the other hand attempts to assess the accuracy of the computational solution to the real world or experimental data. There is no reason to believe that the experimental data will be more accurate than the computational solution but only that the experimental data is the closest benchmarks for validation.

The FE Code Abaqus

Abaqus is a finite element analysis software that is able to accurately simulate the predictions of strength and deformations in structures in both linear and non-linear regime (Hibbitt, Karlsson & Sorensen, 2008). It has a wide range of capabilities for structural modeling with nonlinear implicit and explicit static and dynamic analysis capabilities. Abaqus/Explicit can model brief transient dynamic events well, such as

blast and impact problems while Abaqus/Standard is more suitable for static or quasi-static events.

Abacus/Explicit uses an explicit integration method for the analysis while Abaqus/Standard uses an implicit integration method. Explicit integration method satisfies the equation of motion of a structure at current time t_i, and extrapolates to determine the solution at time t_{i+1}. Because it extrapolates instead of satisfying the equation at time t_{i+1}, the time steps need to be small enough to minimize the error due to the extrapolation. Since the time step used is already small, it is useful for brief transient event such as blast and impact problem. The equation of motion at the i^{th} step is:

$$\left\{F^{ext}(t)\right\}_i = [M]\left\{\ddot{u}\right\}_i + [C]\left\{\dot{u}\right\}_i + \left\{F^{\text{int}}(t)\right\} \tag{2-29}$$

For the implicit integration method in Abaqus Standard, the equation of motion is satisfied at time t_{i+1}. A full matrix inversion is required to determine the solution and the time step used can be larger.

$$\{F(t)\}_{i+1} = [M]\left\{\ddot{u}\right\}_{i+1} + [C]\left\{\dot{u}\right\}_{i+1} + [K]\{u\}_{i+1} \tag{2-30}$$

The disadvantage of implicit integration is that matrix inversion is required to find the solution at each time step and this is computationally expensive as compared to explicit integration. Another advantage of explicit integration is that it is able to handle non-linearity better while implicit integration might have problems converging to a solution.

In a study by Yim (2007) on steel moment connections for structures under blast and collapse loading rates, Abaqus/Standard was used to determine the resistance functions of the steel connectors while Abacus/Explicit is used to develop the three-dimensional finite model (Yim, 2007).

Abaqus Explicit was used by Tran (2009) to validate the effect of short duration-high impulse variable axial and transverse loads on reinforced concrete columns.

Concrete damaged plasticity model

Abaqus has three concrete material models available for modeling plain or reinforced concrete. They are concrete smeared cracking model, cracking model for concrete and concrete damaged plasticity model (CDP). All three models can be used for plain concrete, even though they used primarily for reinforced concrete. However, Concrete smeared cracking model can only be used in Abaqus/Standard while cracking model for concrete can only be used in Abaqus/Explicit. CDP was chosen as the material model of choice for concrete as it can be used in both Abaqus/Standard and Abaqus/Explicit.

CDP is suitable for use in which the structure is subjected to monotonic, cyclic and/or dynamic loading under low confining pressures. The concrete behavior is modeled by the theory of isotropic damaged elasticity combined with isotropic compressive and tensile plasticity. The two main failure mechanisms are the compressive failure and the tensile cracking of the concrete.

Tension stiffening of the cracked concrete is a required input in Abaqus and this effect simulates the interaction between the reinforcement and the concrete. Tension stiffening can either be defined in Abaqus as a postfailure stress-strain curve or by

applying a fracture energy criterion in terms of postfailure stress and cracking displacement.

The unloading portion of the stress-strain curve is characterized by two damage variables, d_t and d_c. These two damage variables govern the slope of the unloading curve. They can range from zero (no damage) to one, a total loss of strength.

Tension stiffening or the unloading portion of the tensile behavior of the concrete is defined by its post failure stress and cracking strain, $\tilde{\varepsilon}_t^{ck}$. The cracking strain is equal to the total strain minus the elastic strain of the post-failure stress.

$$\tilde{\varepsilon}_t^{ck} = \varepsilon_t - \tilde{\varepsilon}_{0t}^{el} \quad \text{where} \quad \tilde{\varepsilon}_{0t}^{el} = \sigma_t / E_0 \tag{2-31}$$

Abaqus will convert the cracking strain to plastic strain, $\tilde{\varepsilon}_t^{pl}$, using the relationship:

$$\tilde{\varepsilon}_t^{pl} = \tilde{\varepsilon}_t^{ck} - \frac{d_t}{(1-d_t)} \frac{\sigma_t}{E_0} \tag{2-32}$$

In CDP, the effects between the reinforcement and concrete interface such as dowel action and bond slip can be modeled by introducing “tension stiffening” (Hibbitt, Karlsson and Sorensen, 2008) to simulate the transfer of load over the cracks along the reinforcement. Abaqus suggest that a good estimate of the strain softening is to reduce the failure stress over a ultimate failure strain of 10 times the initial failure strain. Too little tension stiffening might probably cause local failure of the concrete due to cracking and cause unstable behavior in the concrete affecting the response of the entire model. Generally, increasing the tension stiffening makes it easier to obtain numerical solutions.

Compressive behavior or the unloading portion of the compressive stress-strain curve is defined by its post-failure stress and inelastic (crushing) strain, $\tilde{\varepsilon}_c^{in}$. The inelastic strain is equal to the total strain minus the elastic strain of the post-failure stress.

$$\tilde{\varepsilon}_c^{in} = \varepsilon_t - \tilde{\varepsilon}_{0c}^{el} \text{ where } \tilde{\varepsilon}_{0c}^{el} = \sigma_c / E_0 \quad (2\text{-}33)$$

Abaqus will convert the inelastic strain to plastic strain, $\tilde{\varepsilon}_c^{pl}$, using the relationship:

$$\tilde{\varepsilon}_c^{pl} = \tilde{\varepsilon}_c^{ck} - \frac{d_c}{(1-d_{c)}} \frac{\sigma_c}{E_0} \quad (2\text{-}34)$$

Defining parameters of CDP

φ is the dilation angle in the p-q plane under high confining pressure (Jankowiak and Lodygowski, 2005). Laboratory tests were performed by Jankowiak and Lodygowski to identify the materials for the concrete damage plasticity model. The material parameters are obtained from the analysis of the three-point bending single-edge notched concrete beam specimen and the four-point bending single-edge notched concrete beam under static loadings.

Nielsen (1998) showed the friction angle of concrete against the strength of the concrete and correlated the friction angle of concrete, ϕ, with the dilation angle of concrete, $\sin(\phi) = \tan(\varphi)$. However, Mirmiran, Zagers and Yuan (2000) indicate that dilation angle established the flow rule in the plasticity of concrete. If the dilation angle is equal to the internal friction angle of concrete, plastic straining will occur perpendicular to the yield surface with some volumetric expansion. If the dilation angle is less than the internal angle of friction, less volumetric expansion developed and there will be no

volumetric expansion if dilation angle is zero. It was found that a dilation angle of zero could be used to predict the response of concrete columns wrapped with fiber reinforced concrete polymer.

$fb0/fc0$ is the ratio of the unibiaxial compressive strength to the initial uniaxial strength and the default in Abaqus is 1.16.

ε is the eccentricity of the plastic potential surface and the default value in Abaqus is 0.1.

K is the ratio of the second stress invariant on the tensile meridian to that of the compressive meridian (Hibbitt, Karlsson and Sorenson, 2008). The default value in Abaqus is 0.667.

Viscosity parameter, μ, is used to describe the visco-plastic regularization of the constitutive law for concrete. The default values in Abaqus/Standard is 0.0 but this parameter is ignored in Abaqus Explicit.

Classical metal plasticity

Isotropic hardening found under Classical Metal Plasticity material models in Abaqus (Hibbitt, Karlsson & Sorensen, 2008) may be used to describe the behavior of reinforcement. It uses Mises yield surfaces associated with plastic flow and can be combine with linear elastic material model. In this model, the elasticity is required to define the recoverable portion of the strain. This is the gradient of the stress-strain curve exhibiting linear elastic behavior. Most metals exhibit ductile behavior where the yield strain is orders of magnitudes smaller than the elastic modulus of the material. As such, material data definition in Abaqus is in terms of “true” stress or Cauchy stress and logarithmic plastic strain. Nominal stress-strain data can be converted to true stress and

logarithmic plastic strain by the following equations. In Abaqus, the first set of data must be the “true” initial yield stress corresponding to the plastic strain, which will be equal to zero.

$$\sigma_{true} = \sigma_{nom}(1+\varepsilon_{nom}) = \frac{P}{A_c} \tag{2-35}$$

$$\sigma_{nom} = \frac{P}{A_0} \tag{2-36}$$

$$\sigma_{true} = \sigma_{nom}\frac{A_0}{A_c} \tag{2-37}$$

$$\varepsilon_{\ln}^{pl} = \ln(1+\varepsilon_{nom}) - \frac{\sigma_{true}}{E} \tag{2-38}$$

where E is the Young’s modulus and P is the load onto the metal.

Elements

Linear 8-nodes continuum elements, C3D8R (Figure 2-26), with reduced integration and hourglass control were used to model the concrete. Linear 2-nodes beam elements, B31 (Figure 2-27), are used to model the reinforcement and embedded elements technique is used to embed the reinforcement into the concrete.

In the embedded element technique, the host will be the solid concrete elements while the reinforcement will be the embedded elements. In Abaqus, the nodes of the embedded elements will lose its translational degrees of freedom in the sense that they are constrained to the translational degrees of freedom of the host elements. However, the embedded elements are allowed to retain their rotational degrees of freedoms which are not constrained. The number of rotational degrees of freedom allowed in a node of an embedded element is identical to the number of translational degrees of freedom of the host element. In a three-dimensional model with beam elements in solid elements,

since each node at the solid element have three degrees of translational freedom, each beam elements are able to have three rotational degrees of freedom at each node. For the reinforcement, it will retain its own translational degrees of freedom while taking on the interpolated values of the translational degrees of freedom of the host elements.

January and Krauthammer (2003) found that beam elements are more suitable than truss elements for modeling of the reinforcement because the former exhibit shear and bending behavior while the latter only resist axial forces. The study determined that the shear and bending behavior of the beam elements is necessary when refined meshes are used to obtain convergence of results to test data.

Connector elements

Connector elements are able to connect or join two different parts in Abaqus (Hibbitt, Karlsson & Sorensen, 2008) with discrete geometry but having complex kinetic and kinematic relationships. These elements can have relative displacements and rotations local to the elements and are defined by individual attributes. Most single connector elements are able to describe a connection but connectors can also be used in parallel to describe complicated connection. Connectors available in Abaqus include:

1. Basic translational connectors with available translational degree of freedom at both nodes. The rotational degrees of the first of both nodes might also be available.
2. Basic rotational connectors with available rotational degree of freedom at both nodes.
3. Specialized rotational connectors with available degree of freedoms and also other degree of freedom at the nodes.
4. Assembled connectors which is a combination of the predefined basic translational and rotational connectors or translational and specialized rotational connectors.
5. Complex connectors with specialized degree of freedom at the nodes which cannot be defined by any individual connectors.

Progressive Collapse

During the lifetime of a structure, it might be exposed to abnormal loading that was not designed for and this might result in the local failure of one or more structural elements. As a result, the loading path changes and this might create extreme stress on other structural elements not designed for this sudden increment in load.

> Progressive collapse occurs when a structure has its loading pattern, or boundary conditions, changed such that structural elements are loaded beyond their capacity and fail. (Krauthammer, 2008)

This catastrophic collapse results in destruction of buildings and loss of lives. In a RC structure, it is just as important to understand the behavior of the beam-column connections in addition to the main structural elements such as beams and columns in progressive collapse.

Under UFC 4-010-01, it is compulsory for all buildings more than three stories, new and existing, to be designed for progressive collapse. Under UFC-4-023-03 (2009), the level of design (Table 2-3) for structures against progressive collapse is based on the Occupancy Category (OC) of the structure (Table 2-4).

For tie forces, the abnormal load will be transferred from the damage portion of the building to the undamaged portion. In the Alternate Path method, the abnormal load must be able to “bridged” over the damage area. Finally, in Enhanced Local Resistance, the shear and flexural capacity of the walls and columns are increased to provide stronger resistance and reduced the probability and extend of initial damage.

The GSA guidelines (2005) state that all new buildings must be designed to withstand the loss of column one level above grade at the building perimeter without progressive collapse. This is to ensure adequate load paths redistribution due to a local damage. In the case of the loss of an internal column, the designer has to show that

load redistribution to alternate path is possible. Or the designer can simply ignore progressive collapse calculation by protecting the column such that the column would not have a chance to be damaged critically. The analysis can be performed either statically or dynamically. The following vertical load would have to be applied to the structure for static analysis:

$$\text{Load} = 2\,(DL + 0.25LL) \tag{2-39}$$

where DL is dead load and LL is live load.

Hayes Jr et al. (2005) suggested that seismic upgrading of the Murrah Federal building will improve the resistance to both blast loads and progressive collapse. Increasing the member sizes and the addition of transverse and longitudinal reinforcements increases the flexural and shear strength of the structure, counteracts the abnormal loadings and increase the structure resistance to the blast loads and progressive collapse.

Detailed modeling of the entire RC structure against blast loadings for progressive collapse using Abacus/Explicit will be computationally expensive and time-consuming because of the large amount of elements in the detail model. Yim (2007) used Abaqus/Explicit to develop a simplified building frame model (Figure 2-66) consisting of beam elements instead of beams and columns, and connector element for connection components, while ensuring acceptable accuracy to the detailed model. The connector element mechanical properties are the resistance function of the steel moment connections derived earlier by Abaqus/Standard.

Figure 2-29 shows an elevation view of the RC structure which is scheduled for progressive collapse test by the removal of a column at the first storey. The structure

made up entirely of RC columns, beams and slabs will be attached to very strong steel reaction frame. More details of the RC structure will be shown in the later chapters.

Summary

Different types of RC beam-column connections respond differently to loadings depending on their geometry and detailing of the reinforcements. Different models and theories on the behavior of the concrete connections have also lead to the emphasis on different characteristics and parameters of the connections during analysis which is in turn used for the design and detailing of the connections. Due to the lack of understanding of the RC beam-column connection, many researchers have used experimental and numerical modes in an attempt to better understand and explain connections' behavior. Finally, progressive collapse of a structure is introduced through the study of the effects of a structure's response to an abnormal load or the sudden removal of a structural element.

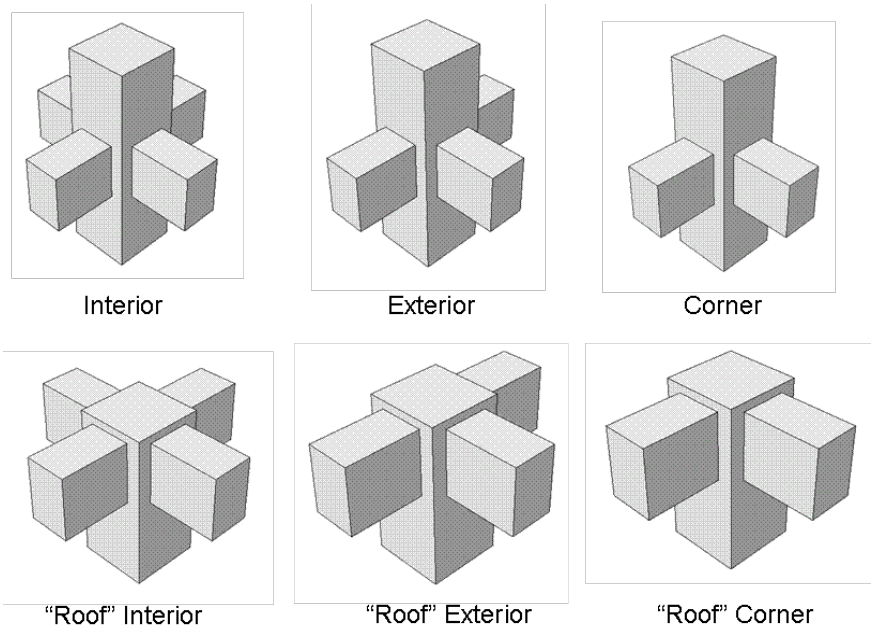

Figure 2-1. RC beam-column connections [Adapted from ACI 352R-02. 2002. ACI 352R-02. (Page 352R-2, Figure 1.1).]

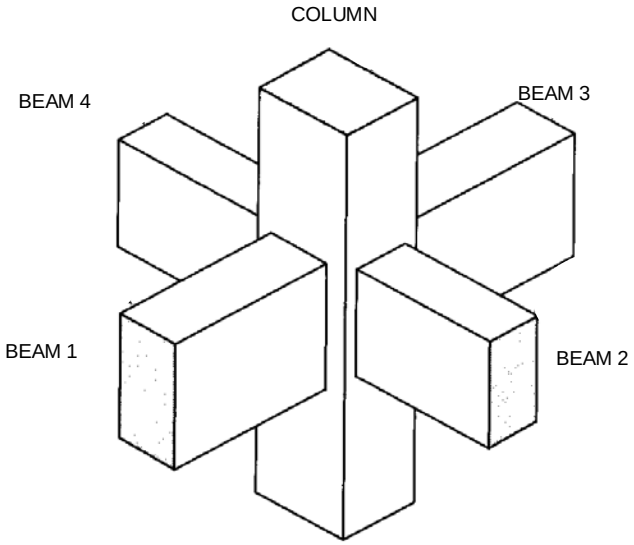

Figure 2-2. Typical monolithic interior beam-column connection [Adapted from Nilson, Darwin and Dolan. 2004. Design of concrete structures. (Page 349, Figure 11.2).]

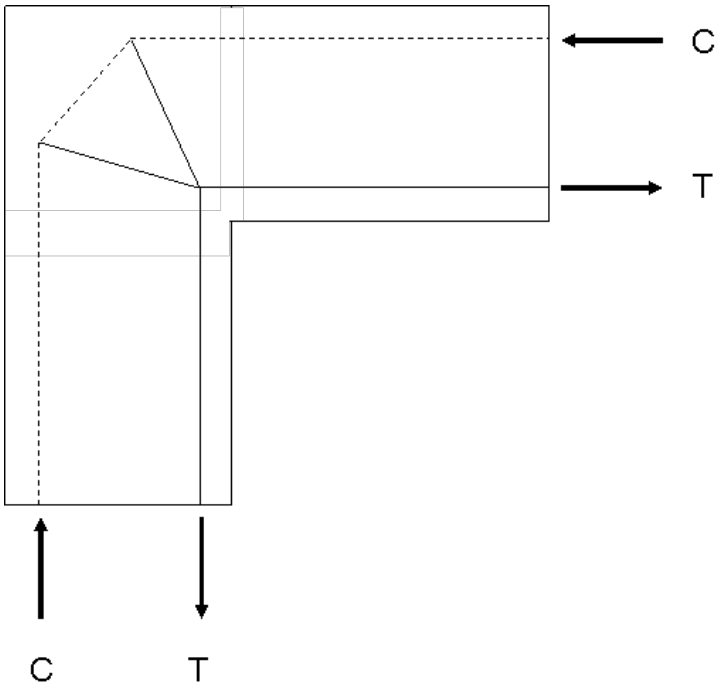

Figure 2-3. Knee-connection subjected to opening loads [Adapted from MacGregor and Wight. 2005. Reinforced concrete mechanics and design. (Page 916, Figure 18-45).]

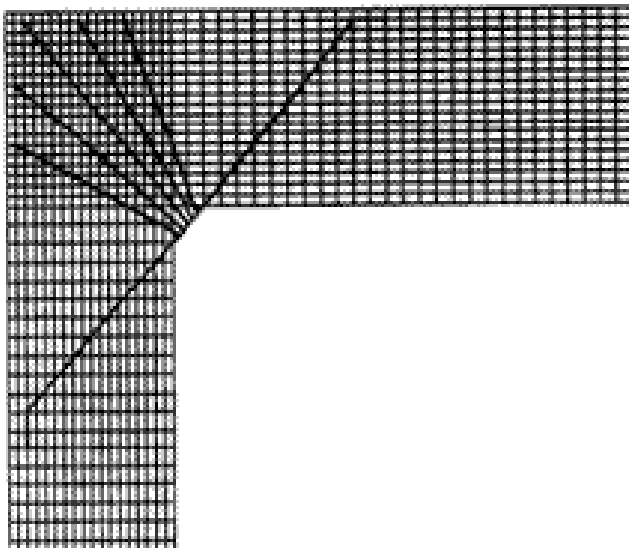

Figure 2-4. Diagonal and radial bars configuration [Reprinted with permission from Krauthammer and Ku. 1996. A hybrid computational approach for the analysis of blast resistant connections. (Page 841, Figure 11).]

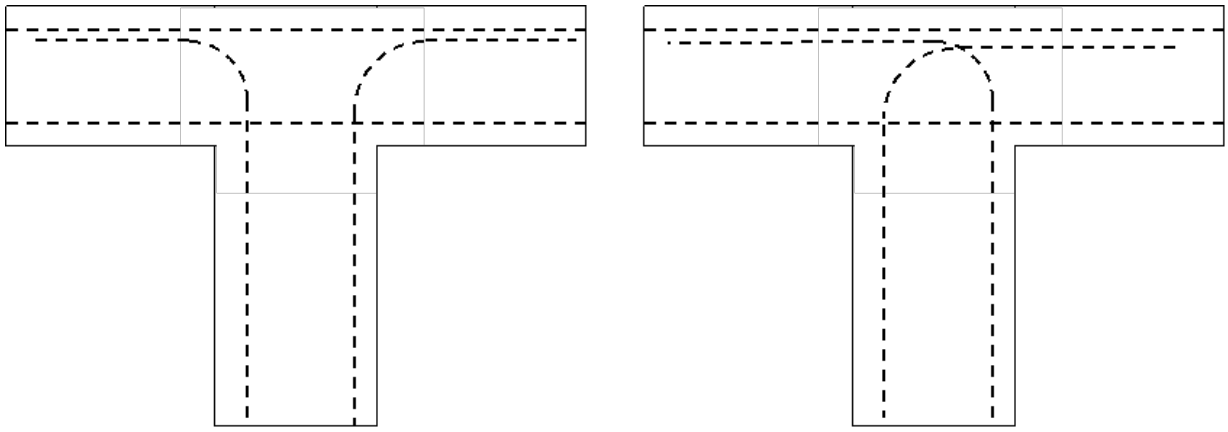

Figure 2-5. Typical three-member connection details [Adapted from Nilson, Darwin and Dolan. 2004. Design of concrete structures (Page 368, Figure 11.21).]

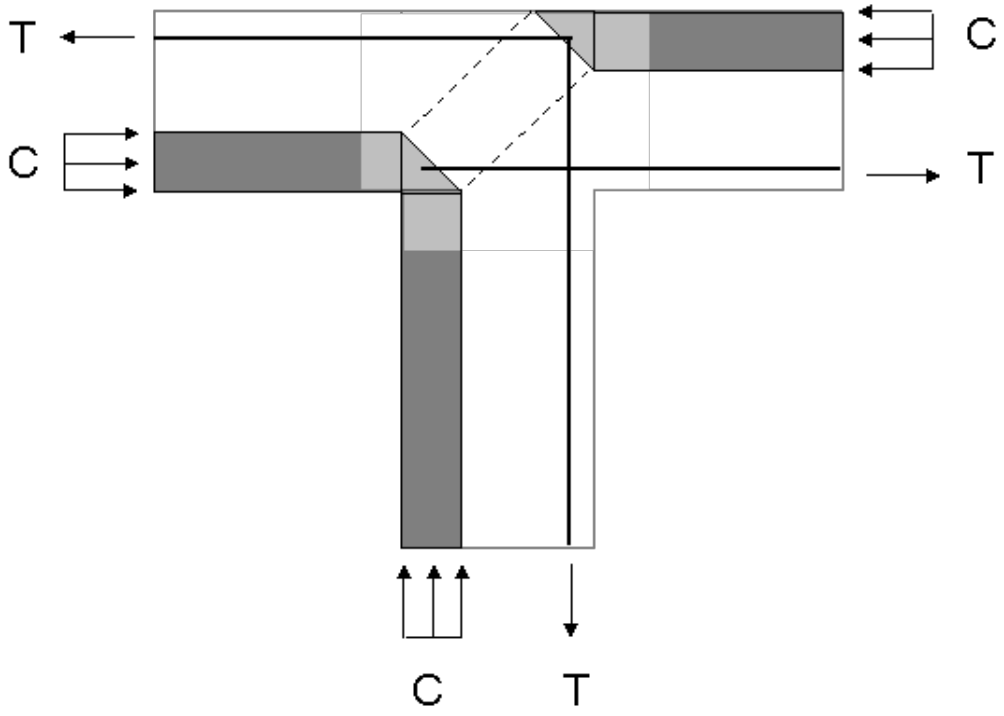

Figure 2-6. Strut-and-tie model [Adapted from Nilson, Darwin and Dolan. 2004. Design of concrete structures (Page 368, Figure 11.22).]

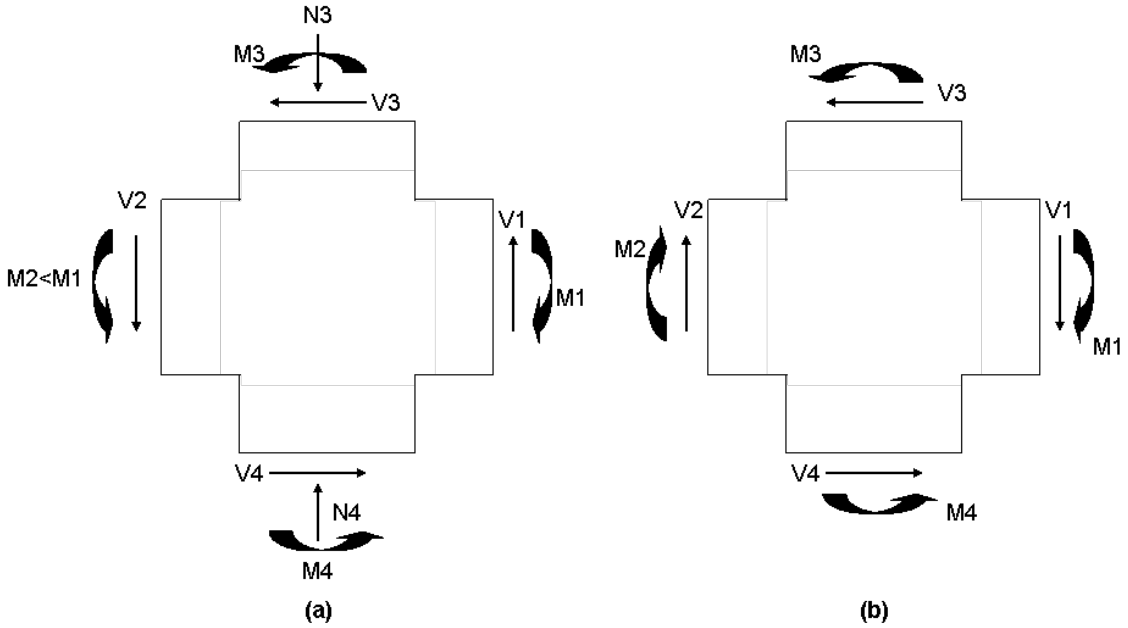

Figure 2-7. Joint loads and forces on an interior connection due to (a) gravity loads and (b) lateral loads [Adapted from Nilson, Darwin and Dolan. 2004. Design of concrete structures (Page 350, Figure 11.3 & 11.4).]

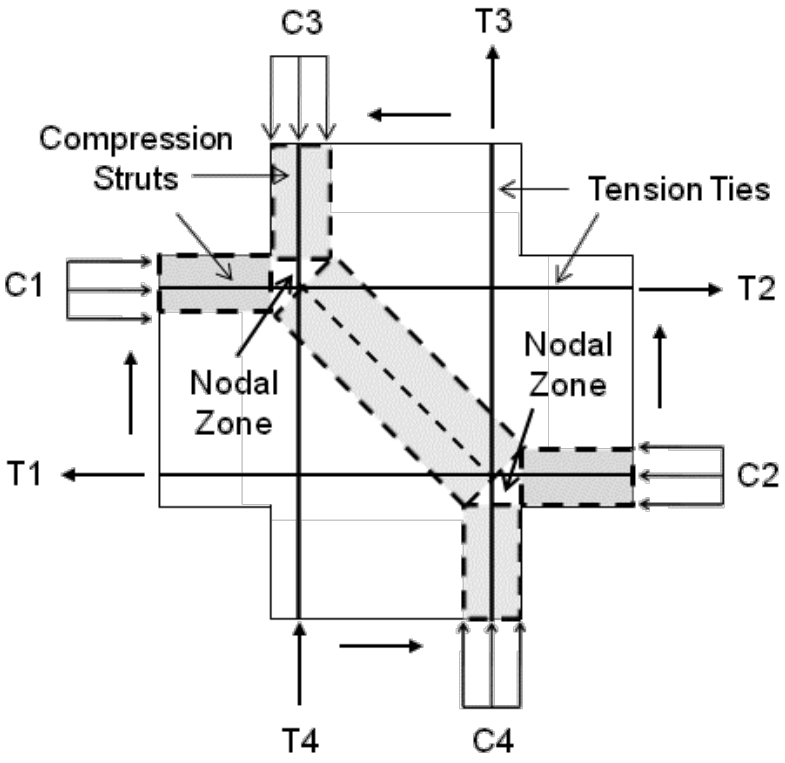

Figure 2-8. Strut-and-tie model [Adapted from Nilson, Darwin and Dolan. 2004. Design of concrete structures (Page 361, Figure 11.12).]

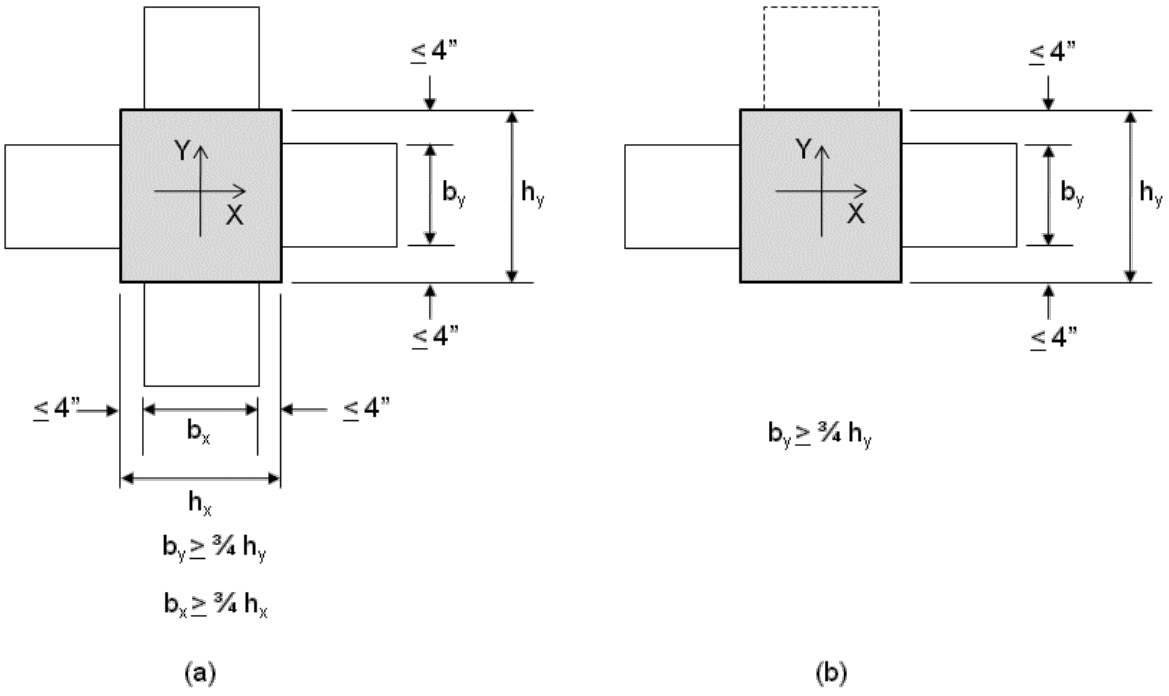

Figure 2-9. Confinement within connections [Adapted from Nilson, Darwin and Dolan. 2004. Design of concrete structures (Page 353, Figure 11.7).]

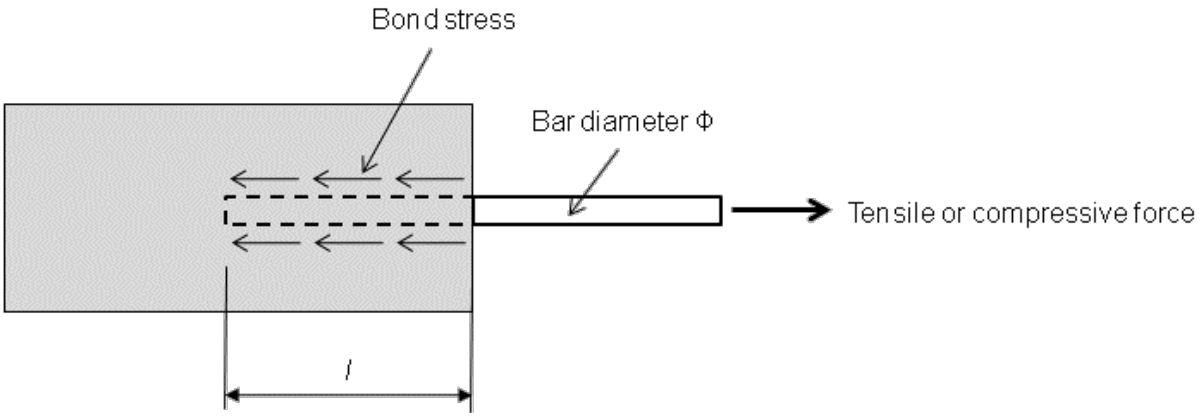

Figure 2-10. Development of reinforcement [Adapted from Holmes and Martin. 1983. Analysis and design of structural connections: Reinforced concrete and steel. (Page 63, Figure 2.30).]

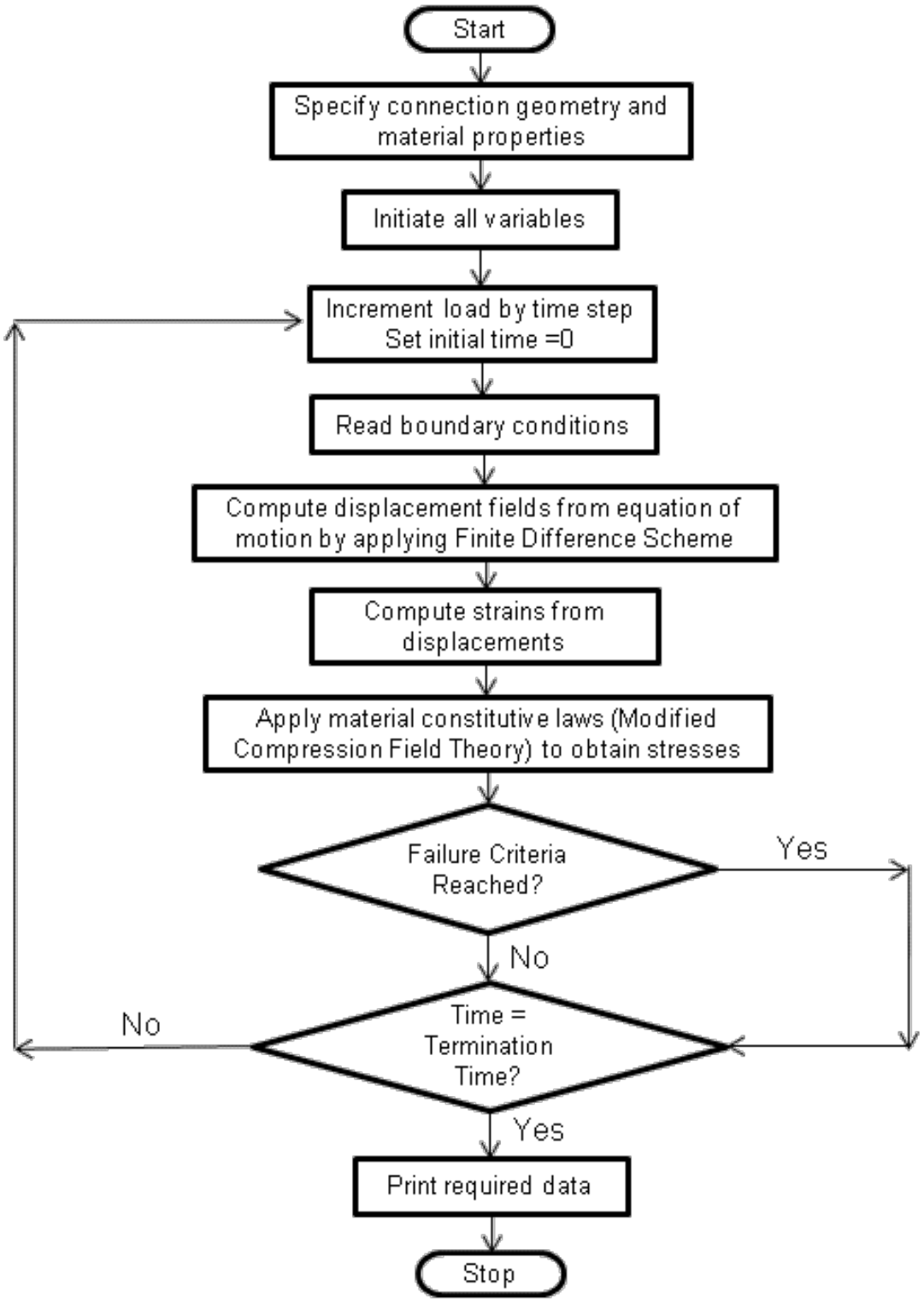

Figure 2-11. Computation flow chart from finite difference scheme. [Adapted from Krauthammer and Ku. 1996. A hybrid computational approach for the analysis of blast resistant connection. (Page 836, Figure 4)]

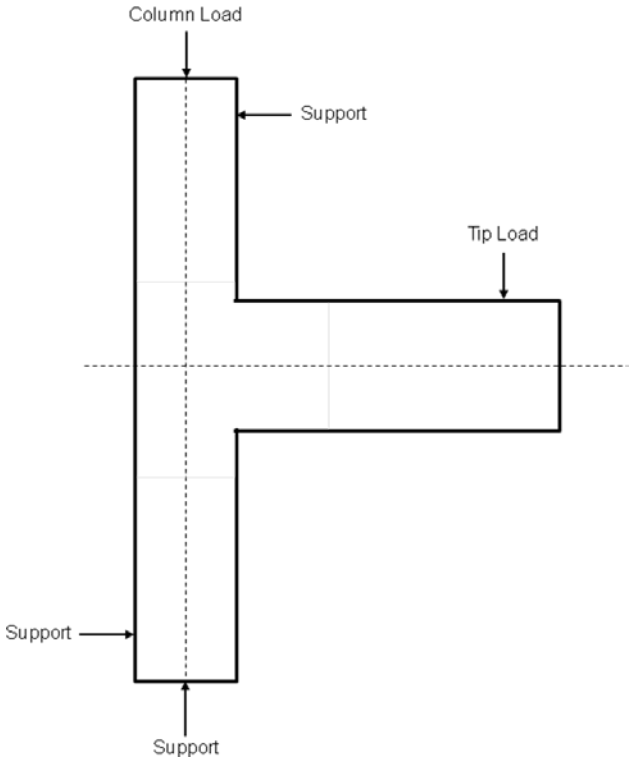

Figure 2-12. Experimental setup [Adapted from Hii. 2007. Influence of concrete strength on the behavior of external RC beam-column joint. (Page 41, Figure 3.7)]

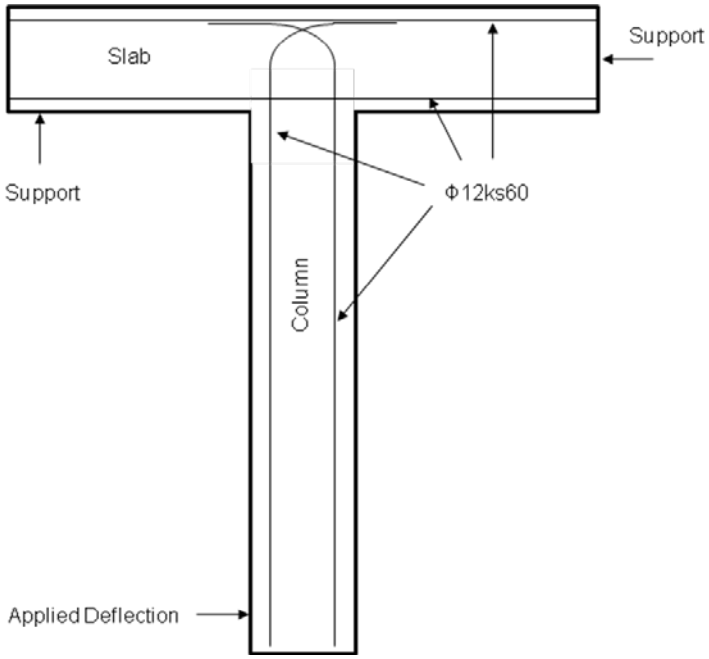

Figure 2-13. T-section testing [Adapted from Nilsson. 1973. Reinforced concrete corners and joints subjected to bending moment. (Page 166, Figure 9.6)]

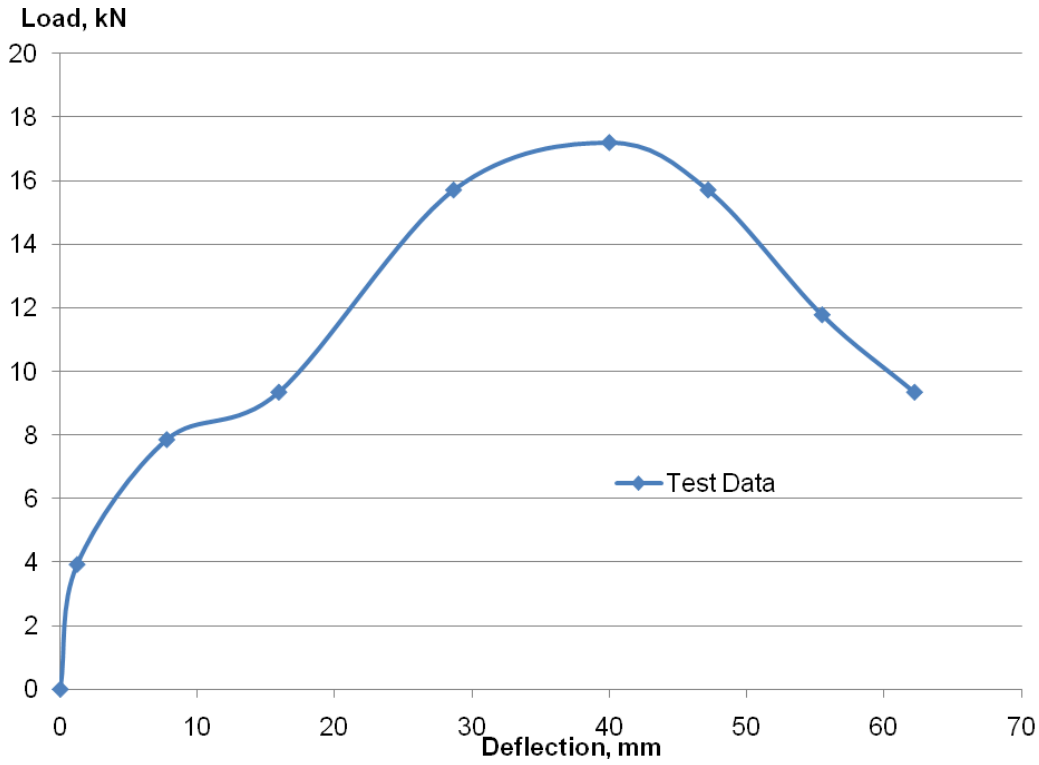

Figure 2-14. T16 Load deflection curve. [Adapted from Nilsson. 1973. Reinforced concrete corners and joints subjected to bending moment. (Page 170, Figure 9.13)]

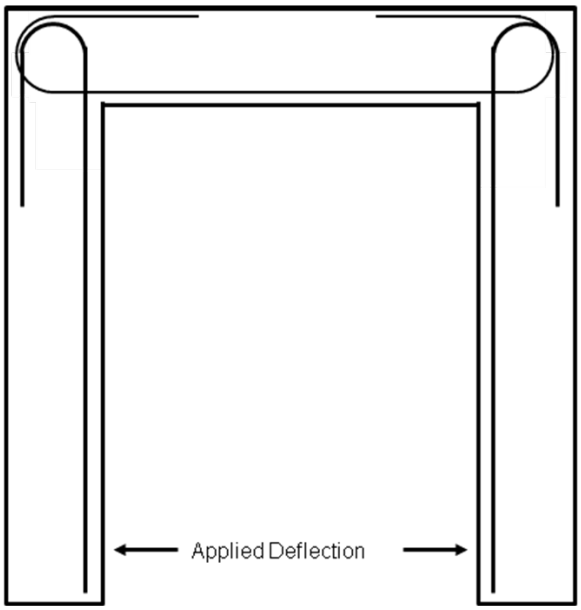

Figure 2-15. Corner section testing [Adapted from Nilsson. 1973. Reinforced concrete corners and joints subjected to bending moment. (Page 209)]

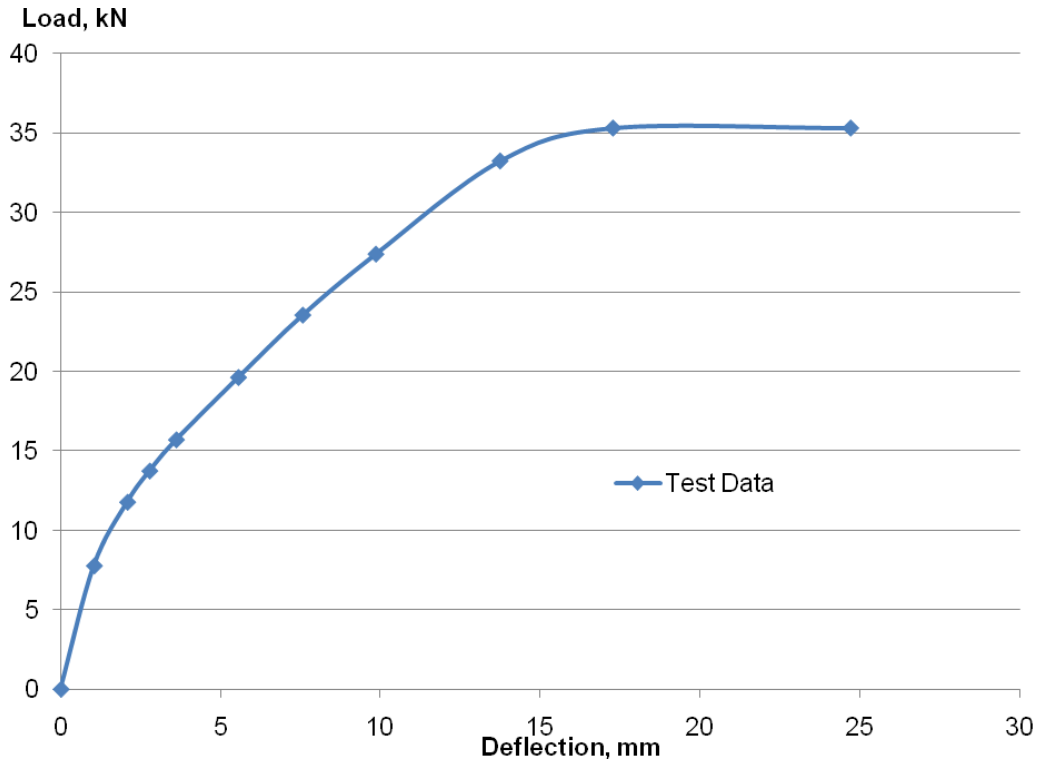

Figure 2-16. Load deflection curve for U25 [Adapted from Nilsson. 1973. Reinforced concrete corners and joints subjected to bending moment. (Page 225, Figure A.5)]

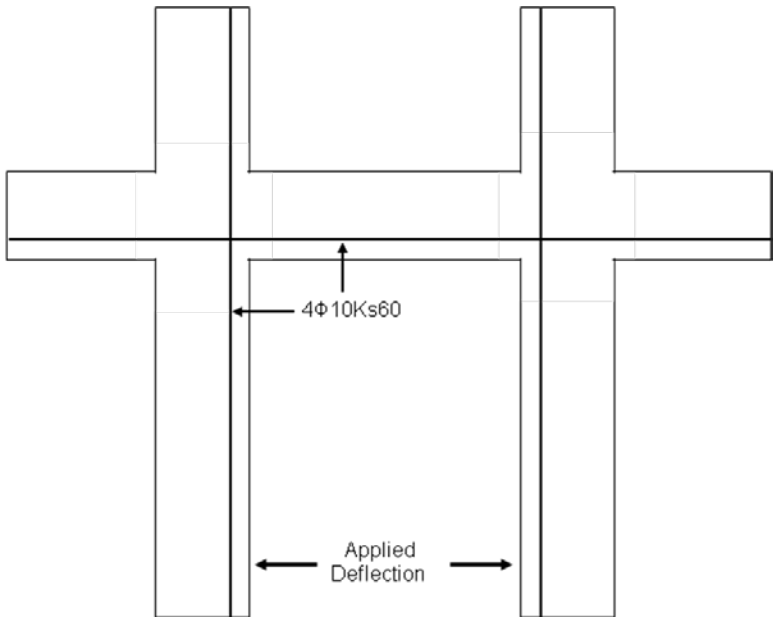

Figure 2-17. Interior connection testing. [Adapted from Nilsson. 1973. Reinforced concrete corners and joints subjected to bending moment. (Page 186, Figure 9.34)]

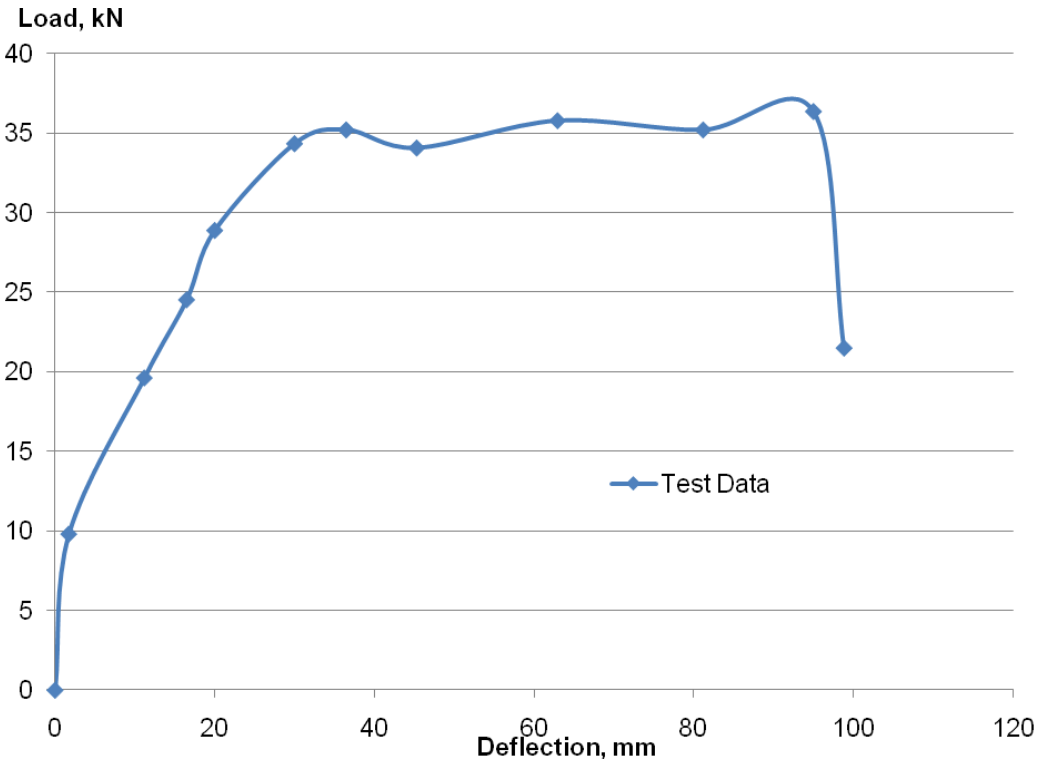

Figure 2-18. Interior connection load deflection curve for U69 [Adapted from Nilsson. 1973. Reinforced concrete corners and joints subjected to bending moment. (Page 186, Figure 9.35)]

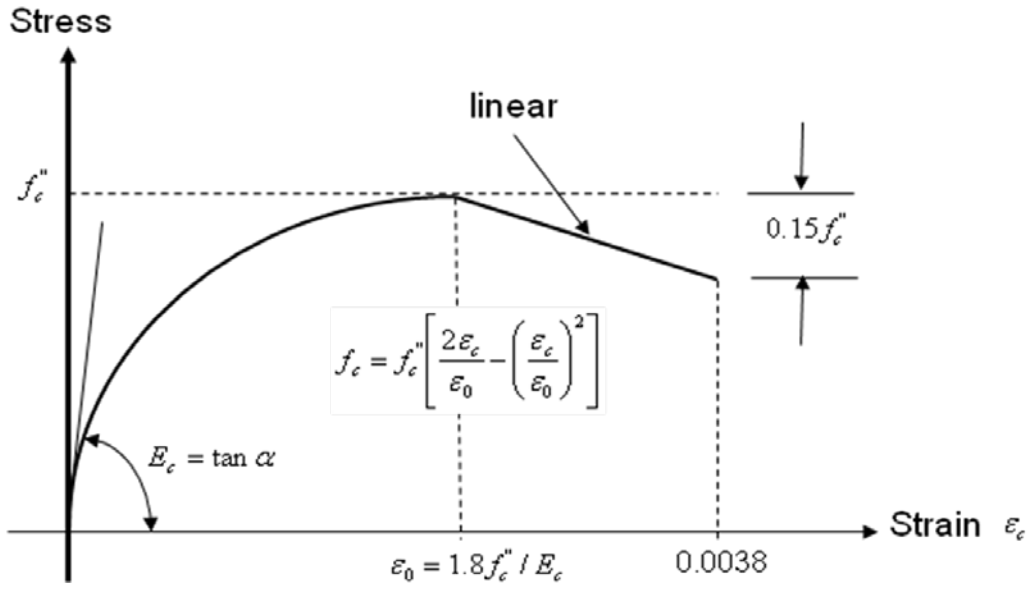

Figure 2-19. Modified Hognestad curve. [Adapted from MacGregor and Wight. 2005. Reinforced concrete mechanics and design. (Page 71, Figure 3-19(a))]

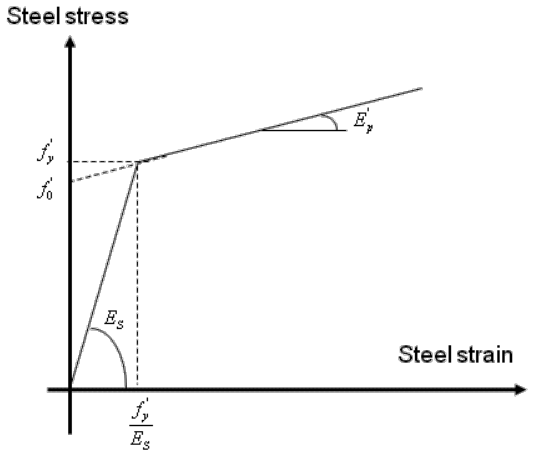

Figure 2-20. Stress-strain curve of reinforcement using bilinear model. [Adapted from Hsu. 1993. Unified theory of reinforced concrete. (Page 206, Figure 7.8)]

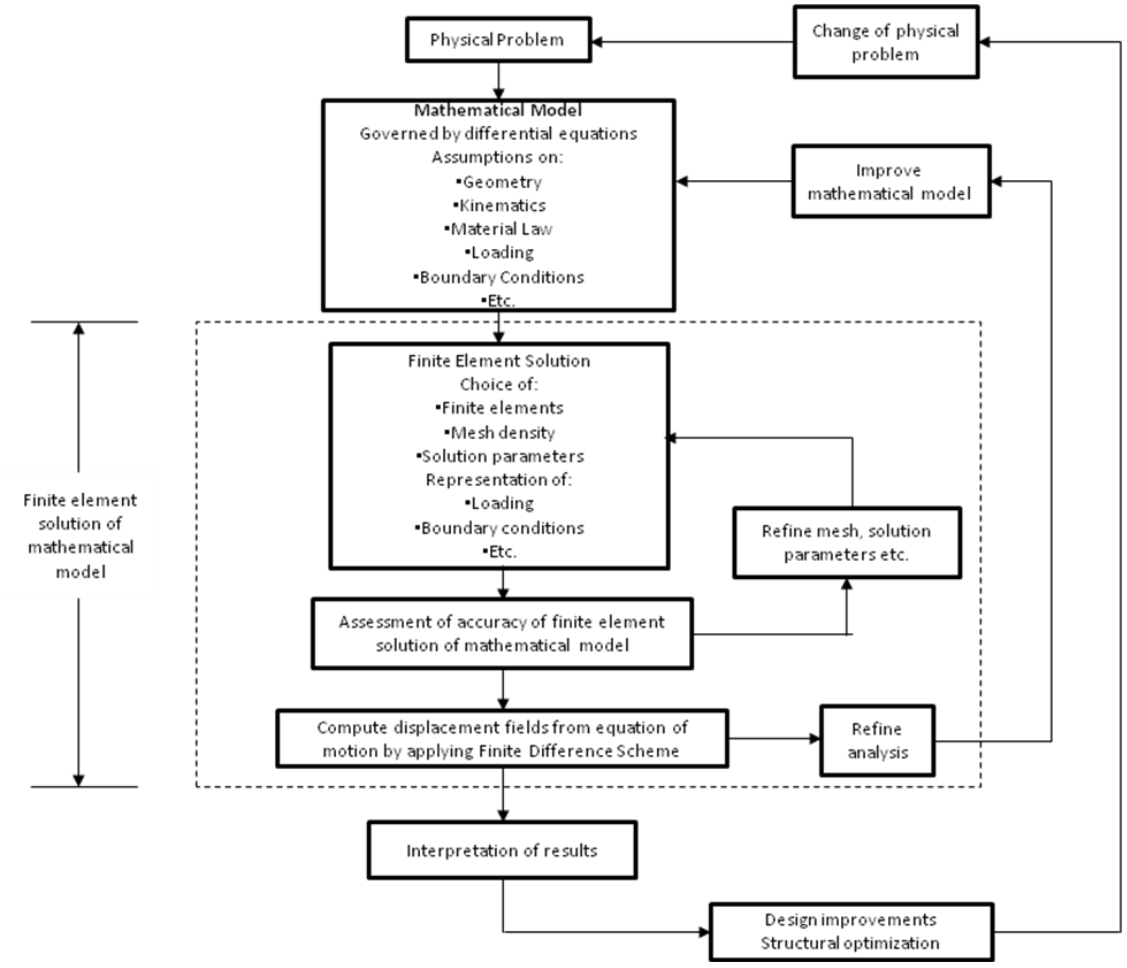

Figure 2-21. Process of finite element analysis. [Adapted from Bathe. 1996. Finite element procedures. (Page 3, Figure 1.1)]

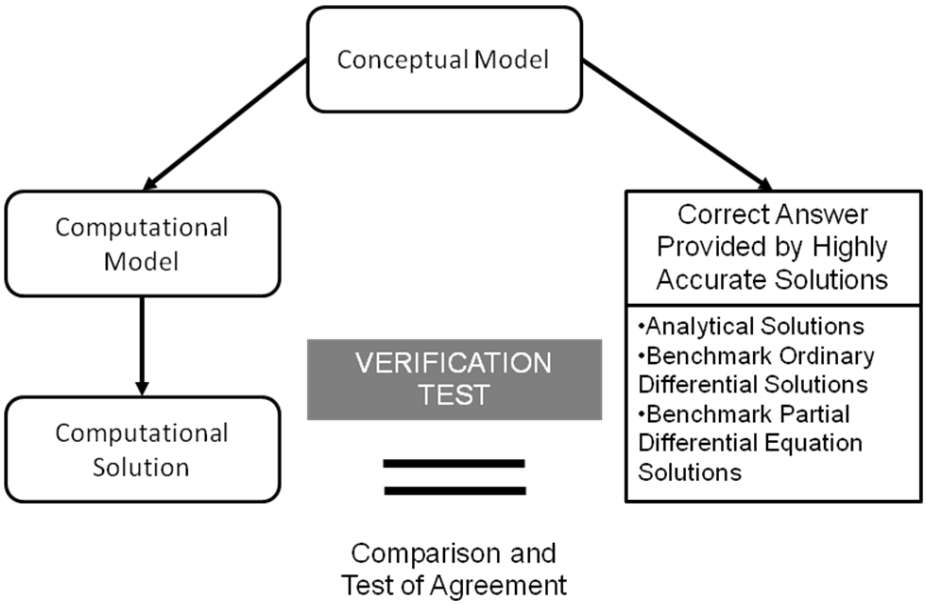

Figure 2-22. Verification process. [Adapted from Oberkampf, Trucano and Tirsch. 2002. Verification, validation, and predictive capability in computational engineering and physics. (Page 10, Figure 2)]

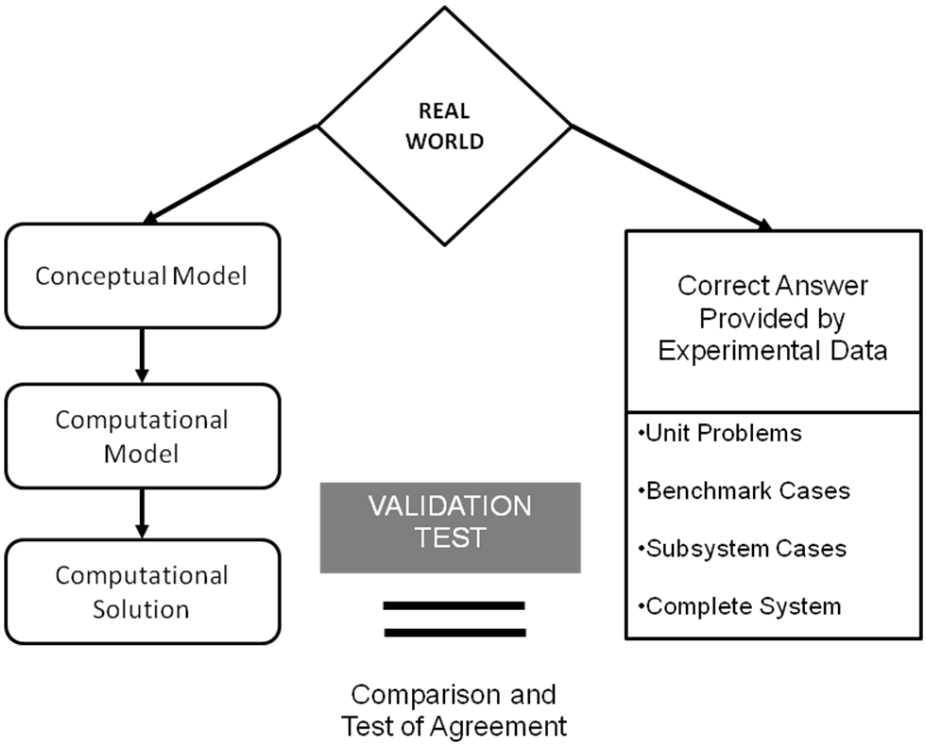

Figure 2-23. Validation process. [Adapted from Oberkampf, Trucano and Tirsch. 2002. Verification, validation, and predictive capability in computational engineering and physics. (Page 11, Figure 3)]

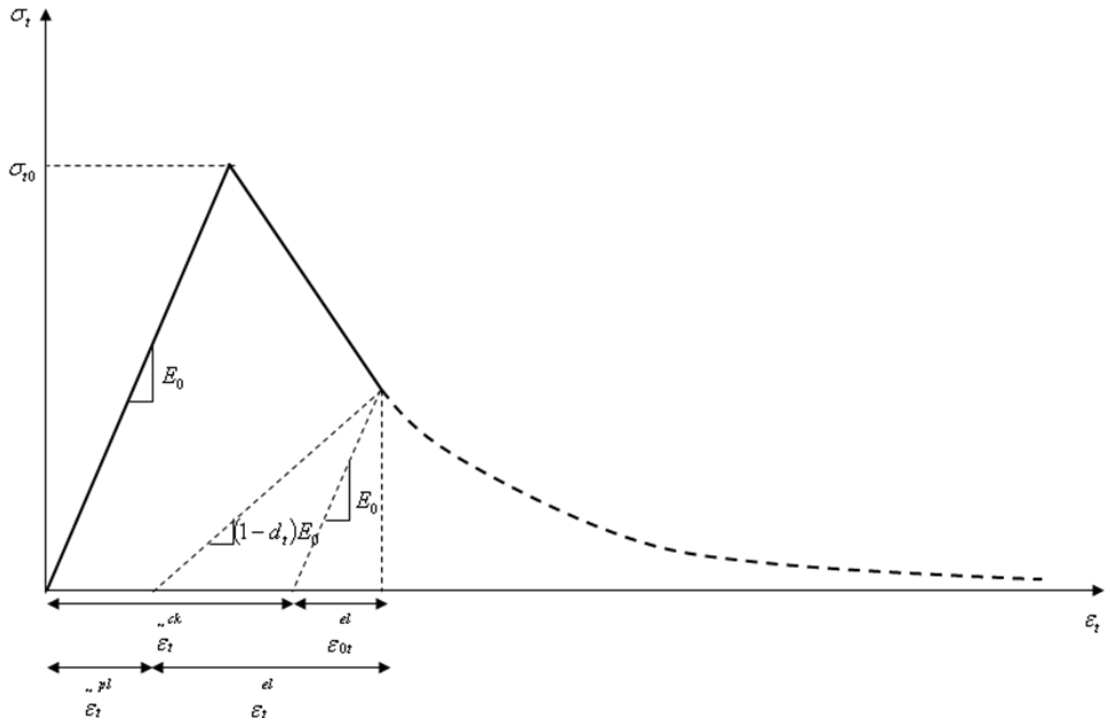

Figure 2-24. Tensile stress-strain curve of CDP. [Adapted from Hibbitt, Karlsson and Sorenson. 2008. Abaqus 6.8 Analysis User's Manual. (Figure 19.6.3-3)]

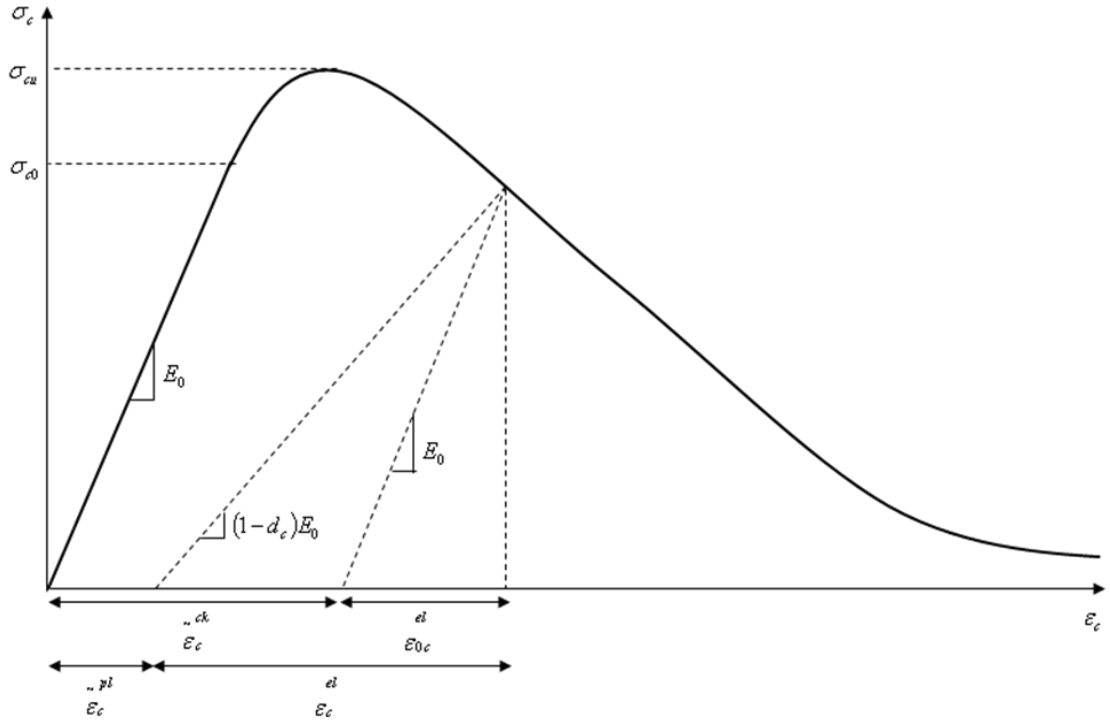

Figure 2-25. Compressive stress-strain curve of CDP. [Adapted from Hibbitt, Karlsson and Sorenson. 2008. Abaqus 6.8 Analysis User's Manual. (Figure 19.6.3-6)]

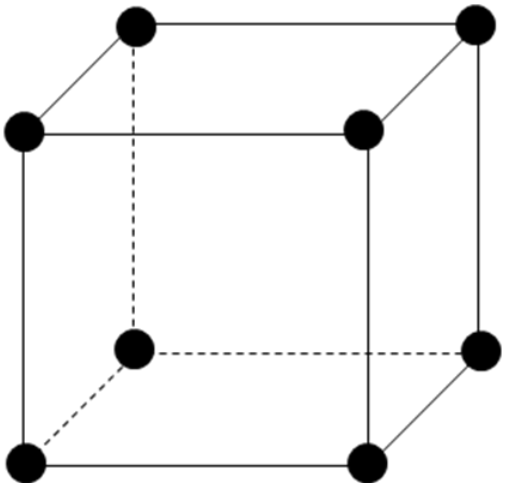

Figure 2-26. C3D8R continuum elements. [Adapted from Hibbitt, Karlsson and Sorenson. 2008. Abaqus 6.8 Analysis User's Manual. (Figure 22.1.1-2)]

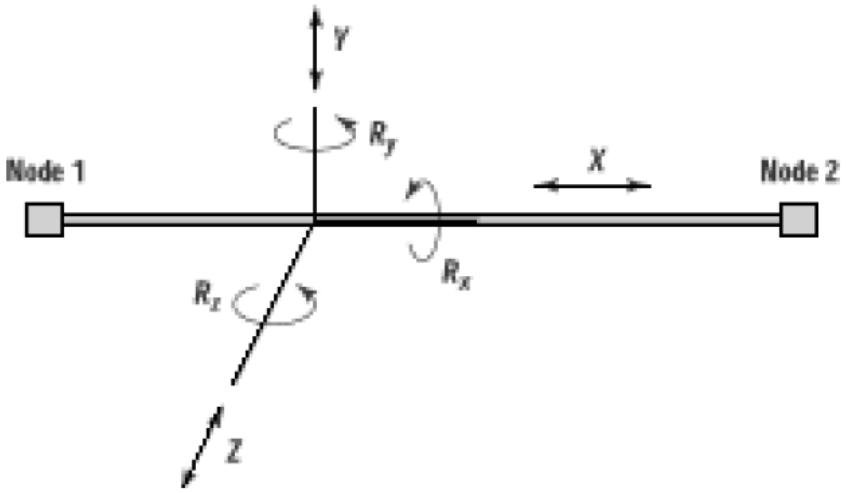

Figure 2-27. Beam elements. [Reprinted with permission from Yim. 2007. A study of steel moment connections for structures under blast and progressive collapse loading rates. Ph.D. dissertation. (Page 33, Figure 2-18). The Pennsylvania State University, Pennsylvania]

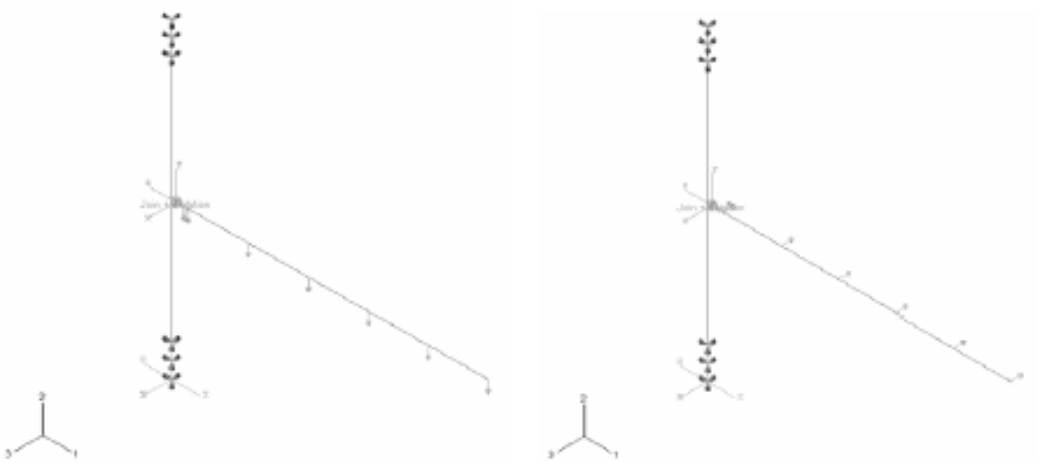

(a) Vertical Loading (b) Horizontal Loading

Figure 2-28. Simplified frame model [Reprinted with permission from Yim. 2007. A study of steel moment connections for structures under blast and progressive collapse loading rates. Ph.D. dissertation. (Page 68, Figure 4-13). The Pennsylvania State University, Pennsylvania]

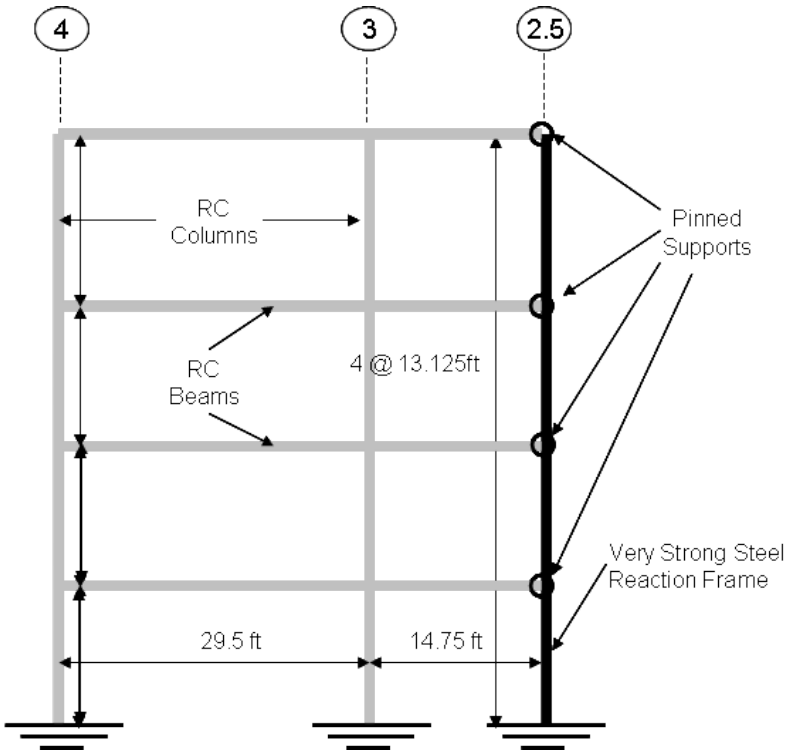

Figure 2-29. Elevation view of RC structure to be subjected to progressive collapse test

Table 2-1. γ values for beam-column connections [Adapted from ACI 352R-02. 2002. (Page 352R-9, Table 1).]

	Classification	Connection Type 1	2
A.	Joints with a continuous column		
A.1	Joints effectively confined on all four vertical faces	24	20
A.2	Joints effectively confined on three vertical faces or on two opposite vertical faces	20	15
A.3	Other faces	15	12
B.	Joints with a discontinuous column		
B.1	Joints effectively confined on all four vertical faces	20	15
B.2	Joints effectively confined on three vertical faces or on two opposite vertical faces	15	12
B.3	Other faces	12	8

Table 2-2. Tensile strength of concrete (Nilson, Darwin and Dolan, 2005)

	Normal Weight Concrete, psi	Lightweight Concrete, psi
Direct tensile strength f_t'	3 to $5\sqrt{f_c'}$	2 to $3\sqrt{f_c'}$
Split cylinder strength f_{ct}'	6 to $8\sqrt{f_c'}$	4 to $6\sqrt{f_c'}$
Modulus of rupture f_r	8 to $12\sqrt{f_c'}$	6 to $8\sqrt{f_c'}$

Table 2-3. Occupancy categories. [Adapted from Unified Facilities Criteria. 2009. Design of buildings to resist progressive collapse. (Page 16, Table 2-1)]

Nature of Occupancy	Occupancy Category
• Buildings in Occupancy Category I in Table 1 of UFC 3-310-01 • Low Occupancy Buildings [A]	I
• Buildings in Occupancy Category II in Table 1 of UFC 3-310-01 • Inhabited buildings with less than 50 personnel, primary gathering buildings, billeting and high occupancy family housing [A,B]	II
• Buildings in Occupancy Category III in Table 1 of UFC 3-310-01	III
• Buildings in Occupancy Category IV in Table 1 of UFC 3-310-01 • Buildings in Occupancy Category V in Table 1 of UFC 3-310-01	IV

[A] As defined by UFC 4-010-01 Minimum Antiterrorism Standards for Buildings

[B] Occupancy Category II is the minimum occupancy category for these buildings, as their population or function may require designation as Occupancy Catergory III, IV or V.

Table 2-4. Occupancy categories and design requirements [Adapted from Unified Facilities Criteria. 2009. Design of buildings to resist progressive collapse. (Page 17, Table 2-2)]

Occupancy Category	Design Requirements
I	No specific requirements
II	Option 1: Tie Forces for the entire structure and Enhanced Local Resistance for the corner and penultimate columns or walls at the first story. OR Option 2: Alternate Path for specified column and wall removal locations.
III	Alternate Path for specified column and wall removal locations; Enhanced Local Resistance for all perimeter first story columns or walls.
IV	Tie Forces: Alternate Path for specified column and wall removal locations; Enhanced Local Resistance for all perimeter first and second story columns or walls.

CHAPTER 3
RESEARCH APPROACH

Introduction

The focus of this study is to use a predominantly continuum typed FE model to simulate an RC beam-column connection and extract a simple mechanical model which can be used along structural typed elements for faster progressive collapse analysis to be used in comprehensive progressive collapse assessment from the analysis.

Before using the FE code to model the actual RC beam-column connection, it is critical to ensure that the FE code is being verified and validated to have confidence in its usage and the computational solution.

Verification of Abaqus is required to provide evidence that the FE code executes correctly the mathematical algorithms. In the Verification Manual for Abaqus (Hibbitt, Karlsson & Sorensen, 2008), there are extensive verification tests for elements, materials and other options in the code. These verification tests are usually done on problems with well known solutions. It does not, however, attempt to relate the relationship of the conceptional model with the real world. Several examples of Abaqus verification will be provided in Chapter 4.

For validation, Abaqus/Explicit (Hibbitt, Karlsson & Sorensen, 2008) will be validated against a RC beam exposed to a dynamic-load by Feldman and Seiss (1956). This is to validate the dynamic behavior of Abaqus/Explicit for reinforced concrete elements against dynamic loadings. Abaqus/Standard (Hibbitt, Karlsson & Sorensen, 2008) against three RC beam-column connections exposed to monotonic loadings by Nilsson (1973). These three connections are chosen because they are the most representative beam-column connections in a RC structure, namely a corner

connection, T-connection and interior connection (Figure 3-1). Although we are only focusing on the interior connection in this study, the validation of the corner-connection and T-connection facilitates the future study of progressive collapse for the entire RC structure.

Once the FE code has being verified and validated, Abaqus/Standard can be used to extract the mechanical model (resistance function) for the RC beam-column connection. Connector elements, with the properties of the mechanical model, will be used together with structural typed elements to replace the predominantly continuum based FE model. The approach will be covered in this chapter in more details.

Characterization of RC Beam-Column Connection

The interior RC beam-column connection together with the attached beams and columns will be modeled and subjected to monotonic load. This is to ensure that the true representation of the actual experiment is being replicated in the FE analysis. The detailed model of the RC beam-column connection (modeled as an interior-joint), up to d distance from the column face, is being modeled as fine mesh of continuum elements for the concrete and beam elements for the reinforcement while coarse mesh of continuum elements are used to represent the RC beams and columns further than d distance away (Figure 3-2). This will enable us to capture in details the behavior of the RC beam-column connection, which is the main focus of the study. Although using coarse continuum elements to model the RC beams and columns might not be very accurate, it will not affect our study as we only need the elements to transfer the force and moments throughout the RC beams and columns to obtain the resistance function of the connection. The main objective is to obtain the moment-rotation resistance function of the RC beam-column connection. Modeling of a detailed continuum FE

model of the entire assemblage is not recommended because it is complicated, computationally expensive and time consuming.

Rotation at connections. The global rotation of the connection can be easily found using the deflection at the tip of the beam and the length of the beam as shown in Figure 3-3. Rotation, θ, is simply $\tan^{-1}\frac{d}{L}$. This, however, does not represent the rotation at the plastic hinge as it does not take into account of the length of the plastic hinge formed.

As such, Figure 3-4 shows a more accurate depiction of the behavior of the connection considering the formation of a plastic hinge. The rotation at the connection can be found considering the plastic hinge and the vertical and horizontal displacement of the points on the plastic hinge shown in Figure 3-5 (Yim, 2007). The rotation will be the average of the calculations taken at the top, middle and bottom of the beam. The rotation, θ will be:

$$\tan\theta = \frac{v_2 - v_1}{u_2 - u_1 + L} \tag{3-1}$$

where L = l_p, plastic hinge length

Simplified FE Model

After obtaining the moment-rotation of the connection from a predominantly continuum based FE model, connector elements will be used to represent the resistance function and beam elements to represent the RC beams and columns to form a simplified structural based FE model (Figure 3-6). Both models must be equivalent and they will be tested by subjecting them to the same loading and boundary conditions. The RC beams and columns of the structural based FE model (Figure 3-6)

will be modeled as beam elements while the beam-column connection will be represented by connector elements, JOIN and CARDAN.

Connector JOIN is a translational basic connector and it freezes the position of two nodes. The Cartesian coordinates of node b relative to node a will always be fixed, regardless of whether the two nodes are located at the same position.

Connector CARDAN is a basic rotational basic connector which provides a rotational connection and relationship between 2 nodes defined by Cardan angles. The three available degree of freedoms are the relative Cardan angles of node b relative to node a and the kinetic moment in a Cardan connection is directly proportional to the relative Cardan angles.

A combination of these two basic translational and rotational connectors will be able to describe the behavior of the moment-rotation relationship at the beam-column connection. The connector JOIN links the RC beam to the RC column while CARDAN allows us to describe the behavior of the RC beam-column connection by a moment-rotation resistance function found earlier.

Power Model (Richard and Abbott, 1975) will be used to see if it is a good fit to the moment-rotational resistance function obtained from the simulation.

The simplified structural based FE model can be tested against progressive collapse by the sudden removal of a column using Abaqus/Explicit. However, this will not be in the scope of this study.

Summary

The above describes the characterization of the resistance function for RC interior beam-column connection from a predominantly based continuum FE model to be incorporated in a simplified predominantly structural based FE model for faster

progressive collapse assessment. The flowchart (Figure 3-9) below describes clearly the research approach discussed.

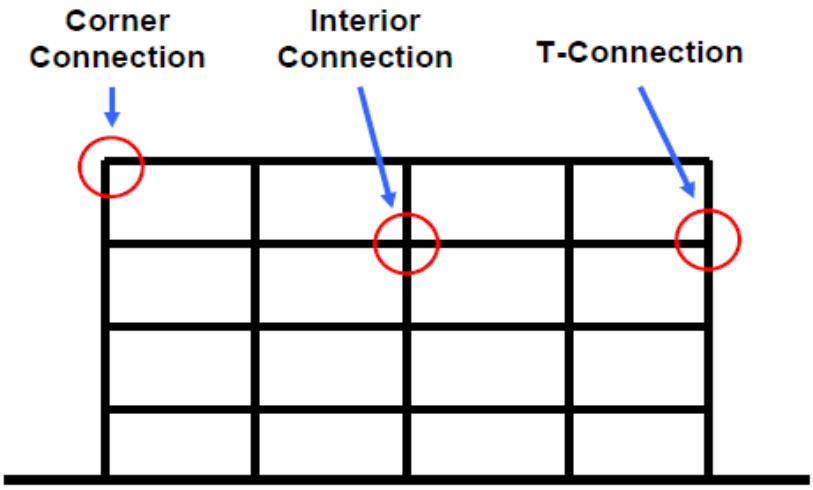

Figure 3-1. Beam-column connections of a RC structure

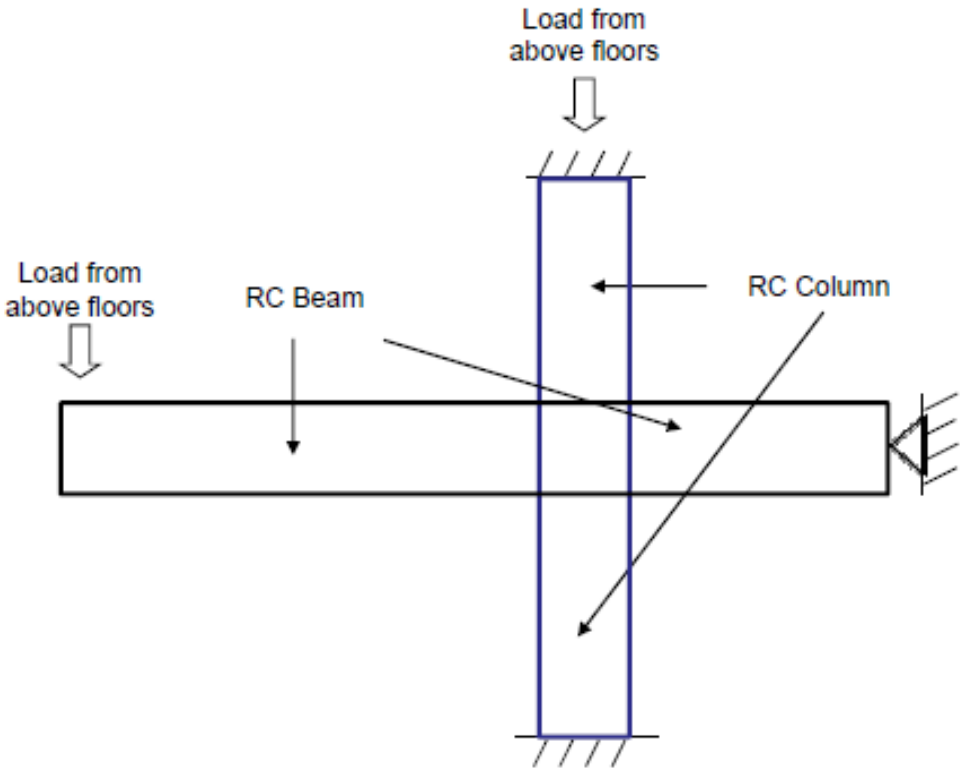

Figure 3-2. Free-body diagram of Abaqus model

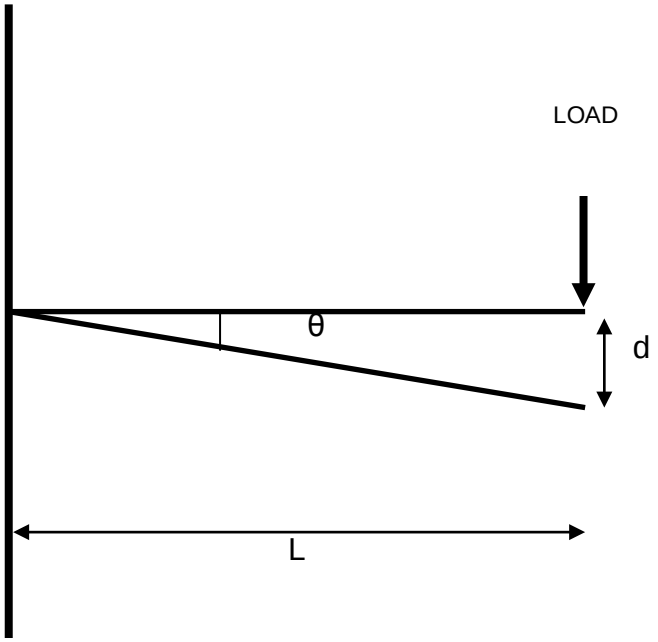

Figure 3-3. Global rotation

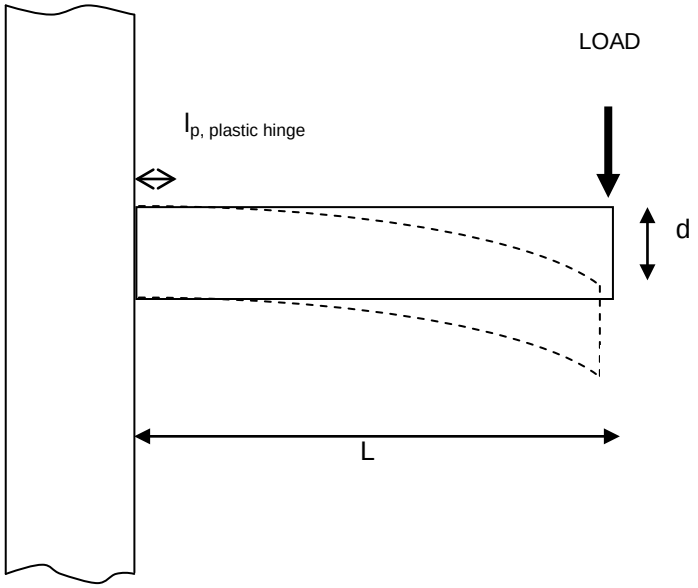

Figure 3-4. Formation of plastic hinge

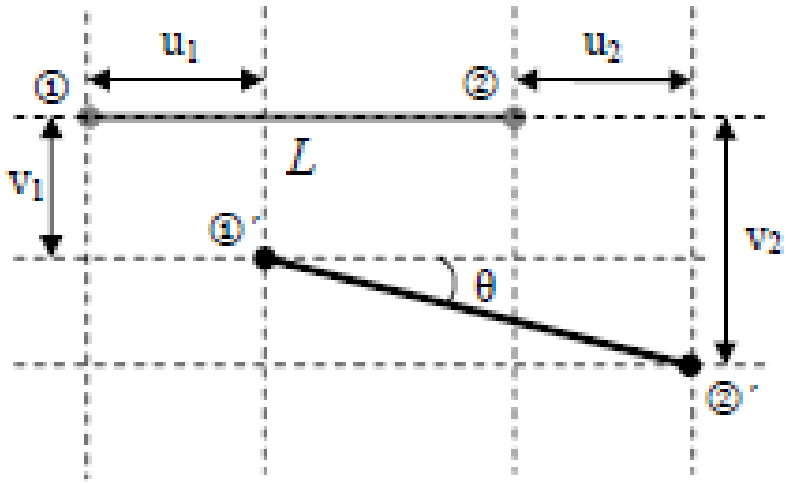

Figure 3-5. Rotation points. [Reprinted with permission from Yim. 2007. A study of steel moment connections for structures under blast and progressive collapse loading rates. Ph.D. dissertation. (Page 41, Figure 3-1(c)) The Pennsylvania State University, Pennsylvania]

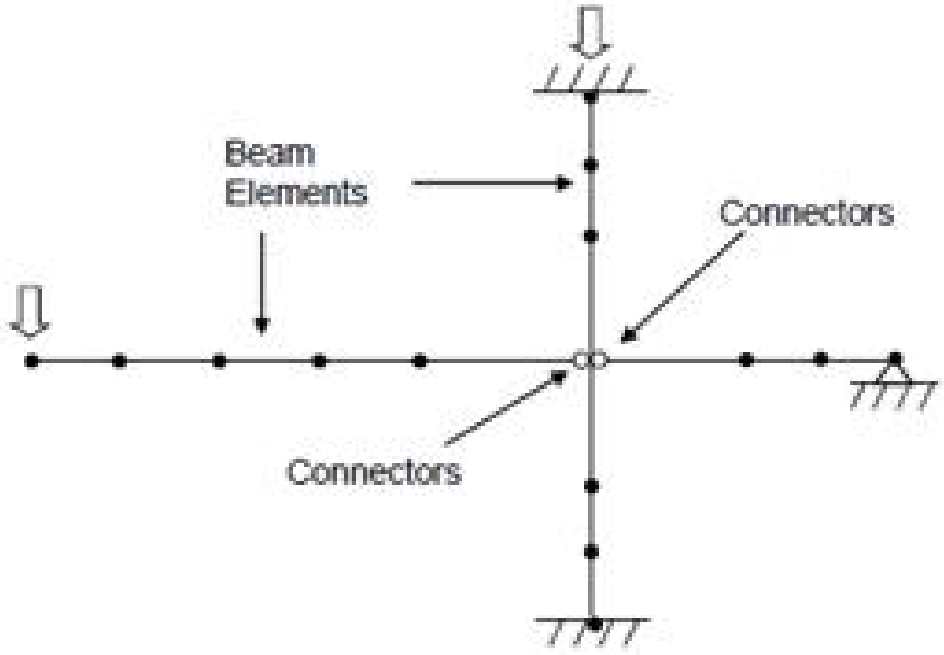

Figure 3-6. Simplified structural based FE model

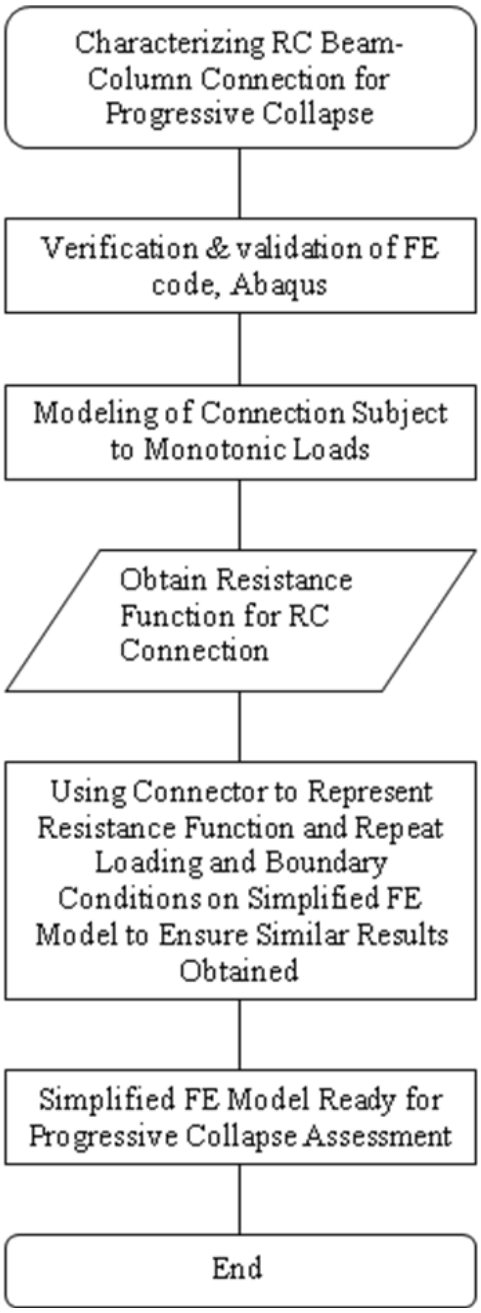

Figure 3-7. Flowchart of research approach

CHAPTER 4
RESULTS AND DISCUSSIONS

Introduction

Firstly, the verification and validation of Abaqus will be described in this chapter. Following this, a brief description of the RC structure containing the beam-column connection will be given. The validated FE code, Abaqus/Standard, will be used to extract the resistance function of the RC beam-column connection by subjecting it to a monotonic load. A connector will be used to replace the resistance function of the RC beam-column connection and beam elements will be used to model the RC beams and columns in a simplified structural based FE model. This simplified structural based FE model is subjected to the same monotonic load and boundary conditions to verify that the same moment-rotation relationship will be obtained as the predominantly continuum based FE model. Finally, the simplified structural based FE model will be ready to be subjected to progressive collapse assessment.

Verification and Validation

Verification of Abaqus

Verification of Abaqus is necessary to have confidence that it can be used to describe reinforced concrete elements and structures. The focus of this study will not be on the verification as the main objective is to characterize the resistance function of a RC beam-column connection. As such, the verification done and reported in Abaqus Verification Manual Version 6.8 (Hibbitt, Karlsson & Sorensen, 2008) will be highlighted.

CDP is verified in Abaqus/Standard and Abaqus/Explicit using continuum elements for inelastic behavior of concrete based upon the theory of isotropic damaged

elasticity of concrete which depends on the isotropic compressive and tensile plasticity behavior.

The CARDAN connector element is verified by testing in Abaqus/Standard and Abaqus/Explicit for elastic behavior and performance when subjected to a damped, free vibration analysis or sinusoidal excitation of a damped spring-mass system.

Continuum C38DR elements are tested for the features of hourglass control, kinematic formulation, tied contact surfaces, multi-point constraints and shear in both Abaqus/Standard and Abaqus/Explicit.

Beam B31 elements are tested for the features of small displacements and large rotations when subjected to loadings in both Abaqus/Standard and Abaqus/Explicit.

Validation of Abaqus

Validation of Abaqus is important to compare its accuracy against experiments of RC elements or structures subjected to dynamic and monotonic loadings. Abaqus/Explicit is validated against RC beams subjected to dynamic loads while Abaqus/Standard is validated against RC beam-column connections subjected to monotonic.

For dynamic behavior of concrete elements, validation is performed for a RC beam subjected to dynamic loading in the Feldman and Seiss tests. For RC beam-column behavior, validations are performed for corner-connections, T-connections and interior connection as these are the most commonly found beam-column connections to be found in RC structures (Figure 4-1). Although this study will look into only a particular interior connection, validating the two other types of connections is useful for future study of progressive collapse of the entire building.

RC beam subjected to dynamic loads

This validation is performed because for future progressive collapse assessment of RC structures, the external or abnormal load might be a blast or impact load which will cause the RC structure to behave dynamically.

Abaqus/Explicit is used to simulate a simply supported RC beam (Feldman and Seiss, 1956) subjected to a dynamic load at its midspan. Beam 1-C has a length of 10 feet simply supported between 106 inches. It has a column stub at midspan to transmit the dynamic load. The concrete beam is reinforced with 2 no. of #7 tensile reinforcements and 2 no. #6 compressive reinforcements with #3 stirrups at 7 inch intervals. The reinforcement details of the RC beam are shown in Figure 4-2. Figure 4-3 shows the loading time history for beam 1-C.

Solid C3D8R elements are used to model the concrete and beam B31 elements are used for the reinforcement. In this validation, it is found that 1 inch mesh (Figure 4-4) is most appropriate for this simulation as the results converge and it takes a relatively short time to run the simulation.

Dynamic Increase Factors (DIF) (Table 4-1) per UFC 3-340-02 were applied to the material properties of concrete and steel to account for the response of structural materials to high loading rates (ASCE, 1999). Hsu's material model (1993) is used for the steel while CDP is used for the concrete. The stress-strain curves for concrete and steel for static loading and high loading rates in Beam 1-C are shown in Figure 4-5 and Figure 4-6.

The default parameters of CDP in Abaqus as described earlier are used (Table 4-2). It was found that varying the value of these parameters do not change the response by a significant amount. A parametric study is done to investigate the optimum value of

dilation angle and it was found to be 31°. Figure 4-7 shows the deflection time history for far design range (DIF) for various dilation angles and the test data.

Abaqus/Explicit obtained very close results with the test data for the peak displacement for far design range for dilation angle of 31°. The peak deflection of the model was less than 1% different compared to the actual test data. The residual response of the beam as the load starts to decrease does not match closely the experimental results.

Damage to a structural element can be classified in terms of peak displacement and in this test; the inelastic demand of the beam is represented by the peak displacement. Based on the closeness between the peak displacements of the test and simulation, we would conclude that Abaqus/Explicit is able to model the dynamic behavior of reinforced concrete beams.

RC beam-column connections subjected to monotonic loads

Abaqus/Standard is used to simulate the response of a RC T-connection, T16 (Figure 2-13), corner-connection U25 (Figure 2-15) and interior connection U69 (Figure 2-17) subjected to monotonic loads (Nilsson, 1973).

The same Abaqus modeling process as described in the RC beams was carried out. The tests are conducted with the RC beam-column assembly that was placed on the floor to eliminate the effects of gravity on the results. Displacement-control testing was carried out to obtain the load-deflection data as recorded in the tests by increasing the displacement followed by measuring the load required.

CDP was used for the concrete and Hsu's model for embedded reinforcement in concrete was used for reinforcement. The stress-strain curve for the concrete and reinforcement for the 3 tests are shown in Figure 4-8 and Figure 4-9. The parameters

for CDP are also set at Abaqus default with the dilation angle of the concrete being varied. It was found that the most appropriate value of the viscosity parameter μ was 0.01 as it allows the results to converge faster.

For T16 (Figure 4-10), the peak failure load of both the simulation and the experiment occurs at nearly the same deflection, 40mm in both the simulation and experiment, at dilation angle of 10. The peak failure load of 18.168 kN in the simulation is about 5.7% compare to that of 17.187kN in the experiment. However, the simulation did not exhibit the same strain softening behavior or ductility as the experiment after the peak failure load. The experiment recorded a maximum deflection of around 62 mm but the maximum deflection in the simulation is around 41 mm. Based on the closeness of the peak failure load and its occurrence, the author believes that the simulation does validate the behavior of the T-connection tested.

For U25 (Figure 4-11), at a dilation angle of 20, the initial failure load of 35.629kN for the simulation and 35.316kN for the experiment is really close, with a difference of just 0.89% between them. Both the initial failure also occurs at around the same deflection of around 17mm. Similar to T-16, the simulation does not exhibit the same strain hardening or ductility as shown in the test. Based on the almost identical initial failure load and occurrence, the author believes that the simulation is able to model the behavior of the corner connection, U25.

For U69 (Figure 4-12), a parametric test by varying the dilation angles was carried out. It was found that for dilation angle of 10, the simulation's peak load of 44.052 kN was about 21.18% from the test peak load of 36.355 kN. Both the peak load of the test and simulation occur near the same deflection. The peak load of the simulation reduces

with reducing dilation angles. But this reduction flattens off after a dilation angle of 10 degrees where it is seen that a dilation of 5 degrees produced similar results.

In the experiment, cracks will be formed in the concrete with increasing load. The reinforcement might not be able to reach its full capacity as the distance in between the cracks might be smaller than the development length of the reinforcement. However, this phenomenal does not occur in the Abaqus simulation where the stress of the reinforcement is only a function of the structure at that particular location. The Abaqus model might be stiffer than the actual test and this might explained the reason why the simulation has a higher load resistance compared to the experiment. Only one test was carried out by Nilsson (1973), and since only one experiment was done, there might be some variability in the results as the materials, testing procedures or equipment might not be functioning as it should during the experiment.

The author believes that Abaqus is able to model the behavior of the internal connection reasonably well at a dilation angle of 10 degrees because the peak load of both the model and the experiment occurs at nearly the same deflection and the 21.18% variation in the peak load could possibly be due to the two reasons stated above.

Parameters of CDP

During the validation of Abaqus/Explicit and Abaqus/Standard, all parameters of the CDP material model were kept constant to the default values in Abaqus except for the viscosity parameter and dilation angle.

In Abaqus/Explicit, viscosity parameter will be zero regardless of what values were assigned to it. For Abaqus/Standard, it was found out that a viscosity value of 0, 0.01

and 0.001 does not have adverse effect on the results of the simulation but having a viscosity parameter of 0.01 makes it faster for the simulation runs faster.

RC Beam-Column Connection in Study

An interior RC beam-column connection of a concrete structure will be modeled using Abaqus/ Standard to determine its moment-rotation resistance function. Figure 4-13 shows the elevation view of the reinforced concrete structure and the interior connection to be modeled. Figure 4-14 and 4-15 shows the details of the beams and columns respectively.

The concrete has an f_c' of 4000psi while the reinforcement used is Grade 60 steel conforming to the latest ASTM specifications A616 or A706. The stress-strain curves for the concrete and reinforcement are shown in Figure 4-16 and Figure 4-17 respectively. Hsu's material model for reinforcement and CDP material model for concrete is used in Abaqus/Standard for the simulation.

Resistance Function of RC Beam-Column Connection

The dashed region (Figure 4-13) shows the beam-column assemblage that will be modeled using Abaqus/Standard. One end of the beams will be loaded by the exterior column transferring the weight from the above floors, when the column beneath is removed, while the other end will be pinned onto a very strong steel resistance frame. The support condition at the steel frame will be a pinned support. Figure 4-18 shows the predominantly continuum FE model of the RC beam-column assemblage.

The focus of the simulation is to determine the behavior of the connection subjected to monotonic loads. As a strong column-weak beam design, the plastic hinge will develop within the RC beam. For the plastic hinge to form on the RC beam and rotate about the edge of the column, the length of the plastic hinge will be d (distance

from the outer most compressive fibers of the beam to the tensile steel) from the edge of the column. Detailed modeling is done up to d the distance from the face of the connection at the beams and columns to accurately capture the behavior of the beam-column connection.

The local rotation at the plastic hinge at each face of the connection is obtained by capturing the translations and θ is obtained as shown in Figure 3-5. The local rotation is taken as the average at the top, middle and bottom faces of the RC beam (Figure 4-19). The moment is simply the product of the load applied and the lever arm. The moment-rotation relationship for the connection for this face of the RC beam-column is obtained.

Further away at more than d distance, the actual behavior of the RC beams and columns are not of importance in this study. They can either be represented by using appropriate beam elements or continuum elements of coarser mesh whose main purpose is to transfer the loading and boundary conditions to the connection to maintain compatibility. In this case, continuum elements (Figure 4-18) are used to represent these sections and they are meshed into coarse mesh to save computing time. Figure 4-20 compares the assemblage consisting of the entire assemblage modeled of continuum and beam elements of 1 inch mesh compared to another model that only models in detailed the beam-column connection in 1 inch mesh. The amount of elements in the former model is about 7.5 times more than that in the latter model. We can save tremendous resources and computing time by just modeling in detail up to d distance of the beam-column connection as we are only interested in the connection behavior.

Since the RC beam is not symmetrical, the moment-rotation resistance function of the RC beam-column connection is not symmetrical either. Therefore, separate moment-rotation resistance functions have to be determined for a load pushing towards the ground and another in the opposite direction (Figure 4-21).

Moment-Rotation Resistance Function

Figure 4-22 shows the moment-rotation resistance function generated by subjecting the continuum FE model in both directions in Abaqus/Standard. Three simulations are run with dilation angles of 31, 20 and 10.

For all the runs, it was found out that the local rotations at the top, middle and bottom face of the beam is similar and this further reinforced our assumption that the plastic hinge will developed at d distance away from the column face.

The maximum moment-rotation results from the simulations are shown in Table 4-3. For gravity loading, simulation with dilation angle of 10 has the highest moment of 7530 kips-inches while simulation with dilation angle of 31 has the highest moment of 5258 kips-inch for loading in the opposite direction.

Dynamic Structure Analysis Suite (DSAS) Version 3.0 (Astarlioglu and Krauthammer, 2009) was used to determine the maximum moment resistance based on the section details of the RC beam at the face of the connection. The maximum moment resistance when subjected to gravity loading based on the section properties is about 4884 kips-inch and 3919 kips-inch when subjected to loading in the opposite direction. Based on these figures, a dilation angle of 20 is a good estimate to use for the simulation as it is the closest to the moment resistance calculated from the section properties.

Figure 4-23 compared the Power Model (Richard and Abbott, 1975) against the simulation for gravity loading. It can be seen that the Power Model over estimates the moment and is not a good fit for the simulation results. However, using a 3rd degree polynomial can fit the simulation results perfectly. This behavior is consistent for the simulation when the load was applied in the opposite direction. A 3rd degree polynomial (Figure 4-24) can fit the simulation results perfectly.

Replacing Moment-Rotation Resistance by Connector

Connector elements will replace the resistance function of the RC beam-column connection in a structural based FE model. The connectors to be used in Abaqus/Standard are the combination of the basic translational connector JOIN and rotational connector CARDAN. The RC column and beams will be represented by beam elements and JOIN will connect the node of the beam and the column at the intersection point. At the same location, CARDAN will provide a rotational connection between the node at the beam and the node at the column, parameterized by CARDAN angles through a moment-rotation resistance constitutive relationship of the connection found earlier.

In Abaqus, this constitutive moment-rotation resistance function will be defined by both linear elastic behavior and non-linear elastic behavior. The linear elastic behavior will be the moment over rotation at initial failure while the non-linear elastic behavior will be the corresponding sets of yield moment and plastic rotation values after initial failure that described the isotropic hardening behavior. Figure 4-25 shows the isotropic hardening behavior of the connectors in both loading directions.

Verification of Predominantly Structural Based FE Model

The simplified structure based FE model shown in Figure 3-6 consists of beam elements to represent the RC beams and columns and connectors to represent the RC beam-column connection. When subjected to the same loading and boundary conditions used in the characterization of the moment-rotation resistance of the connection, the CARDAN connector must exhibit the same moment-rotation output for verification that the simplified predominantly structure based FE model is performing its intended function.

Figure 4-26 and 4-27 compares the output of the simplified structural based FE model against the moment-rotation resistance function obtained earlier from the predominantly continuum based FE model. The results show that the outputs of the two models are exactly the same. This gives us confidence to replace the detailed RC beam-column assemblage with the simplified predominantly structural based FE model.

More importantly, for the same output, the simplified structural based FE model was able to perform the simulation around 10 minutes compared to about 150 minutes for the predominantly continuum FE model (Table 4-4) .

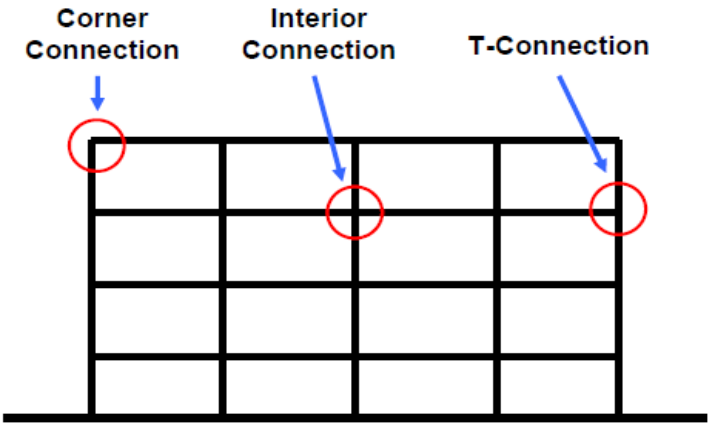

Figure 4-1. Elevation of a common RC structure

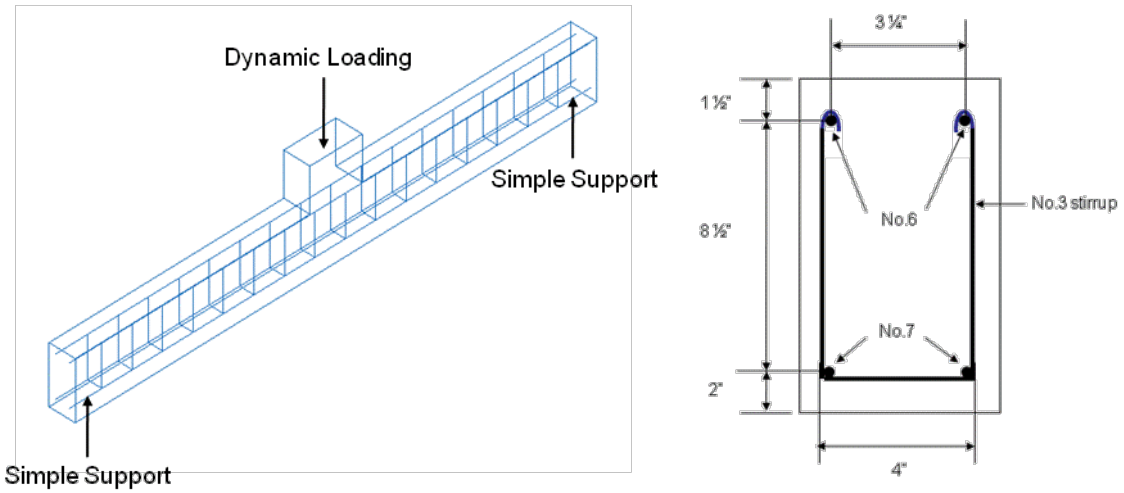

Figure 4-2. Section properties and details for RC beam 1-C. [Adapted from Feldman and Seiss. 1956. Investigation of resistance and behavior of reinforced concrete members subjected to dynamic loading. (Figure 20)]

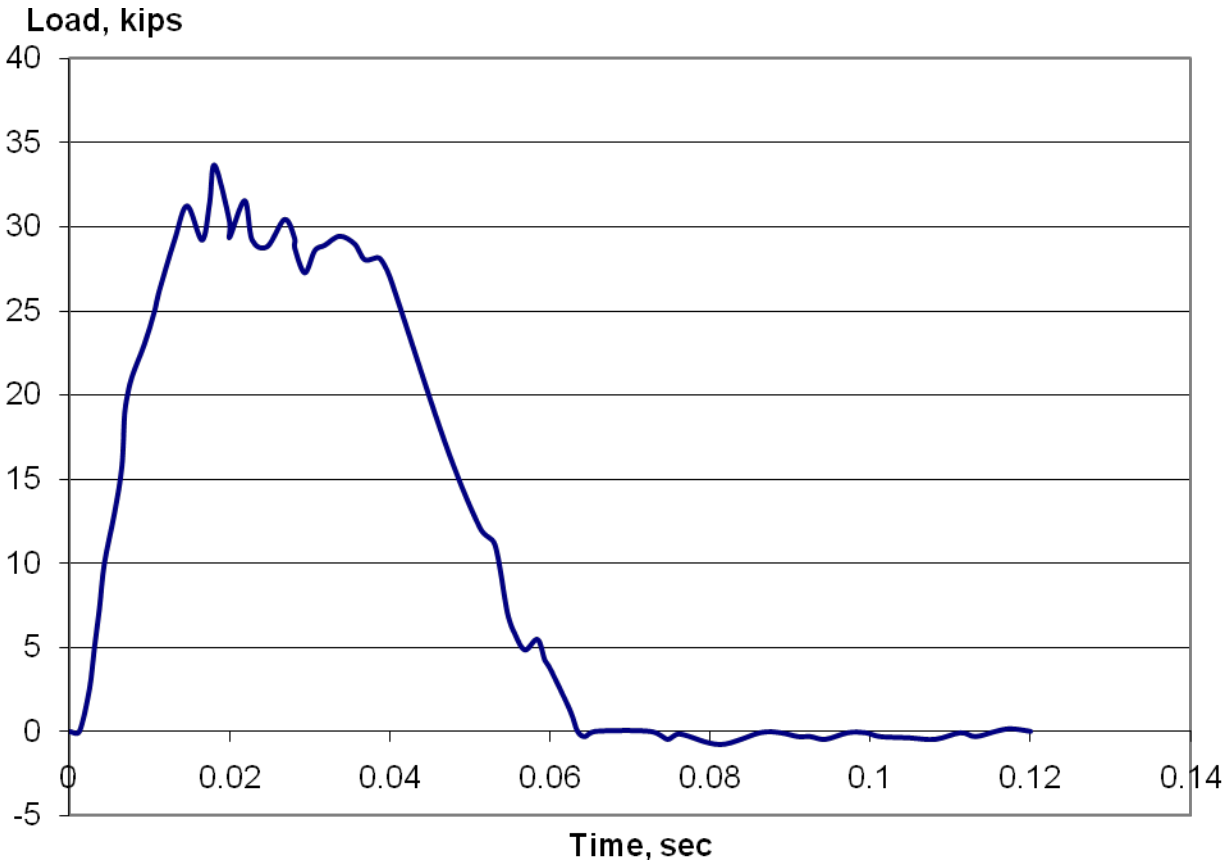

Figure 4-3. Loading time history for beam 1-C

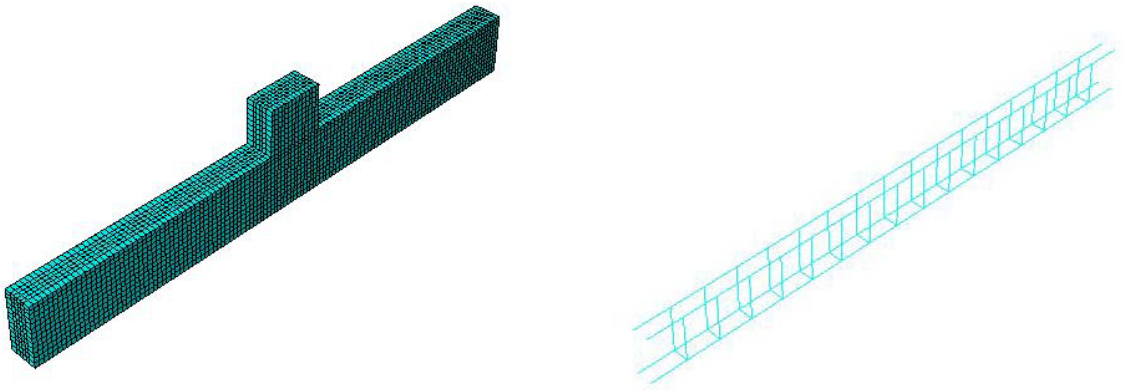

Figure 4-4. Abaqus model showing 1 inch mesh and reinforcement

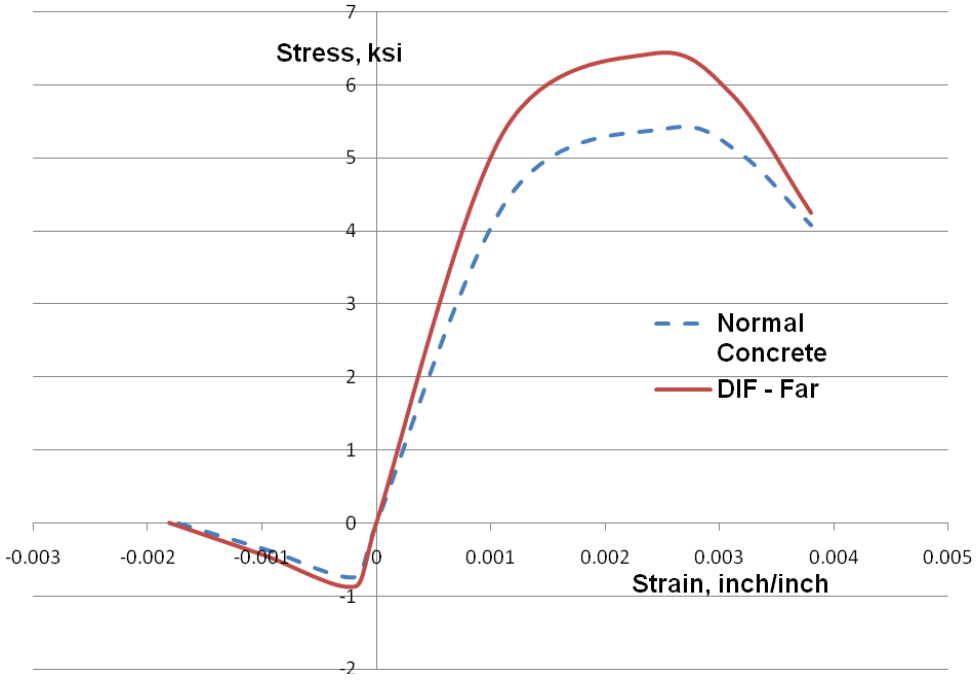

Figure 4-5. Stress-strain curve of concrete for Beam 1-C

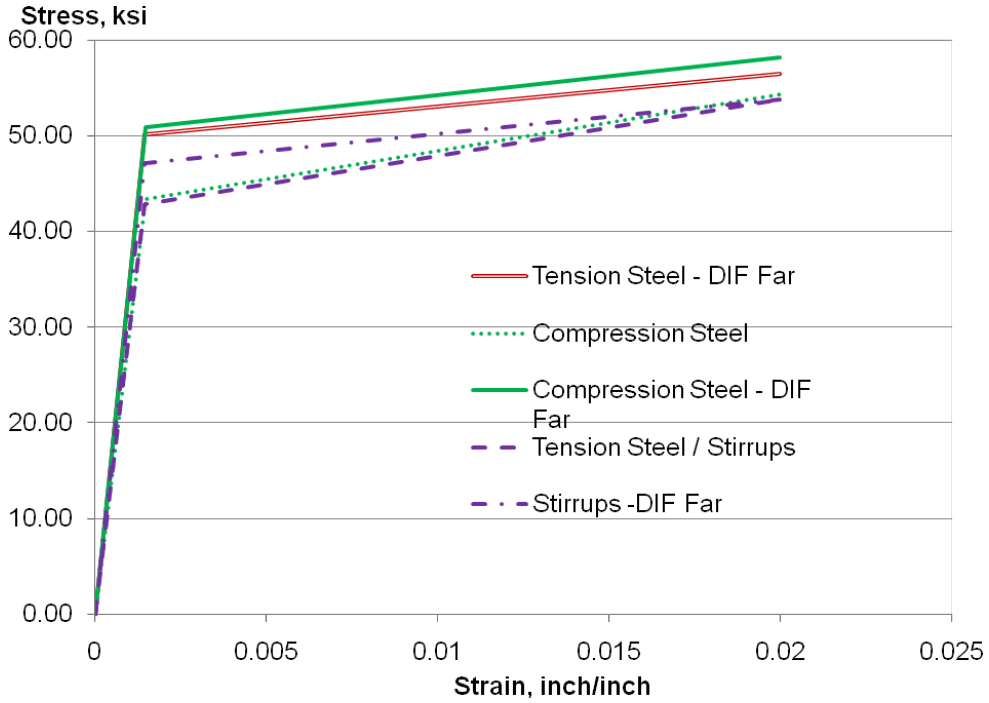

Figure 4-6. Stress-strain curve of steel for Beam 1-C

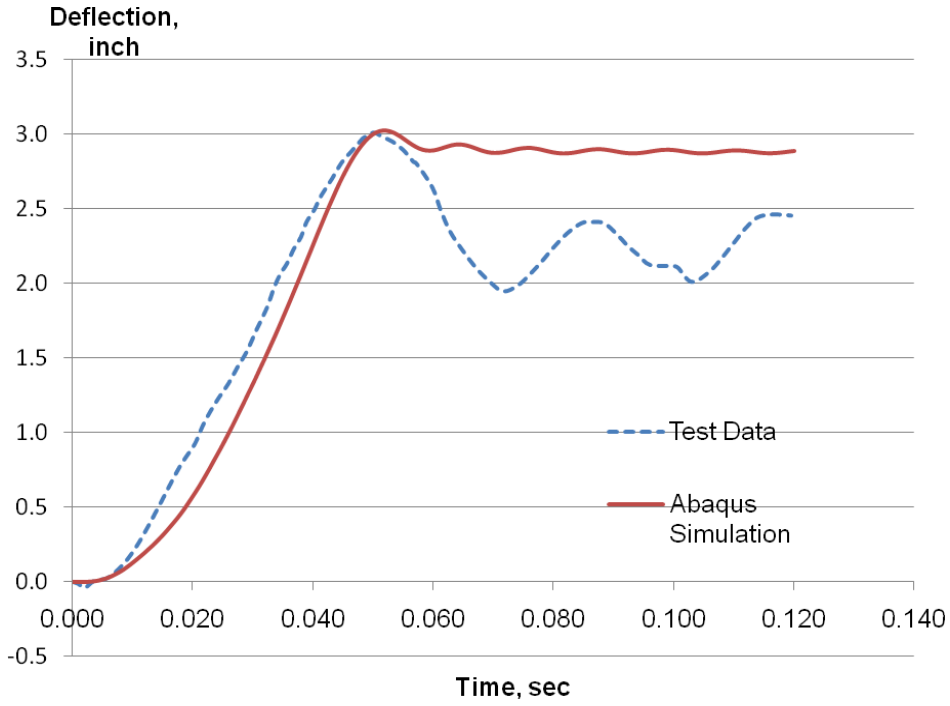

Figure 4-7. Deflection time history for RC beams subjected to dynamic loads

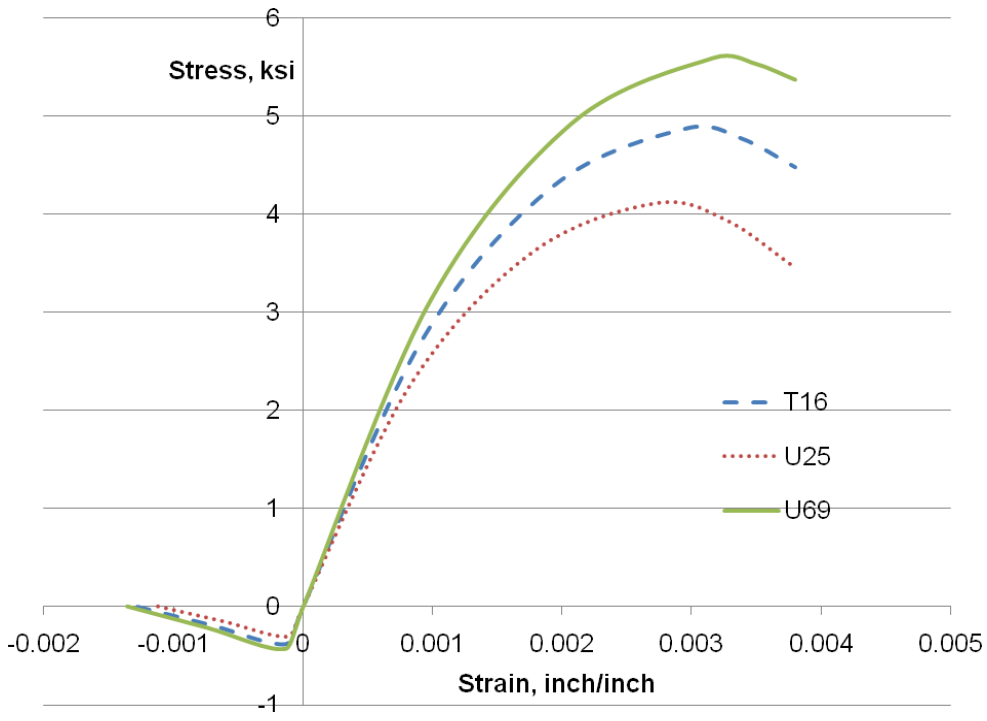

Figure 4-8. Concrete stress-strain curve for T16, U25 & U69

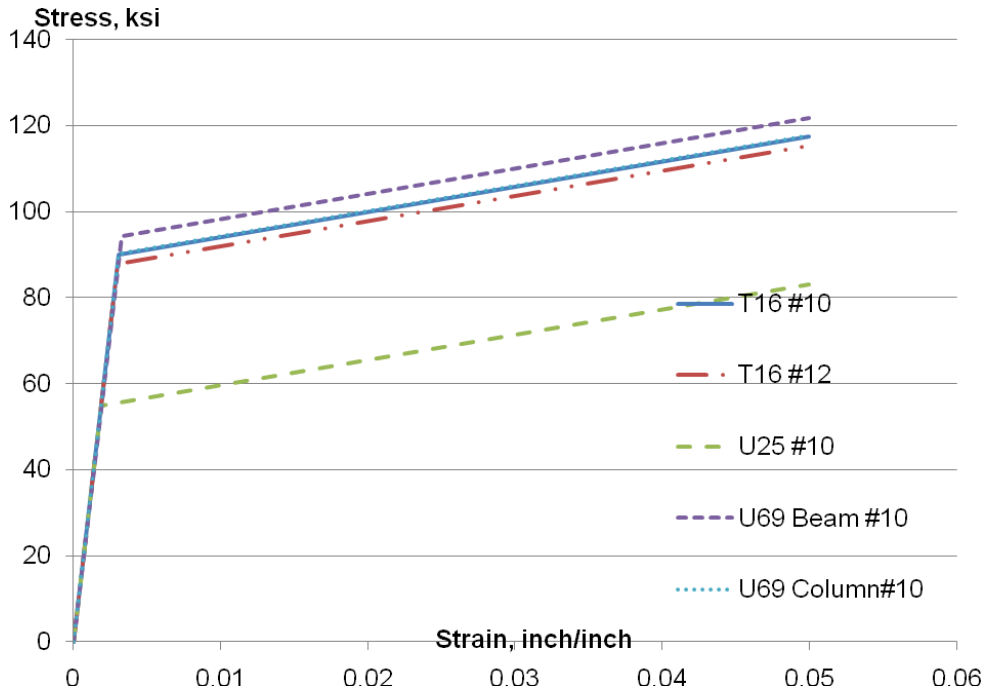

Figure 4-9. Reinforcement stress-strain curve for T16, U25 & U69

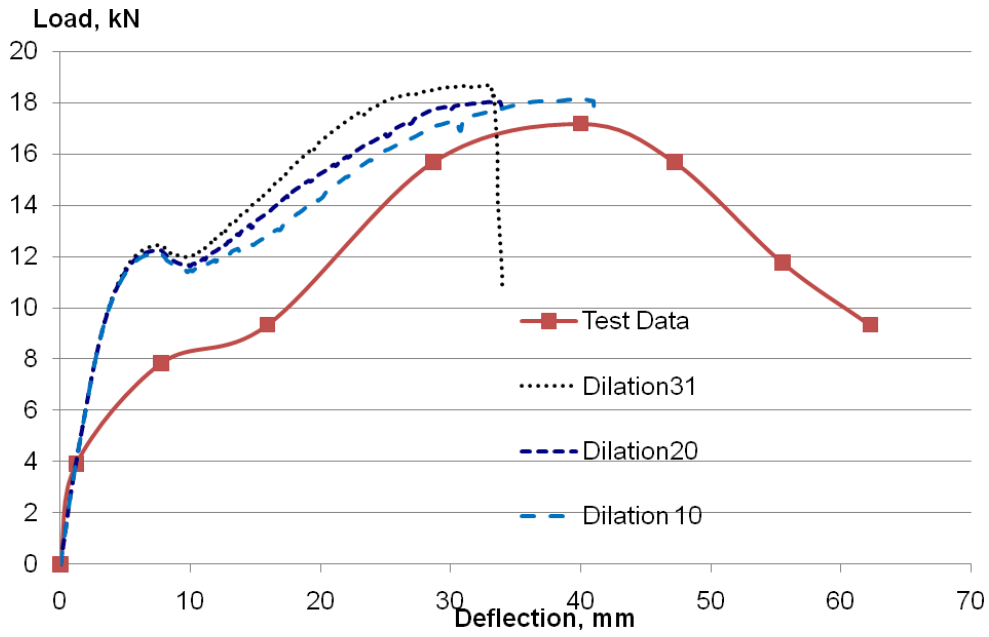

Figure 4-10. Load-deflection curve for T16

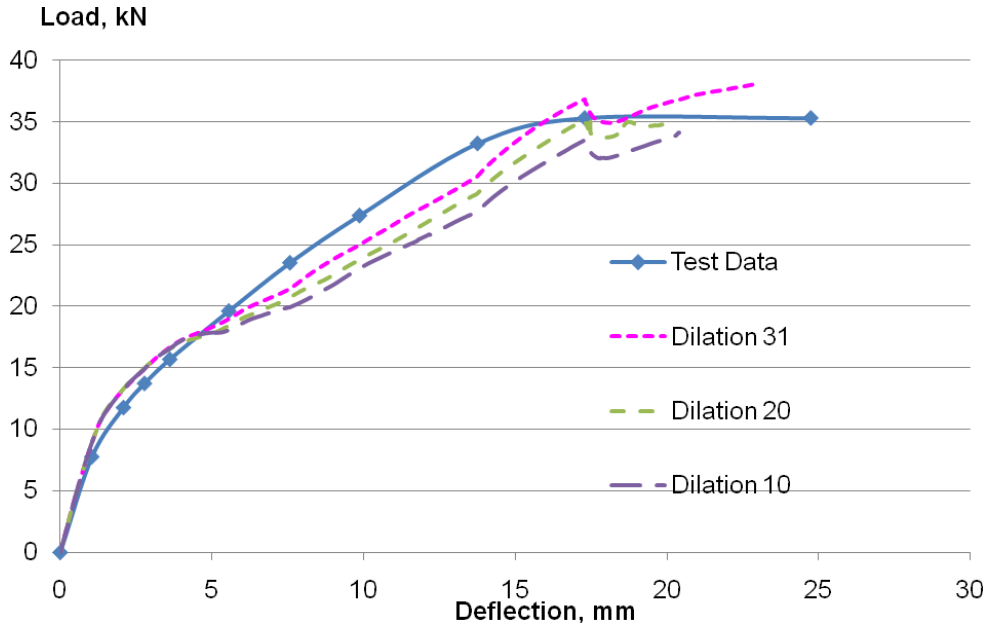

Figure 4-11. Load-deflection curve for U25

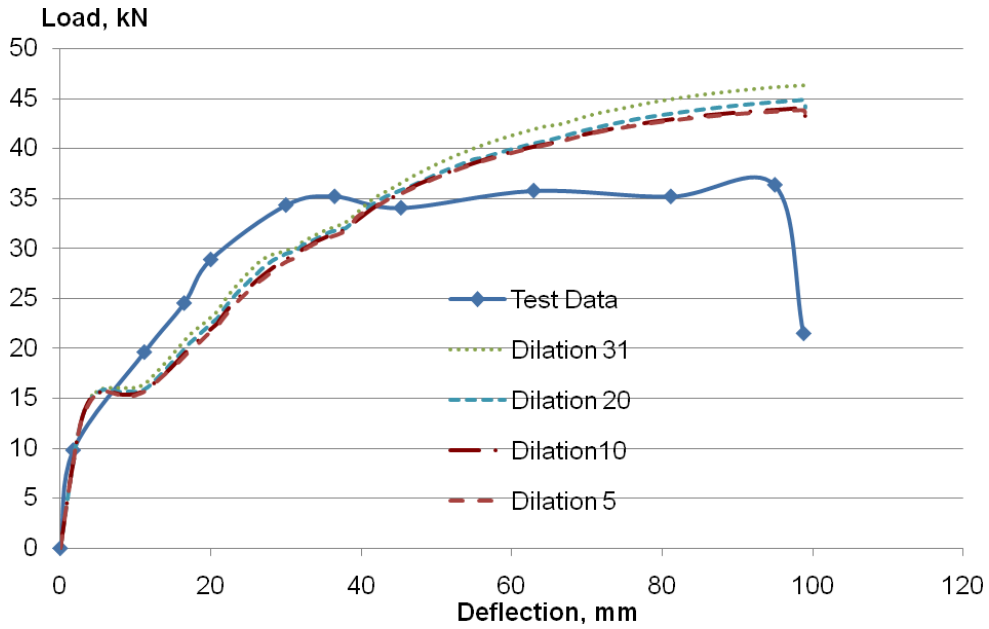

Figure 4-12. Load-deflection curve for U69

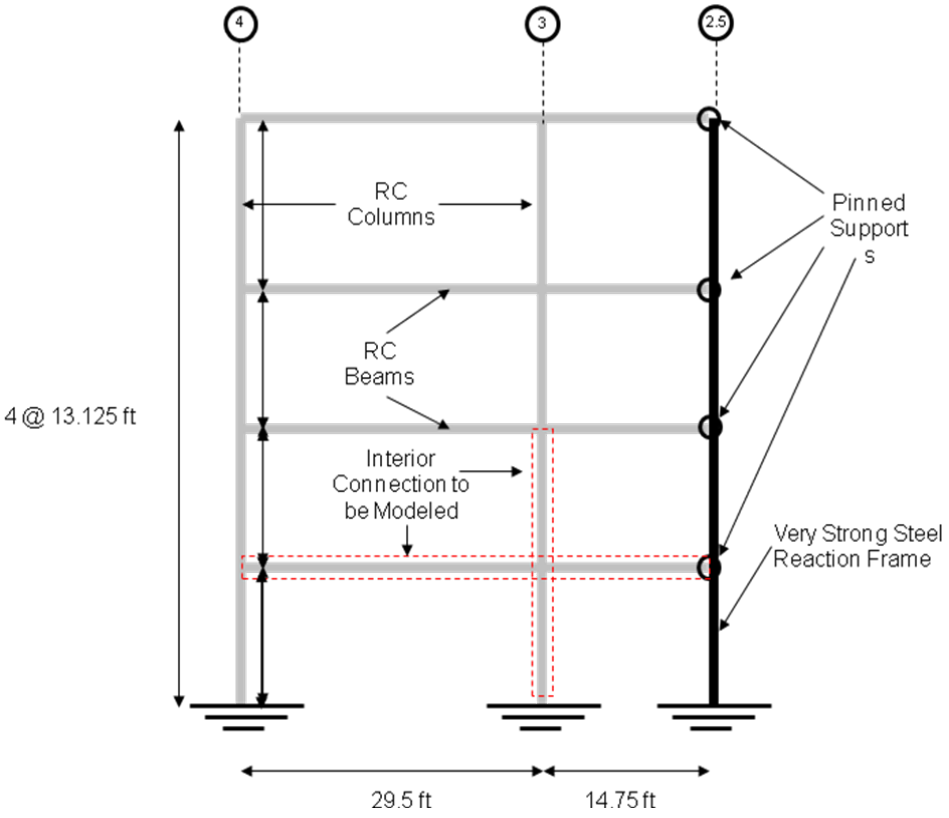

Figure 4-13. Elevation view of RC structure and interior connection

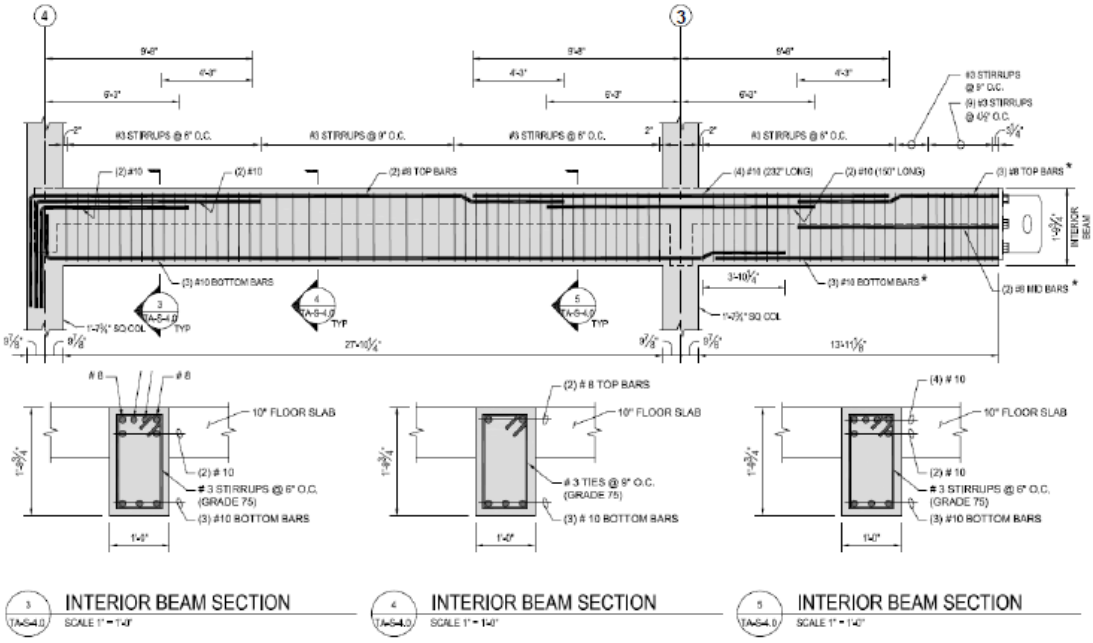

Figure 4-14. Details of RC beams

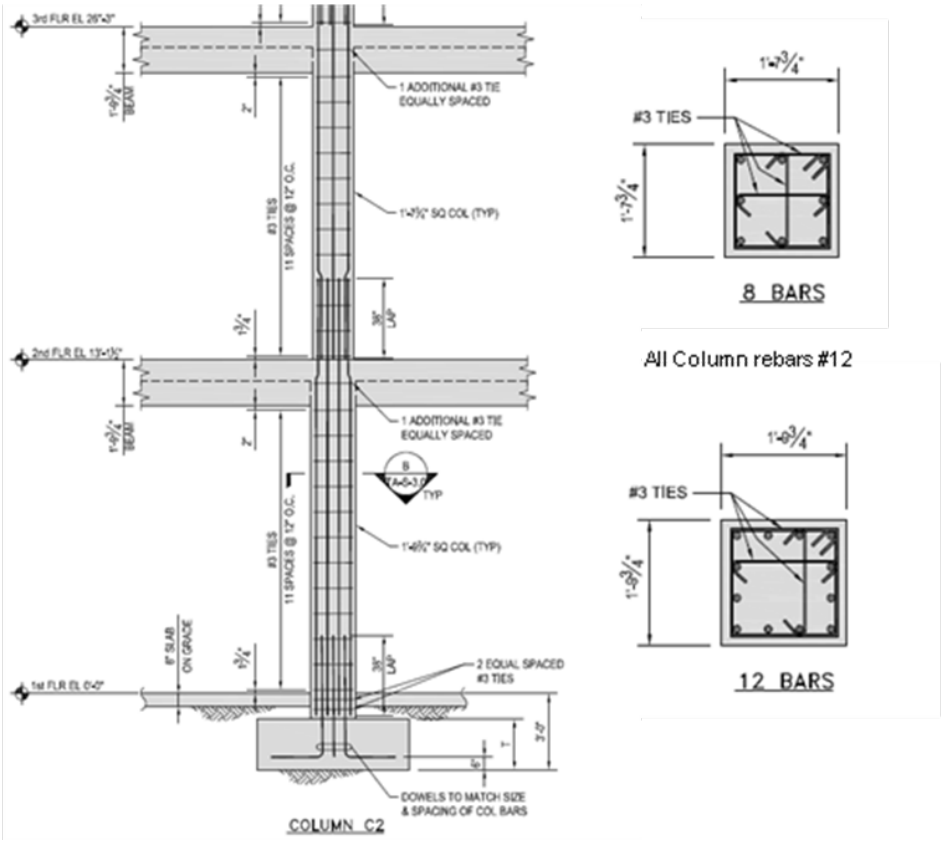

Figure 4-15. Details of columns

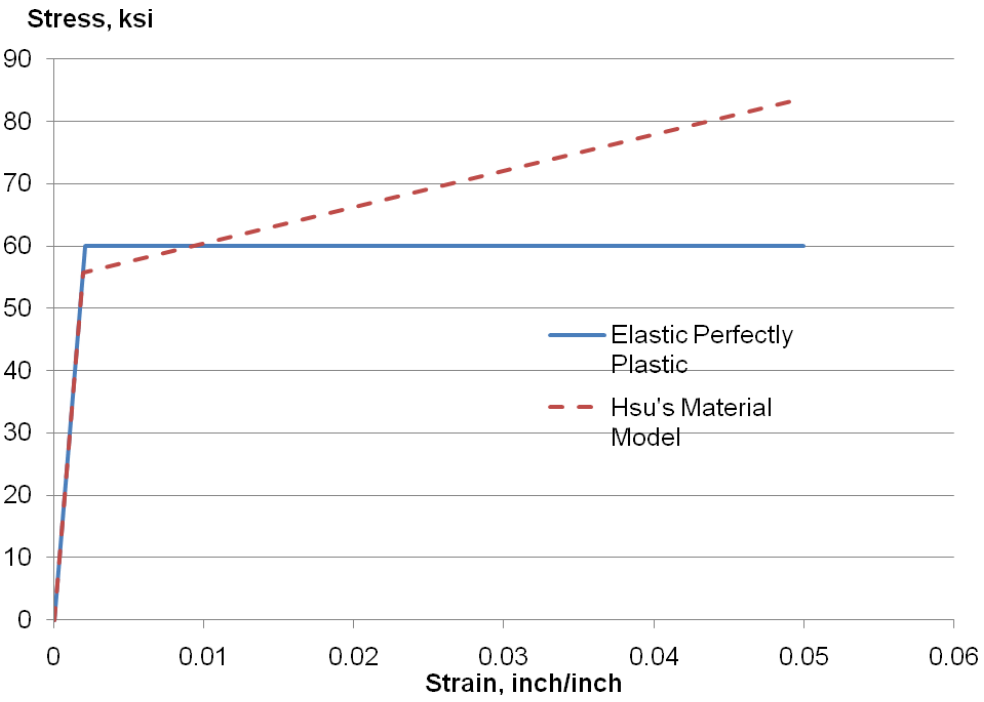

Figure 4-16. Reinforcement stress-strain curve

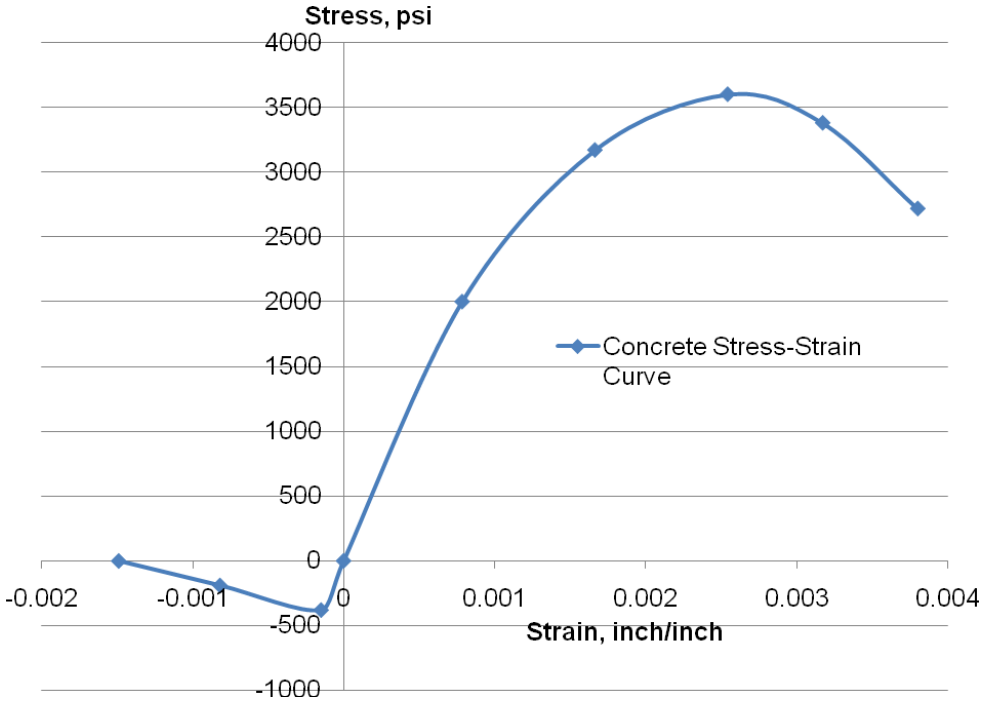

Figure 4-17. Concrete stress-strain curve

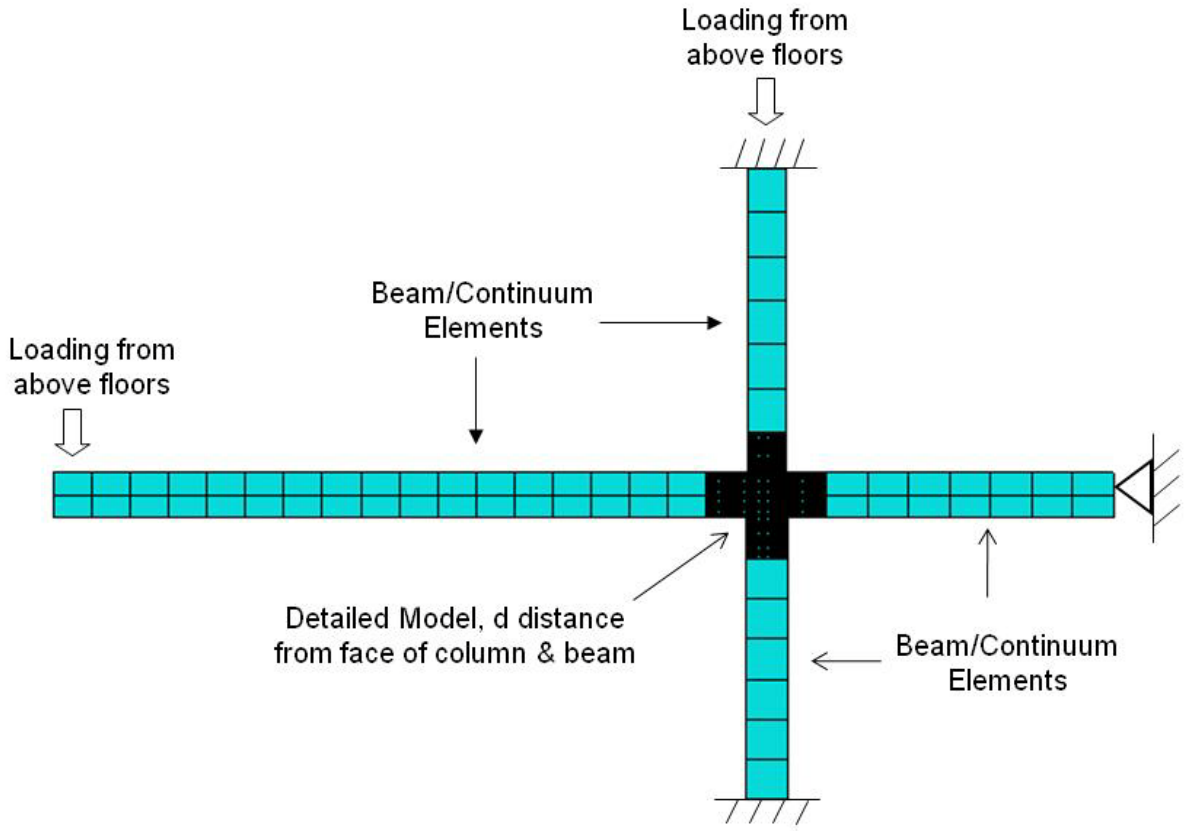

Figure 4-18. Continuum FE model of RC beam-column assemblage

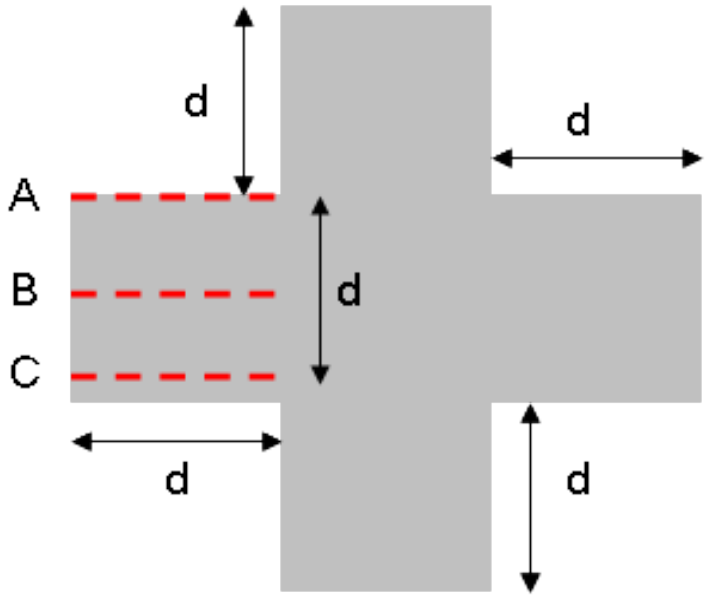

Figure 4-19. Positions of measurement for local rotation

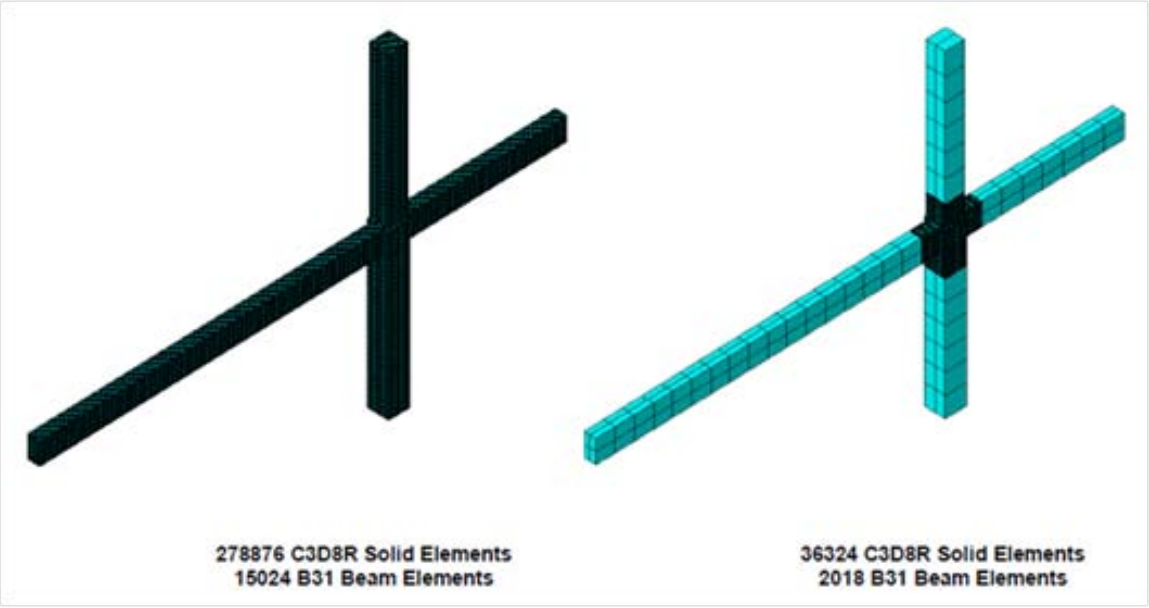

Figure 4-20. Comparison of dense and simple model of beam-column assemblage

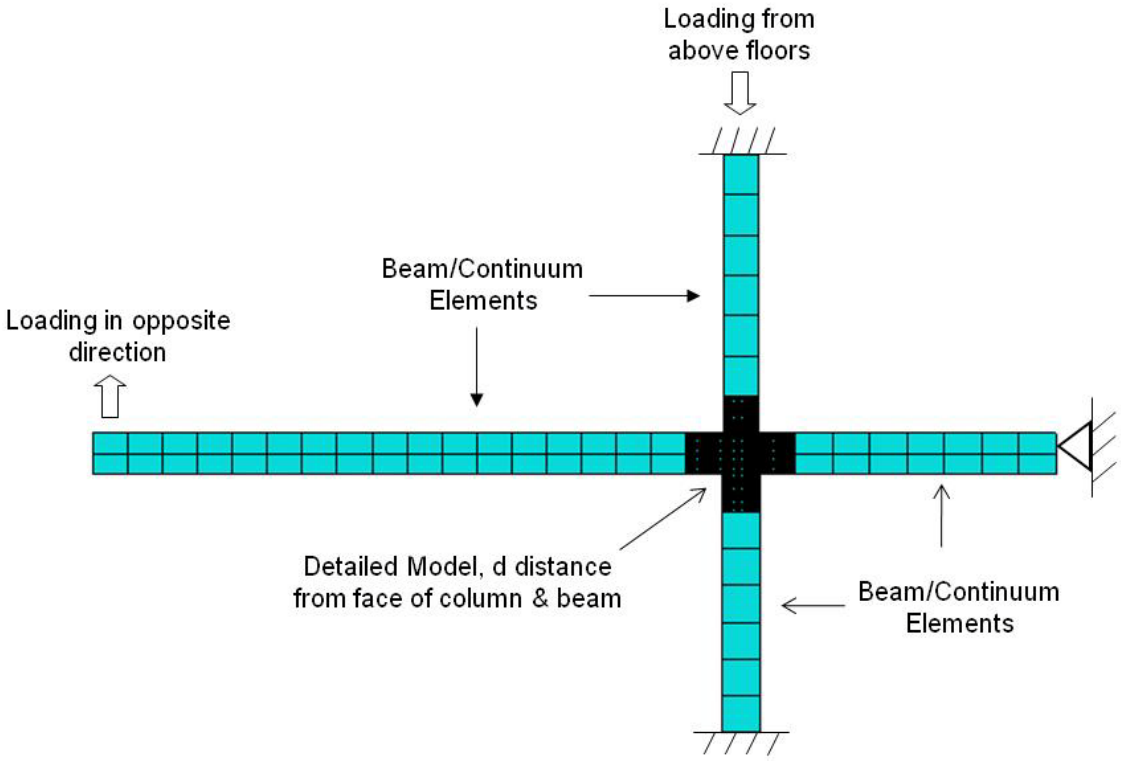

Figure 4-21. Loading of RC beam-column assemblage in opposite direction

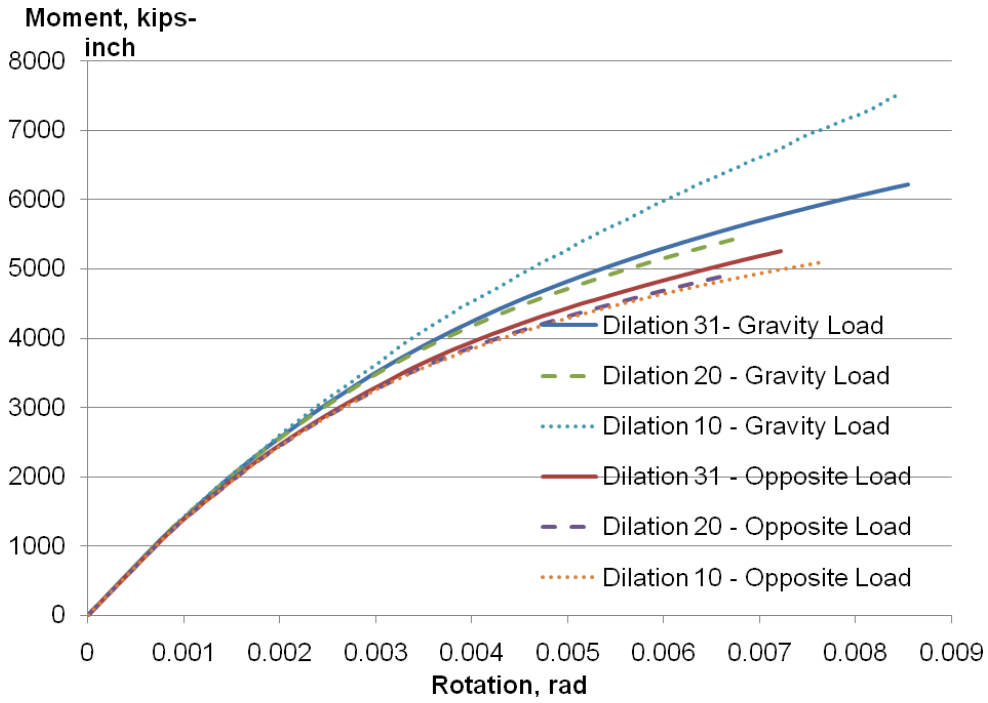

Figure 4-22. Moment-rotation resistance functions

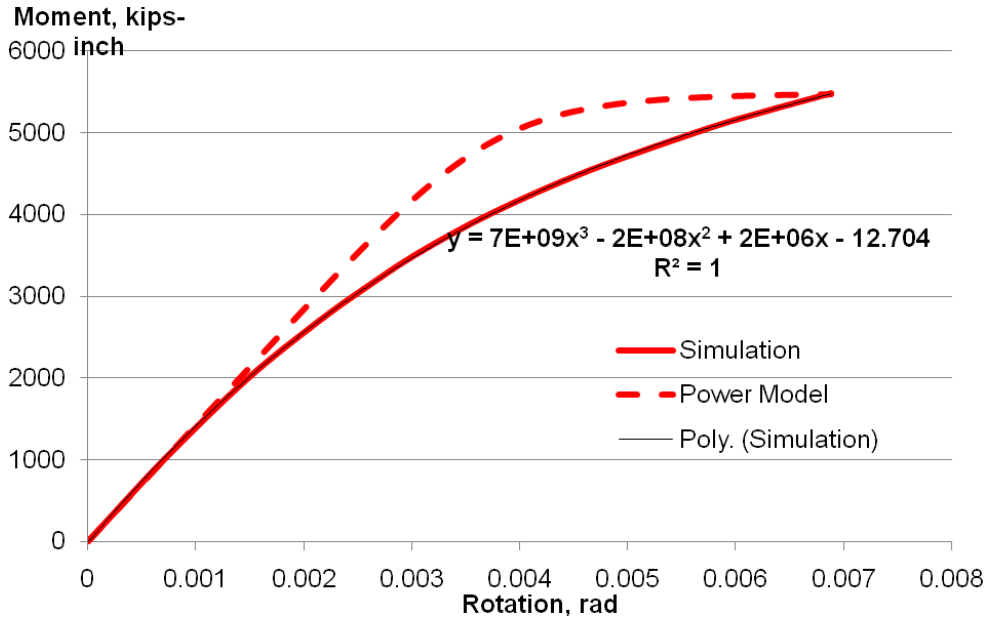

Figure 4-23. Moment-rotation resistance functions subjected to gravity load

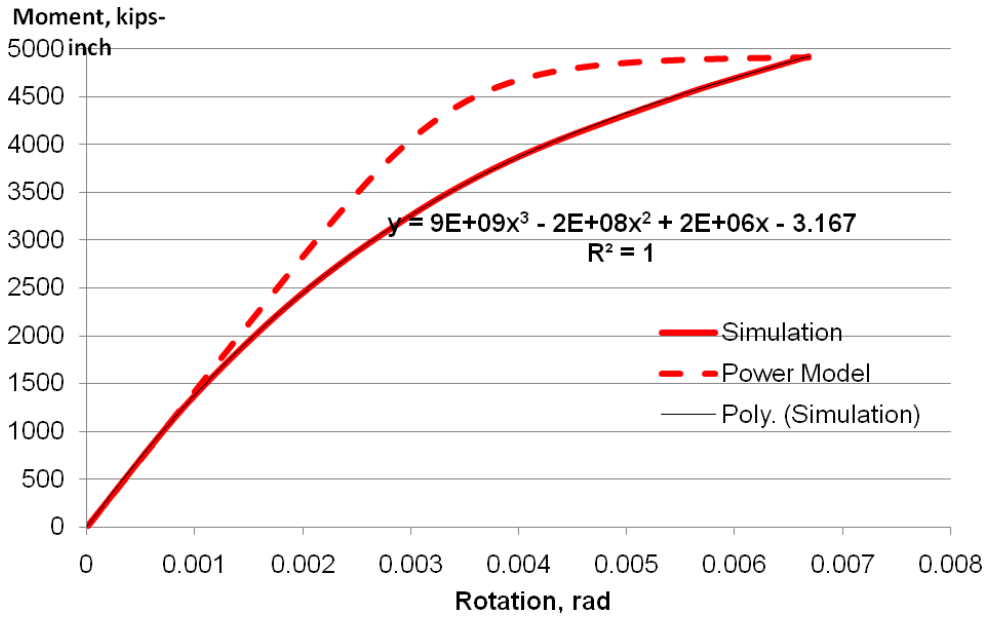

Figure 4-24. Moment-rotation resistance functions subjected to opposite load

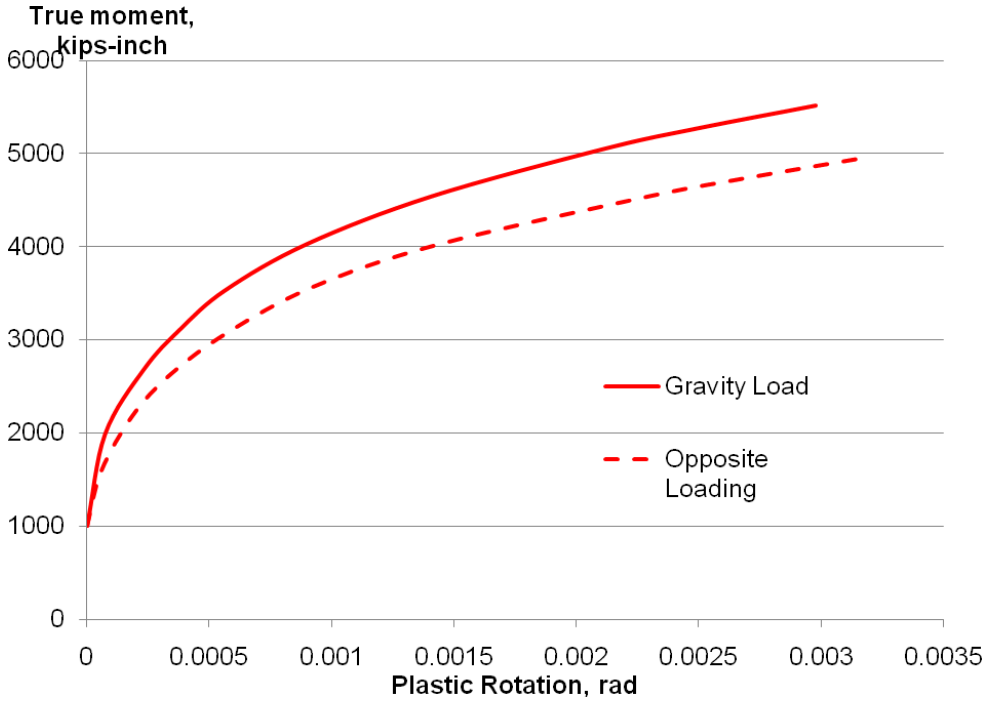

Figure 4-25. Isotropic hardening behavior for connectors

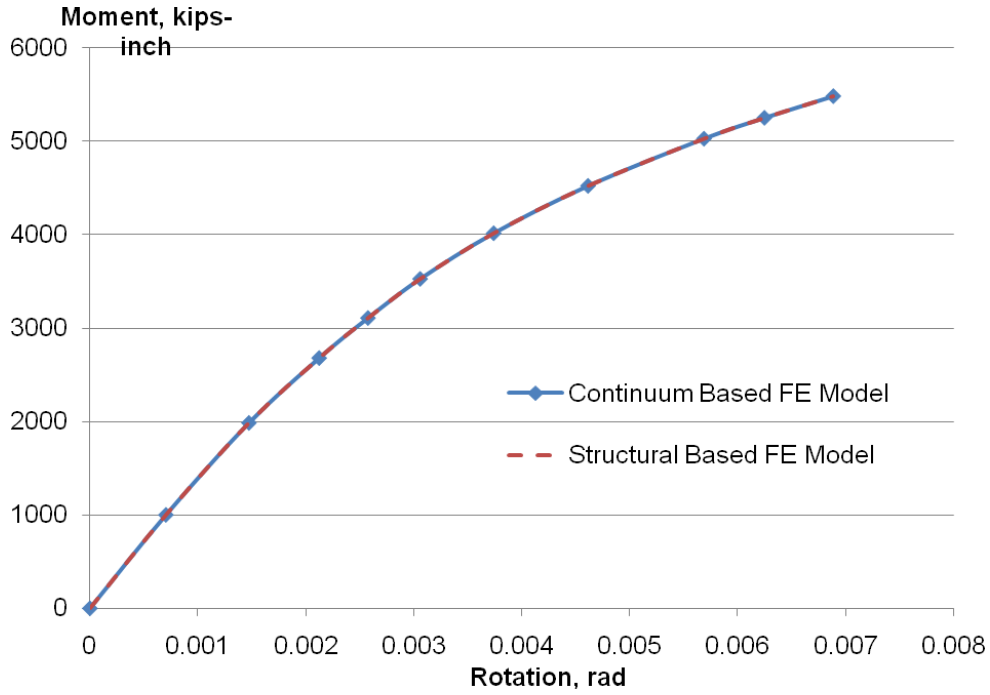

Figure 4-26. Output for connector for gravity loading

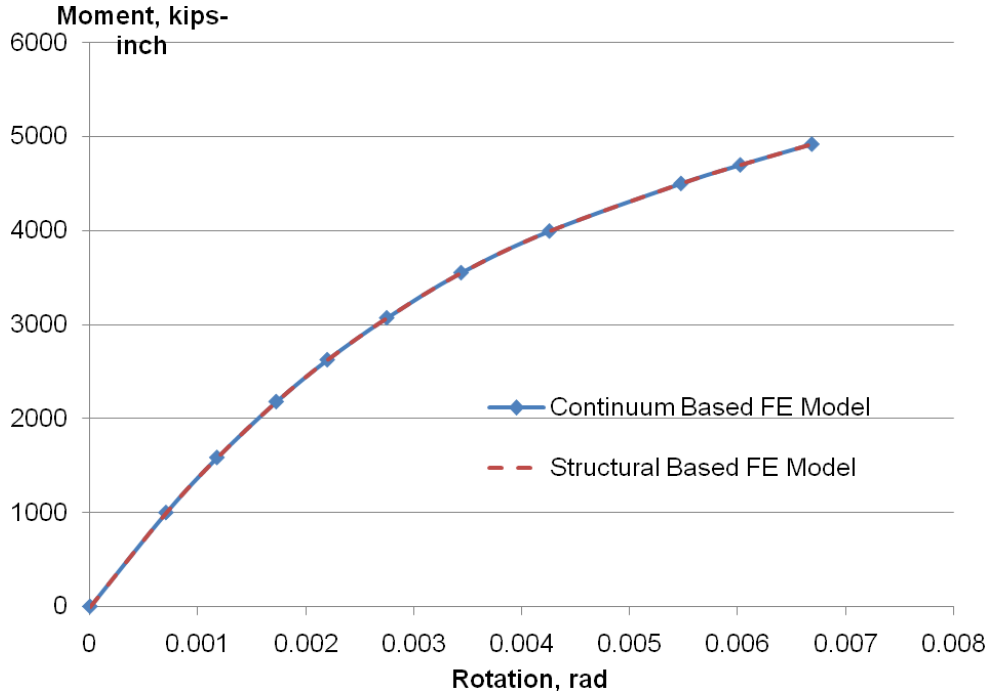

Figure 4-27. Output for connector for opposite loading

Table 4-1. Dynamic increase factor [Adapted from Unified Facilities Criteria. UFC 3-340-02: Structures to resist the effects of accidental explosions. (Page 1068, Table 4-1)]

Type of Stress	FAR DESIGN RANGE			CLOSE-IN DESIGN RANGE		
	Reinforcing Bars		Concrete	Reinforcing Bars		Concrete
	f_{dy} / f_y	f_{du} / f_y	$f_{dc}^{'} / f_c^{'}$	f_{dy} / f_y	f_{du} / f_y	$f_{dc}^{'} / f_c^{'}$
Bending	1.17	1.05	1.19	1.23	1.05	1.25
Diagonal Tension	1.00	-	1.00	1.10	1.00	1.00
Direct Shear	1.10	1.00	1.10	1.10	1.00	1.10
Bond	1.17	1.05	1.00	1.23	1.05	1.00
Compression	1.10	-	1.12	1.13	-	1.10

Table 4-2. Parameters of CDP

Description	Symbol	Value
Flow Potential Eccentricity	ε	0.1
Ratio of Initial Equibiaxial Compressive Yield Stress to Initial Uniaxial Compressive Yield Stress	$\frac{\sigma_{b0}}{\sigma_{c0}}$	1.16
Ratio of Second Stress Invariant on Tensile Meridian to Compressive Meridian	K_c	0.666
Viscosity Parameter	μ	0

Table 4-3. Ultimate moment-rotation of simulations

	Gravity Loading		Opposite Loading	
Dilation Angle	Moment, kips-inch	Rotation, rad	Moment, kips-inch	Rotation, rad
31	6223	0.008547	5258	0.007224
20	5479	0.006883	4925	0.006687
10	7530	0.008458	5091	0.007637

CHAPTER 5
CONCLUSION AND DISCUSSION

Summary

A numerical method employing an advanced nonlinear finite element (FE) code to extract the moment-rotation curve from an internal RC beam-column connection was presented.

Chapter 2 introduced the different types of RC beam-column connections and the different structural behavior and connection design parameters associated with it. Material models for concrete and reinforcement were being reviewed. Finite element analysis was introduced as a tool commonly used to solve engineering analysis problems and Abaqus was discussed in more details. Finally, progressive collapse was briefly examined through the effects of a structure's response to an abnormal load or from the sudden removal of a structural element.

Chapter 3 described the research methodology to extract the mechanical resistance function of an internal RC beam-column connection subjected to monotonic loads.

The actual process and the results of validation were described in Chapter 4. Extraction of the mechanical resistance of the interior RC beam-column connection was done and a simplified structural based FE model with connector elements, representing the RC beam-column connection, was developed to replace the RC beam-column assemblage.

Conclusions

Validations

The behavior of a RC beam under dynamic loadings was validated using Abaqus/Explicit. This is to validate the behavior of concrete elements under dynamic loadings.

The behavior of three different types of RC beam-column connections, namely corner-connection, T-connection and interior connection, under monotonic loadings were being validated with existing test data using Abaqus/ Standard. This ensured confidence in the usage of Abaqus/Standard to derive the mechanical resistance of these three different types of RC beam-column connections for further study.

Characterization of Moment-Resistance of Interior Connection

The RC beam-column connection, interior connection, in our study was modeled using Abaqus/Standard and a moment-rotation resistance function was successfully derived.

A Simplified Structural FE Model

A simplified structural FE model consisting of beam elements to represent the RC beams and columns and connectors to replace the moment-rotation resistance function of the RC beam-column connections was developed and shown to exhibit the same behavior as the detailed model. Most importantly, the new model was able to save much computing time and resources. This simplified structural FE model can be used for progressive collapse analysis on an entire structure in future studies.

Limitations

The simulation of the RC beam-column assemblage was done with fine mesh of continuum elements (concrete) and embedded beam elements (reinforcement) in the

interior connection up to d distance but further away, continuum elements of coarse mesh was used to represent the RC beams and columns. This is because the behavior of the connection is of interest, while the role of the RC beams and columns is to transfer the loads to the connection. Due to the large dimensions of the RC beams and columns, simulating the RC beams and columns in detail similar to the interior connection will take a very long time. This limitation can be resolved with faster computers or computers that are connected in parallels to run the simulations. With that, the entire assemblage could be simulated in details within just a few days and will provide a better simulation of load transfer from the beams and columns to the connections.

Currently, the material models for concrete and reinforcement in Abaqus could not couple together and adjust the stress in the reinforcement because of the reduction in the bonding length between the reinforcement and the concrete due to cracks. This might result in a stiffer or stronger Abaqus model than the actual behavior of RC elements. This limitation can be solved by introducing a material model or code that could take into considerations the effect of the development length of the reinforcement.

Recommendations

Progressive collapse of an entire structure subjected to abnormal loadings or the sudden removal of a structural element can be carried out using the simplified structural based FE model and Abaqus/Explicit in future study.

The RC beams and columns was represented by continuum elements having very coarse mesh and a linear elastic material property with yield stress ten times of normal concrete. A detailed study to represent the RC beams and columns by single resistance functions or material property can be carried out such that simpler continuum or beam

elements can replace the RC beams and columns to save time and resource during the analysis.

Material tests to be carried out for concrete and reinforcement to better describe the parameters required in Abaqus for a more accurate simulation.

Future study can investigate the influence of transverse RC beams and adjoining RC slabs on the moment-resistance function of the RC beam-column connection.

LIST OF REFERENCES

ACI Committee 318. (2008). *Building code requirements for structural concrete (ACI 318-08) and commentary (ACI 318R-08)*, Farmington Hills, Mich., American Concrete Institute.

ACI Committee 352. (2002). *Recommendations for design of beam-column connections in monolithic reinforced concrete structures (ACI 352R-02)*, Farmington Hills, Mich., American Concrete Institute.

Alath, S. and Kunnath, S.K. (1995). "Modeling inelastic shear deformations in RC beam-column joints." *Proc., 10th Conference, University of Colorado at Boulder*, Colorado, U.S., 822-825.

ASCE. (1999). *Structural design for physical security*, ASCE Publications.

Astarlioglu, S. and Krauthammer, T. (2009) "Dynamic Structural Analysis Suite (DSAS) User Manual." *Rep. No. CIPPS-TR-003-2009*, CIPPS, University of Florida.

Balint, P.S. and Taylor, H.P.J. (1972). "Reinforcement detailing of frame corner joints." *Rep. No. 42.462*, Cement and Concrete Association, London,U.K.

Bathe, K. (1996). *Finite element procedures*, Prentice-Hall, N.J.

Beres, A., El-Borgi,S., White, R.N. and Gergely,P. (1992). "Experimental results of repaired and retrofitted beam-column joint tests in lightly reinforced concrete frame buildings." *Tech. Rep. NCEER 92-0025*, National Center for Earthquake Engineering Research, Buffalo, U.S.

Bonnaci, J. and Pantazopoulou, S. (1993). "Parametric investigation of joint mechanics." *ACI Struct. J.*, 90(1), 61-71.

Carrasquillo, R.L., Nilson, A.H. and Slate, F.O. (1981). "Properties of high strength concrete subject to short-term loads." *ACI J., Proc.*, 78(3), 171-178.

Chen, W.F. (1982). *Plasticity in reinforced concrete*, McGraw-Hill Book Company.

Cook, R.D., Malkus, D.S., Plesha, M.E.and Witt, R.J. *Concepts and applications of finite element analysis*, Wiley.

Cook, W.D. and Mitchell, D. (1988). "Studies of disturbed regions near discontinuities in reinforced concrete members." *ACI Struct. J.*, 85(2), 206-216.

Ehsani, M.R. and Wight, J.K. (1984). "Reinforced concrete beam-to-column connections subjected to earthquake-type loading." *Proc., 8th World Conference on Earthquake Engineering*, S.F., U.S., 6, 421-428.

El-Metwally, S.E. and Chen, W.F. (1988). “Moment-rotation modeling of reinforced concrete beam-column connections.” *ACI Struct. J.*, 85(4), 384-394.

Feldman, A. and Siess, C.P. (1956). “Investigation of resistance and behavior of reinforced concrete members subjected to dynamic loading.” *Tech. Rep. to The Office of the Chief of Engineers*, Department of the Army, University of Illinois, Illinois, U.S.

GSA. (2005). *Facilities standards for the public buildings service*, U.S. General Services Administration Office of the Chief Architect.

Hanson, N.W. and Conner, H.W. (1967). “Seismic resistance of reinforced concrete beam-column joints”, *J. of the Struct. Div., ASCE*, 93(5), 535-560.

Hayes Jr, J.R., Woodson, S.C., Pekelnicky, R.G., Poland, C.D., Corley, W.G. and Sozen,M. (2005). “Can strengthening for earthquake improve blast and progressive collapse resistance?” J. of Struct. Eng., 131(8), 1157-1177.

Hibbitt H.D., Karlson, B.I. and Sorenson, E.P. (2008). *Abaqus version 6.8 documentation*, Hibbitt, Karlson & Sorenson, Inc.

Hii, H.N. (2007). “Influence of concrete strength on the behavior of external RC beam-column joint.” M.S. thesis, Universiti Teknologi Malaysia, Malaysia.

Holmes, M. and Martin, L.H. (1983). *Analysis and design of structural connections: Reinforced concrete and steel*, Ellis Horwood, N.Y.

Hsu, T.T. (1993). *Unified theory of reinforced concrete*, CRC Press.

Jankowiak, T. and Lodygowski, T. (2005). “Identification of parameters of concrete damage plasticity constitutive model.” *Foundations of Civil and Environmental Engineering*, Publishing House of Poznan University of Technology, 6, 53-69.

January L. M. and Krauthammer, T., (2003). “Finite element code validation using precision impact test data on reinforced concrete beams.” *Rep. to U.S. Army Engineering Research and Development Center, Vicksburg, Mississippi*, Protective Technology Center, The Pennsylvania State University.

Krauthammer, T. (2008). *Modern protective structures*, CRC Press.

Krauthammer,T. and Ku, C.K. (1996). “A hybrid computational approach for the analysis of blast resistant connections.” *Computers and Structures*, 61(5), 831-843.

Leon, R.T. (1990). “Shear strength and hysteretic behavior of interior beam-column joints.” *ACI Struct. J.*, 87(1), 3-11.

Lowes, L.N. and Altoontash, A. (2003). “Modeling reinforced-concrete beam-column joints subjected to cyclic loading.” *J. of Struct. Eng.*, 129(12), 1686-1697.

MacGregor, J.G. and Wight, J.K. (2005). *Reinforced Concrete: Mechanics and design*, Pearson Prentice Hall, N.J.

Mirmiran, A., Zagers, K. and Yuan, W. (2000). “Nonlinear finite element modeling of concrete confined by fiber composites.” *Finite Elements in Analysis and Design*, 35(1), 79-96.

Nielsen, M.P. (1999). *Limit analysis and concrete plasticity*, CRC Press.

Nilson, A.H., Darwin, D. and Dolan, C.W. (2004). *Design of concrete structures*, McGraw-Hill, N.Y.

Nilsson, I.H.E. (1973). “Reinforced concrete corners and joints subjected to bending moment.” *Document. No. D7:1973*, National Swedish Building Research, Stockholm, Sweden.

Nilsson, I.H.E. and Losberg, A. (1976). “Reinforced concrete corners and joints subjected to bending moment.” *Proc., ASCE, J. of the Struct. Div.*, 102(6), 1229-1254.

Oberkampf, W.L., Trucano, T.G. and Hirsch, C. (2002). “Verification, validation, and predictive capability in computational engineering and physics.” *Proc., Foundations for Verification and Validation in the 21st Century Workshop*, Johns Hopkins University/ Applied Physics Lab.,Maryland, U.S.

Pantazopoulou, S. and Bonnaci, J. (1992). “Consideration of questions about beam-column joints.” *ACI Struct. J.*, 89(1), 27-36.

Park, R. and Paulay, T. (1973). “Behavior of reinforced concrete external beam-column joints under cyclic loads.” *Proc., 5th World Conference on Earthquake Engineering*, Rome, I(88).

Park, R. and Paulay, T. (1975). *Reinforced concrete structures*, Wiley, N.Y.

Paulay, T. (1989). “Equilibrium criteria for reinforced concrete beam-column joints.” *ACI Struct. J.*, 86(6), 635-643.

Paulay, T. and Priestley, M.J.N. (1992). *Seismic design of reinforced concrete and masonry buildings*, Wiley-Interscience.

Richard, R.M. and Abbott, B.J. (1975). “Versatile elastic plastic stress-strain formula.” *J. of Struct. Eng.*, ASCE, 101(4), 511-515.

Sarsam, K.F. and Phipps, M.E. (1985). “The shear design of in situ reinforced concrete beam-column joints subjected to monotonic loading.” *Mag. Of Concrete Res.*, 37(130), 16-28.

Taylor, H.P.J. (1974). “The behavior of in-situ concrete-to-column joints.” *Rep. No. 42.492*, Cement and Concrete Association, London,U.K.

Tran, P.T. (2009). “Effect of short-duration-high-impulse variable axial and transverse loads on reinforced concrete column.” M.S. thesis, University of Florida, Gainesville, U.S.

UFC. (2008). UFC 3-340-02, Structures to resist the effects of accidental explosions, Unified Facilities Criteria.

UFC. (2003). UFC 4-010-01, *DoD minimum antiterrorism standards for buildings*, Unified Facilities Criteria.

UFC. (2009). UFC-4-023-03, *Design of buildings to resist progressive collapse*, Unified Facilities Criteria.

Uma, S.R. and Prasad, A.M. (2006). “Seismic behavior of beam-column joints in RC moment resisting frames: A review.” *The Indian Concrete Journal*, 80(1), 33-42.

Viwathanatepa, S., Popov, E.P. and Bertero, V.V. (1979). “Seismic behavior of reinforced concrete interior beam-column subassemblages.” *Rep. No. UCB/EERC-79/14*, Earthquake Engineering Research Center, University of California, Berkley, California, U.S.

Watson, A.J. and Inkester, J.E. (1982). “Impact loading of a reinforced concrete beam-to-column joint”, *Special Publications, ACI J.*,73, 143-164.

Yim, H.C. (2007). “A study of steel moment connections for structures under blast and progressive collapse loading rates.” Ph.D thesis, The Pennsylvania State University, Pennsylvania, U.S.

.

BIOGRAPHICAL SKETCH

Loo Yong Tan was born in Singapore in 1976. He attended secondary school and junior college in Singapore. He was drafted into the army for his national service from 1995 to 1997.

He began his undergraduate studies in civil and structures engineering at Nanyang Technological University, Singapore, in July 1997 and obtained his Bachelor of Engineering degree in July 2001. In September 2001, he joined the Defence Science and Technology Agency, Singapore, as a project engineer. He continued with his part-time graduate studies in industrial and systems engineering at the National University of Singapore, Singapore, in January 2004 and obtained his Master of Science degree in December 2006.

In 2008, he was awarded a postgraduate scholarship to pursue a master's degree in civil engineering at the University of Florida, specializing in the field of protective structures.